“Flow characteristics within the scour hole around inclined circular bridge pier”

A PROJECT

Submitted in partial fulfilment of the requirements for the award of the degree of

BACHELOR OF TECHNOLOGY

IN

CIVIL ENGINEERING

By

Gaurav Sharma (131694)
Praveen Kumar (131700)

Under the supervision of

Dr. Ashish Kumar

Associate Professor

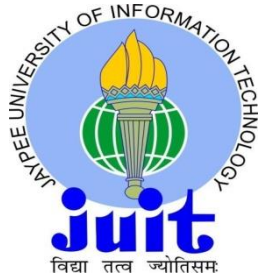

JAYPEE UNIVERSITY OF INFORMATION TECHNOLOGY

WAKNAGHAT SOLAN – 173 234

HIMACHAL PRADESH INDIA

May, 2017

CERTIFICATE

This is to certify that the work which is being presented in the project title **"Flow characteristics within the scour hole around inclined circular bridge pier"** in partial fulfillment of the requirements for the award of the degree of Bachelor of technology and submitted in Civil Engineering Department, Jaypee University of Information Technology, Waknaghat is an authentic record of work carried out by **Gaurav Sharma (131694) and Praveen Kumar (131700)** during a period from July 2016 to June 2017 under the supervision of **Dr. Ashish Kumar,** Associate Professor, Department of Civil Engineering, Jaypee University of Information Technology, Waknaghat.

The above statement made is correct to the best of my knowledge.

Date: - ……

Dr. Ashok Kumar Gupta	Dr. Ashish Kumar	External Examiner
Professor & Head of Department	Associate Professor	
Department of Civil Engineering	Department of Civil Engineering	
JUIT, Waknaghat	JUIT, Waknaghat	

ACKNOWLEDGEMENT

It is our pleased benefit and obligation to recognize the sort of help and direction got from a few people in arrangement of this report. It would not have been conceivable to set up this report in this frame without their profitable help, collaboration and direction.

The topic **"Flow characteristics within the scour hole around inclined circular bridge pier"** was very helpful to us in giving the necessary background information and inspiration in choosing this topic for the project. Our sincere thanks to our Project Guide **Dr. Ashish Kumar,** Associate Prof. for having supported the work related to this project. Their contributions and technical support in preparing this report are greatly acknowledged**.**

Gaurav Sharma **(131694)**

Praveen Kumar **(131700)**

ABSTRACT

In the present study flow pattern and turbulence characteristics around an inclined circular bridge pier have been investigated experimentally in the presence of a scour hole and compare with vertical pier. An Acoustic Doppler Velocimeter (ADV) was used to observe the velocity components, turbulence intensities and Reynolds stresses in the vertical planes, at α = 0˚,30˚,60˚,90˚,120˚and 180˚. Run were conducted under the clear-water approach flow condition. Flow characteristics around a vertical pier in the presence of a scour hole will be compared with flow characteristics similarly observed around an inclined circular uniform pier by utilizing the observations made in radial planes at 0°, 90°, and 180°. Approaching to the pier *i.e.* while *r* is small and below the level of initial bed in the scour hole region the *u* component shows negative values, which indicates reversal of flow near the pier. The *v* component of the velocity is mostly small in this plane. Approaching to the pier, the *w* component of velocity has larger values in downward direction which is being considered as negative. This means there is dominancy of strong down flow in this region. In the plane at α = 180°, close to the pier *i.e.* while *r* is small, the *u* component shows a reversal of flow near the water surface also far away from the pier the value of *w* component is always positive at revealing that upward flow in the wake region. The local scour depth around inclined pier was found to be 7 % lesser than scour depth around vertical pier due to weaker value of turbulent characteristics in case of inclined pier. Results obtained are presented herein.

CONTENTS

List of Figures

List of Table

List of symbols

b = diameter or width of bridge pier

B = flume width

d = size of uniform sediment

d_{50} = median sediment grain diameter

F_r = Froude number

g = gravitational acceleration

h = depth of flow

k = turbulent kinetic energy

Q = discharge

r = distance in radial direction

R_{eb} = pier Reynolds number

S = energy slope

u, v, w = Cartesian velocity components in x, y and z directions respectively

u', v', w' = fluctuation of u, v, and w components of velocity respectively

u = bed shear velocity of approach flow

U_∞ = velocity of approach flow

U_c = velocity of approach flow corresponding to incipient motion of sediment

$\sqrt{u'u'}, \sqrt{v'v'}$ = longitudinal and transverse components of turbulence intensity

$\sqrt{w'w'}$ = vertical component of turbulence intensity

$u'w', v'w'$ = components of Reynolds' Stress

CHAPTER 1
INTRODUCTION

1.1 General

The knowledge of the maximum possible scour around a bridge pier is essential for the safe design of bridges. Countless studies have been led to anticipate the scour depth around piers. Based on these studies, semi-empirical equations are given for the maximum scour depth. A continuous concern is that most of these equations are over-predicting the maximum scour depth for field, or even for laboratory conditions. Knowledge of the Complex flow field and erosion mechanism can provide a way out this problem. An extensive understanding of the turbulent flow structure can provide more insight into the scouring process and aid to predict scour depth precisely. For a superior comprehension of the flow pattern and turbulent flow around piers, many researchers have focused on the flow around piers with different cross section area along length, different pier shapes, cohesion and cohesion less bed material. Most of these studies are related to vertical piers and provide detailed information on the flow pattern around them but very less studies are present on flow characteristics around inclined bridge pier. The main purpose of the present study is to carry out a detailed experimental inspection of the flow pattern around a single inclined pier in a rough flat bed in order to provide a better knowledge of the three-dimensional flow. The experiments were carried out under clear water conditions. All the measurements were taken by an Acoustic Doppler Velocimeter (ADV). The contours of the time-averaged velocity components, turbulence intensities and Reynolds shear stresses at different horizontal and vertical planes are presented. Streamlines and velocity vectors observed from the velocity fields are used to study the details of flow structure.

1.2 Mechanism of scour

The boundary layer in the flow past a bridge element undergoes a three-dimensional separation. This separated shear layer rolls up together with the obstruction to form a vortex system in front of element which is swept downstream by the river flow. See from the top, this vortex system has the characteristic shape of a horseshoe and thus called a horseshoe vortex. The formation of the horseshoe vortex and the associated down flow around the bridge pier results in increased shear stress and hence a local increase in sediment transport capacity of the flow. This leads to the development of a deep hole (scour hole) surrounding the bridge element, which in turn changes the flow structure causing a reduction in shear

stress by the flow thus reducing its sediment transport capacity. The temporal variation of scour and the maximum scour depth at bridge pier therefore mainly depend on the flow pattern, characteristics of pier and river-bed material. The development of the horseshoe vortex and the associated down flow cause scour at different elements of a bridge such as pier, abutment and spur dike. The mechanism of scour around bridge elements has been studied by Kothyari *et al* (1992) whereas studies on the mechanism of scour around abutments and spur dikes are available in Kothyari & Ranga Raju (2001). Vittal *et al* (1994) and Kumar *et al* (1999) investigated the effectiveness of different appurtenances for reduction of scour around bridge piers.

1.3 Objectives of the study

In the present study, an ADV is used to study and compare velocity components, turbulence intensities, Reynolds' shear stresses with the available experimental data. The objectives are therefore to:

a. To study the flow and the turbulence characteristics around the inclined circular uniform pier in the presence of scour hole.
b. To compare flow pattern around vertical circular pier in the presence of scour hole with the inclined circular pier in the presence of scour hole.

1.4 Scope of the work

a. Since 1950 over 500 bridges in USA have failed and that majority of the failures were related to the scour of foundation material.

b. A bridge pier can be inclined towards downstream because of construction fault or even due to lateral settlement so it is necessary to know the flow pattern and scour depth around inclined pier in perceptive of its stability.

c. Use of inclined bridge pier in future due to its lesser scour depth development property. The degree of inclination for the pier should be decided after taking structural aspect into consideration as well.

1.5 Limitations of the study

The following are the main limitations of the present study:

1. The study is confined to clear-water scour around circular pier.

2. Uniform cohesion less sediment of size 0.28 mm with relative density of 2.72 was used.

CHAPTER 2

LITERATURE REVIEW

2.1 General

A main cause of bridge failure mostly is scour around its piers and abutments. The process of scour around bridge elements involves the complexities of both the three dimensional flow patterns and the sediment transport. The estimation of scour extent and its depth at bridge sites therefore continues to be a major concern for the hydraulic engineers. In the present study flow structure and turbulence characteristics around inclined circular bridge pier have been investigated experimentally in presence of a scour hole. An Acoustic Doppler Velocimeter (ADV) was used to observe the velocity components, turbulence intensities and Reynolds stresses in the vertical planes, at different horizontal angles in front and downstream of the pier.

2.2 Introduction

Bridges are required in order to cross the waterways by transport carriers. Thus bridges provide a smooth way to the transportation system. A main cause of bridge failure is scour by the flow around its pier and abutment. The process of scour around bridge elements involves the complexities of both the three dimensional flow patterns and the sediment transport. The estimation of scour extent and its depth at bridge sites therefore continues to be a major concern for the hydraulic engineers. Extensive research work has been carried out on the topic of scour. Less work however is reported on study of flow pattern around the inclined pier. In the present study flow patterns and turbulence characteristics in the vertical planes, upstream and downstream of the inclined pier have been investigated experimentally.

2.3 Brief Review

The subject of scour at bridge elements has been widely investigated in the past. A large number of laboratory studies have been conducted, mainly focused on estimating the equilibrium scour depth and its relationship with sediment parameters and pier parameters. A numbers of studies are reported on the flow field around vertical pier in presence of a scour hole. Relatively little studies on comparison of scour hole around bridge pier inclined at different angles but till now there is no work reported on study of flow pattern around inclined

pier in presence of scour hole. The present study therefore, was taken up with the objective of comparing the flow characteristics around inclined circular pier at different angles in presence of scour hole with the flow characteristics around vertical circular pier in presence of scour hole. Such studies were made by Zafer Bozkus and Osman Yildiz (2004) "Effect of inclination of bridge pier on scouring depth" ASCE 0733-9429(2004)130:8(827).Zafer Bozkus and Murat Cesme (2010) "Reduction of scouring depth by using inclined pier" NRC research press web site at cjce.nrc,ca on 30 oct. 2010.

Melville and Raudkivi (1977) conducted experiments around the circular bridge pier in three stages of scour *viz.* initial flat bed, the intermediate scour depth after 30 minutes from the starting of erosion and the final equilibrium scour hole. The measurements of flow field and turbulence structure around the pier were made with hot film wire anemometer and pitot tube. From the observations they described that horseshoe vortex travels along the perimeter of the pier. Strength of horseshoe vortex was also quantified. Ahamed and Rajaratnam (1998) described the velocity profiles in upstream plane of symmetry by Clauser type defect scheme. The velocity vectors and bed shear stress vector were measured with two 3-tube yaw probes. They also summarized experimental results by reporting that in presence of scour hole, the upstream flow accelerates into the scour hole rather than separating from the bed. They also reported that down flow velocity was as much as 95 percent of the approach velocity in front of pier. Graf and Yulistiyanto (2002**)** conducted experiments in a established (equilibrium) scour hole. They used an Acoustic Doppler Velocity Profiler to measure instantaneously the three components of velocity in the plane before and after the cylinder in the scour hole. Results of the study present that a vortex system is formed in front of the pier and a trailing wake vortex system of strong turbulence is formed behind the cylinder.

Zafer Bozku and Omen Yildiz (2004) given a technical note in which scour depth around pier at different inclination is compared. They showed that scour depth decreases as the inclination of the pier increases toward downstream. "They stated that rate of scour hole development is higher in the earlier stage of each run and decrease as time passes and approach asymptotically to an equilibrium value and maximum scour depth are observed on the plane of symmetry at the upstream face of the pier. It is found as the pier inclination angle β increases the local scour depth around a bridge pier is reduced substantially". This kind of vertically inclined pier system, also may well have advantages with respect to scour depth over both vertical pier and tapered piers. It should keep in mind however that there might be a certain limit to the inclination of a bridge pier from the construction viewpoint. Scour depth may increase around the downstream pier, which is inclined toward the upstream direction in the vertical plan. Those pier configurations will be studied in the near future.

CHAPTER 3

EXPERIMENTAL SET-UP, EQUIPMENTS AND PROCEDURE

3.1 General

Extensive data are available in literature on depth of scour around vertical circular uniform piers. No information however, is available on flow structure around inclined circular piers. Therefore, it is designated to study the flow pattern and variation of velocity around inclined pier towards downstream during the present investigation, Keeping this in view experiments were planned and conducted in the Hydraulics Laboratory of the Department of Civil Engineering, Jaypee University of Information and Technology, Waknaghat. The present chapter contains the description of the material, equipment used and the experimental procedure adopted for the investigation.

3.2 Details of Experimental Setup

3.2.1 Flume

A fixed bed masonry flume of 10.0 m length, 0.75 m width and 0.60 m depth was used in the experiments. The flume receives its water supply from a controlled water pump. The water supply in the flume was regulated with the help of a valve provided at the inlet of the pump. A working section in the flume is 3.0m long, 0.75m wide and 0.4m deep, consisting of a 20 cm thick sand layer at its bottom which is located 4 m downstream of the flume entrance.

An adjustable iron gate is provided at the downstream end of the flume to enable adjustment of the depth of the flow in the flume. Adjustable rails and trolleys were mounted on the two walls of the flume to carry the pointer gauge and other equipment used for measurements of flow pattern, water surface and bed level. The working section was filled with the desired sediment to the level of the flume bed. The piers were placed at the center of the working section of the flume. The photographic view of the experimental set-up is given Figure 3.1 shows the general layout of the flume used in experimentation.

Fig. 3.1 Flume used in experiment with all arrangement.

3.2.2 Sediment

River sediment retained and passed between two successive sieves were used in all experiments as the sediment. Uniform size non-cohesive river bed sediment having size = 0.28 mm, was used in all experiments as the bed material. These sediments have a relative density of 2.72.

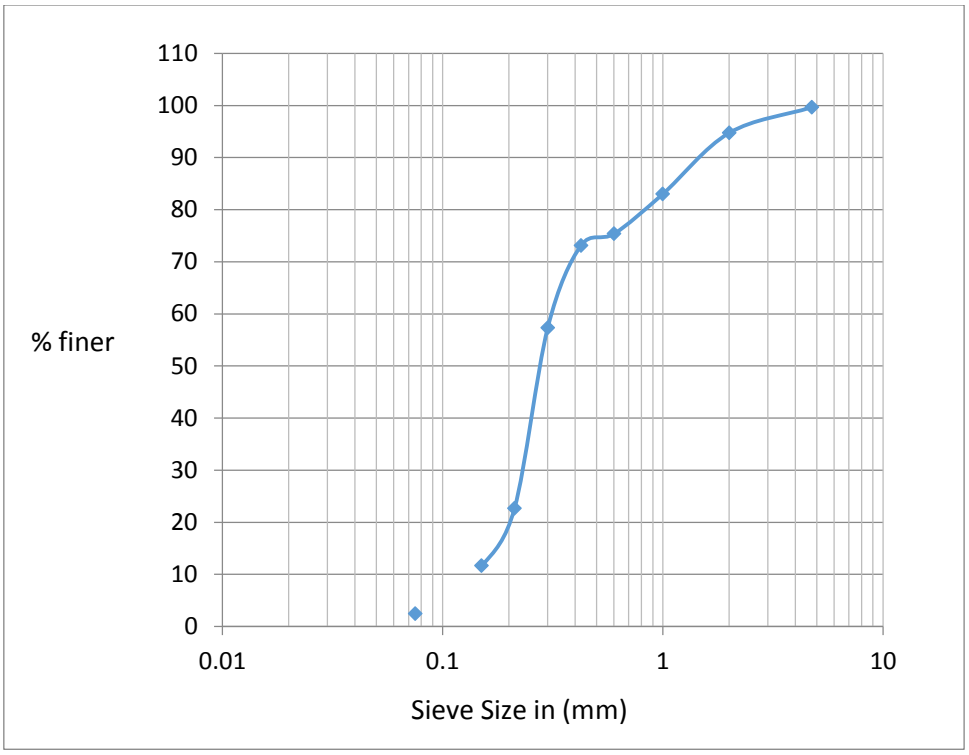

Fig. 3.2 Particle size distribution.

3.2.3 Piers

The models of circular uniform piers were prepared using concrete. Concrete circular pier of uniform section having diameters of 7.5 mm were used.

3.3 Measuring equipments

3.3.1 Acoustic Doppler Velocimeter (ADV)

The ADV is an instrument for measuring the point velocity of water flow. With the use of appropriate software, the values of the velocity are gathered and stored in a computer. The probe head includes one transmitter and between two to four receivers. The remote sampling volume is situated typically 5 cm from the tip of the transmitter, but little studies showed that distance might change slightly. The sampling volume size is decided by the sampling conditions and manual setup. In a standard arrangement, the sampling volume is like a cylinder of water with a diameter of 6 mm and a height of 9 mm, however newer laboratory ADVs may have smaller sampling volume (e.g. Sontek microADV, Nortek Vectrino+). A standard ADV system provided with N receivers records simultaneously 4.N values with each sample. That is, for every receiver, a velocity component, signal strength value, a signal-to-noise (SNR) and a correlation value. The signal strength, SNR and correlation quality are used primarily to determine the quality and exactness of the velocity data, in spite of the fact that the signal strength (acoustic backscatter intensity) may related to the immediate suspended sediment collection with proper calibration. The velocity component is measured along the line connecting the sampling volume to the receiver.

Fig. 3.3 Acoustic Doppler Velocimeter.

3.3.2 Pitot Tube

Pitot tube is a pressure measurement instrument used to measure fluid flow velocity. The pitot tube was design by the French engineer Henri Pitot in the early 18th century and was adjusted to its current shape in the mid-19th century by French scientist Henry Darcy. It is widely used to find the airspeed of an aircraft, water speed of a boat, and to determine liquid, air and gas flow velocities in industrial applications. The pitot tube is used to determine the local flow velocity at a given location in flow stream and not the average flow velocity in the pipe or conduit.

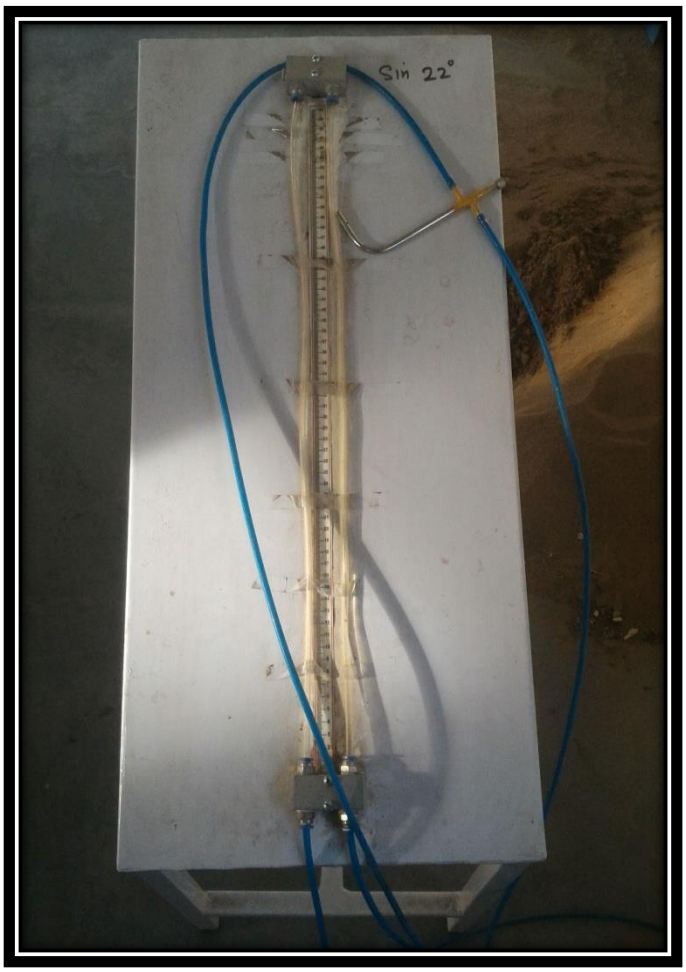

Fig 3.4 Pitot Tube.

3.3.3 Pointer Gauge

Pointer gauge is an instrument used in leveling of initial bed and also used for recording scour depth with time. It has a long square ruler below which a sharp pointed nail is fixed to gauge the distance accurately without damaging bed of the flume.

Fig. 3.5 Pointer gauge.

3.4 Experimental Procedure

For present study, the experiments were carried out in a 10 m long, 0.75 m wide rectangular channel, situated in the Hydraulic Engineering Laboratory of Department of Civil Engineering, Jaypee University of Information Technology. A working section was located 4 m downstream of the flume entrance, having the dimensions; length = 3 m, depth = 0.6 m and width = 0 .75 m. The working section was filled with uniform cohesion less material (sand) having d_{50} = 0.28 mm.

A discharge Q of 0.023 m^3/s and flow depth h of 110 mm was determined such that sediment particles in the test section were subjected to the condition of threshold of their motion. The vertical distributions of the time-averaged velocity were measured in the test section much upstream of the pier. This yielded the average approach velocity U_∞ of flow equal to 0.28 m/s. The shear velocity u_* of the approach flow was obtained through the law of the wall. The critical shear velocity u_{*c} for the corresponding grain size was determined by Shield's diagram. The clear water condition prevailed during the experiment as u_*/u_{*c} value was ≤ 1. The hydraulic parameters used for the experiment are summarized in Table 4.1.

Table 3.1 Hydraulic parameters for the experiment run.

B (m)	S_0	h (m)	Q (m^3/s)	B/h	U_∞ (m/s)	F_r	Re_h	d_{50} (mm)	b (m)	β
0.75	0.00021	0.11	0.023	6.82	0.28	0.21	24151	0.28	0.075	0˚,5˚,10˚,15˚

B - Width of flume, S_0 - energy slope , Re_h – Reynolds number , b – diameter of pier, F_r - Froude Number, β = angle of inclination towards downstream.

3.4.1 Vertical pier (setup 1)

A circular pier having diameter b = 75 mm was installed vertically in the middle of the test section and the flow condition described in Table 3.1 was established. The run was performed under clear water condition. The run was performed for duration of 7 hrs and scour hole of 8.7 cm developed. Geometry of scour hole was measured after the run with the help of pointer gauge having least count of 0.1mm. Figure 3.6 shows 2-D & 3-D view of conture map of scour hole.

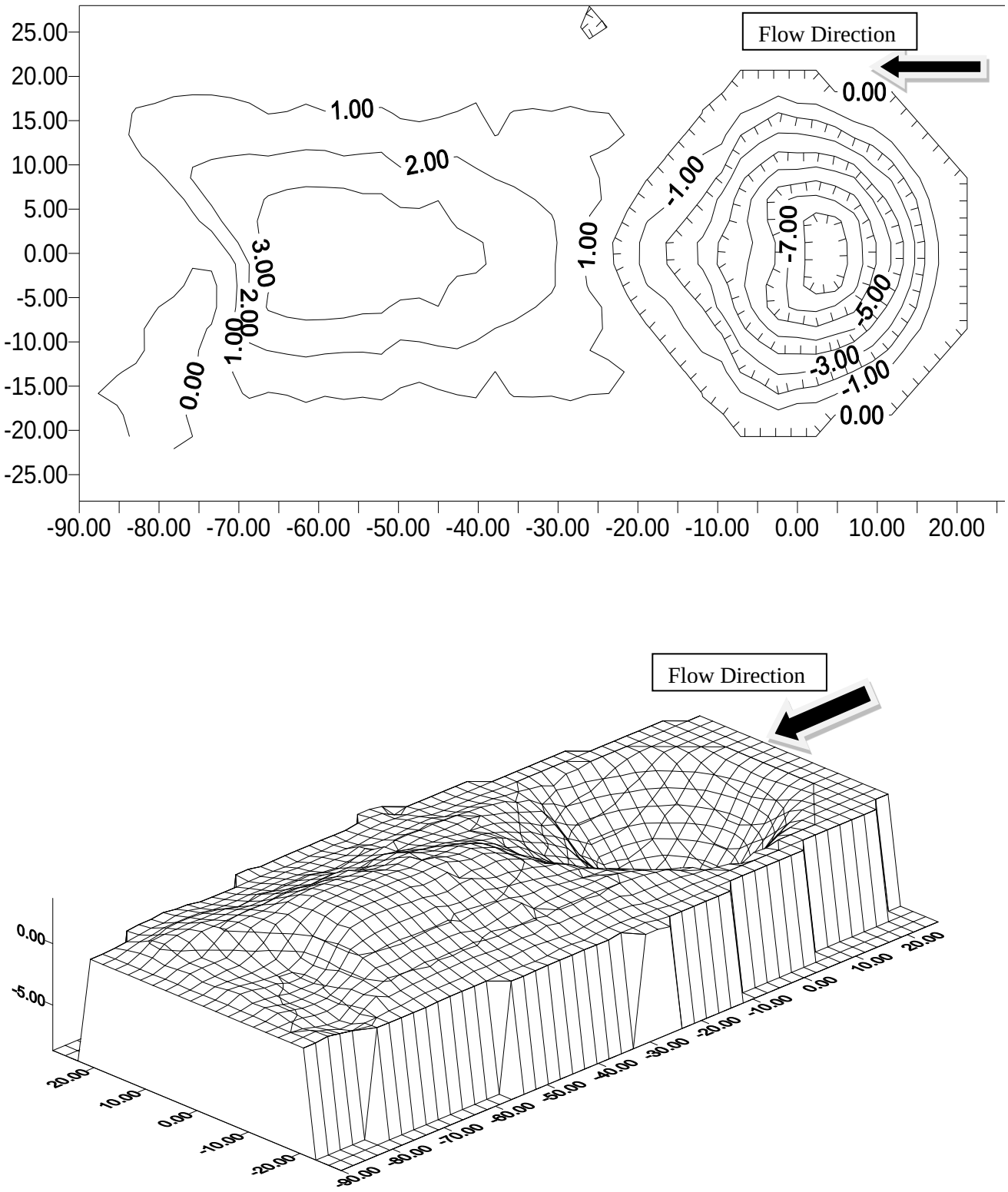

Fig.3.6 2-D & 3-D view of conture map of scour hole around vertical pier.

3.4.2 5° Inclined pier towards downstream (setup 2)

The run was performed for the same time and under same conditions as for vertical pier then a scour hole of 8.1 cm developed. Geometry of scour hole was measured after the run with the help of pointer gauge having least count of 0.1mm. Figure 3.7 shows 2-D & 3-D view of conture map of scour hole. Rather the main objective of the study is to show the effect of the inclination of the pier on flow characteristics.

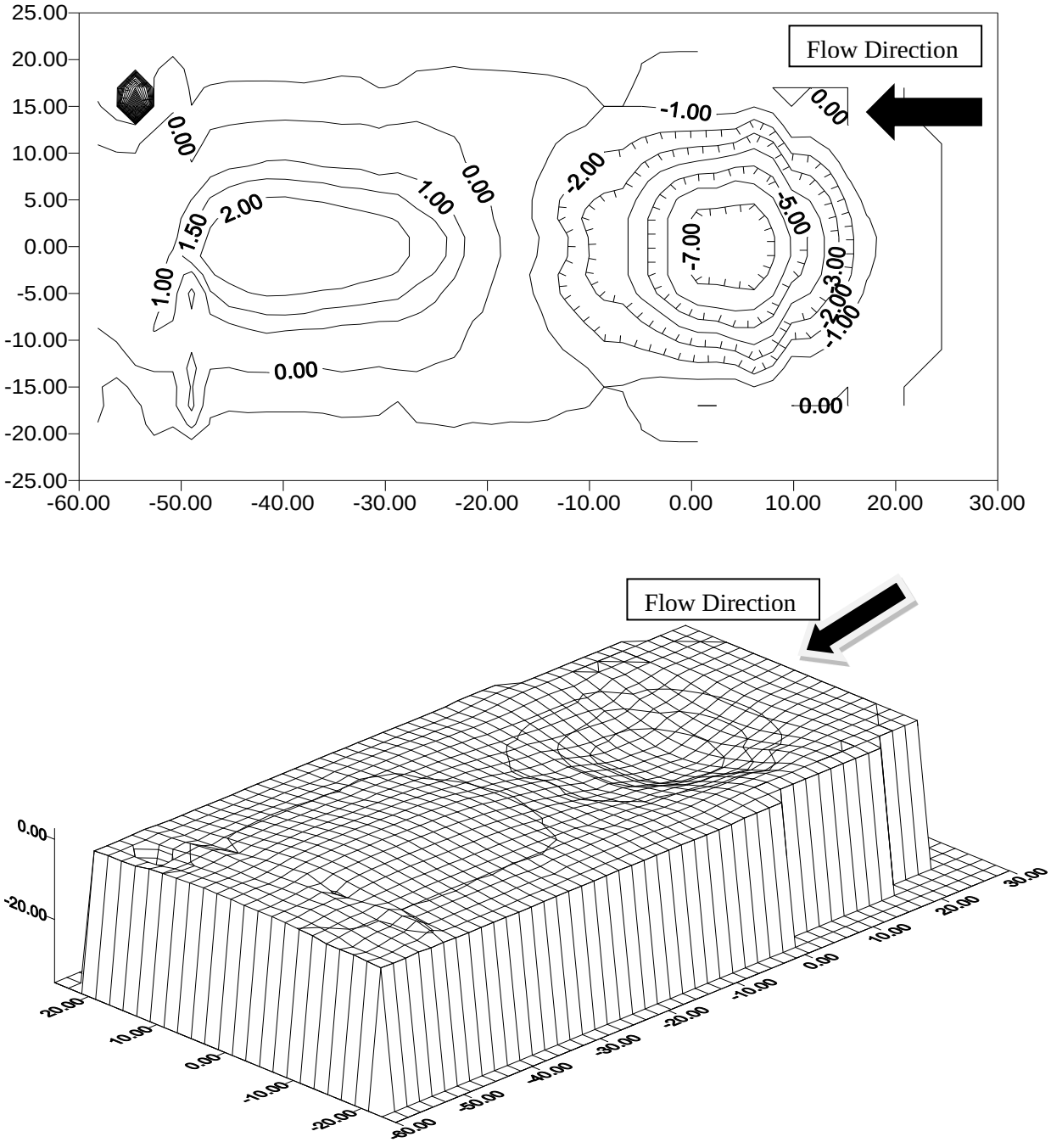

Fig.3.7 2-D & 3-D view of conture map of scour hole around inclined pier.

3.5 Velocity Measurements

The geometry of scour hole developed around the pier was stabilized by spraying cement over its surface after the water was completely drained from it at the end of the scour activity in every experimental set up. The measurement for the flow velocity components, turbulence intensities and Reynolds stresses were made in a vertical plane of symmetry ahead of pier at α = 0˚,30˚,60˚,90˚,120˚and 180˚ using an Acoustic Doppler Velocimeter (ADV) as shown in fig 3.8. Here α is the angular direction of the plane with $\alpha = 0°$ corresponding to upstream central line of the channel. Velocity distributions were measured along eight vertical planes at different radial distances (r) from the centre of pier *i.e.* r = 7.5, 9.5, 11.5, 13.5, 15.5, 17.5, 19.5, 21.5, 23.5 and 25.5, 27.5 cm at each α as shown in fig, 3.8. The coordinates of every point is defined by (r, α, z) with z being vertical distance above the general bed level of the channel.

The three-dimensional velocity measurements were taken using the ADV. An ADV can instantaneously measure all the three components of velocity at a given point in the flow domain. The measurements were taken at any particular point for long durations in order to ensure that observations become stationary. The measurements were made at a frequency of 25 Hz over duration of 4 minutes at each location. Each time series on velocity components was edited for a minimum signal to noise ratio of 17 and minimum correlation coefficient of 70%.

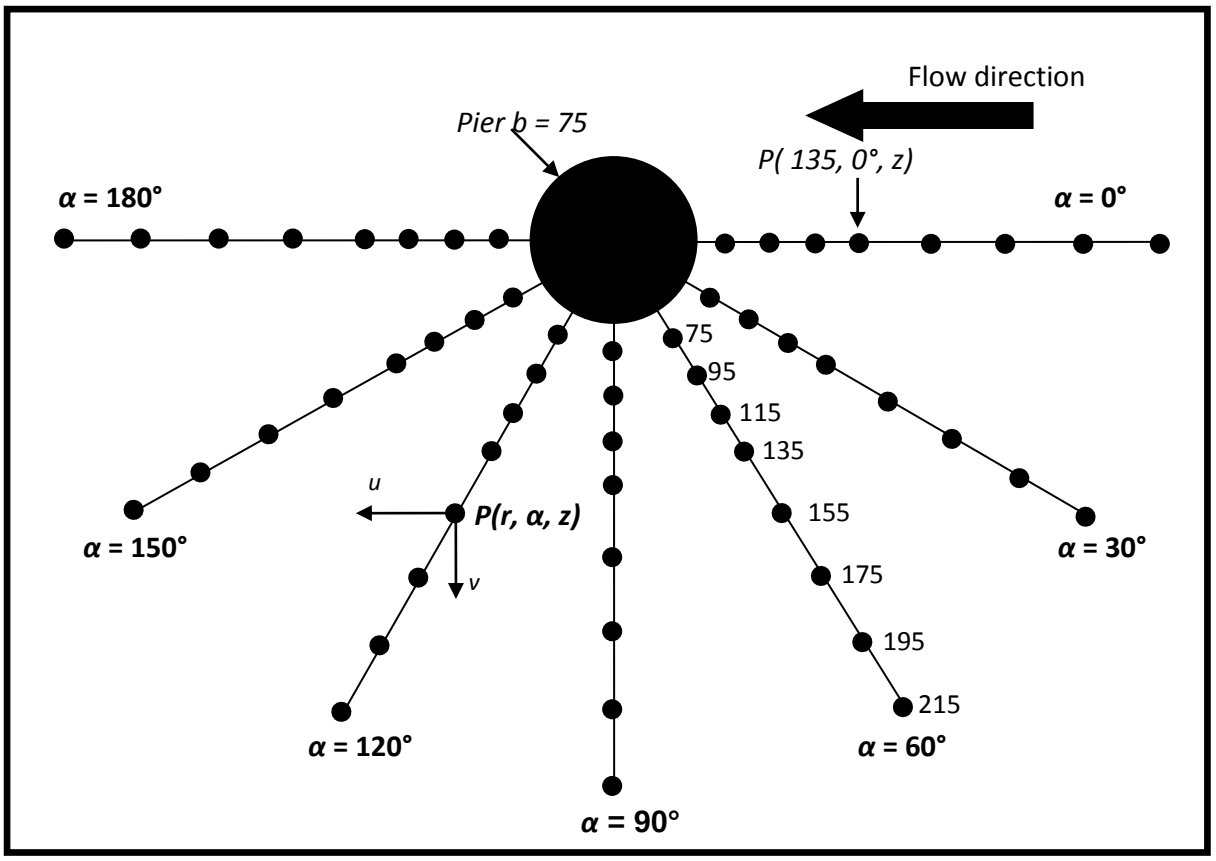

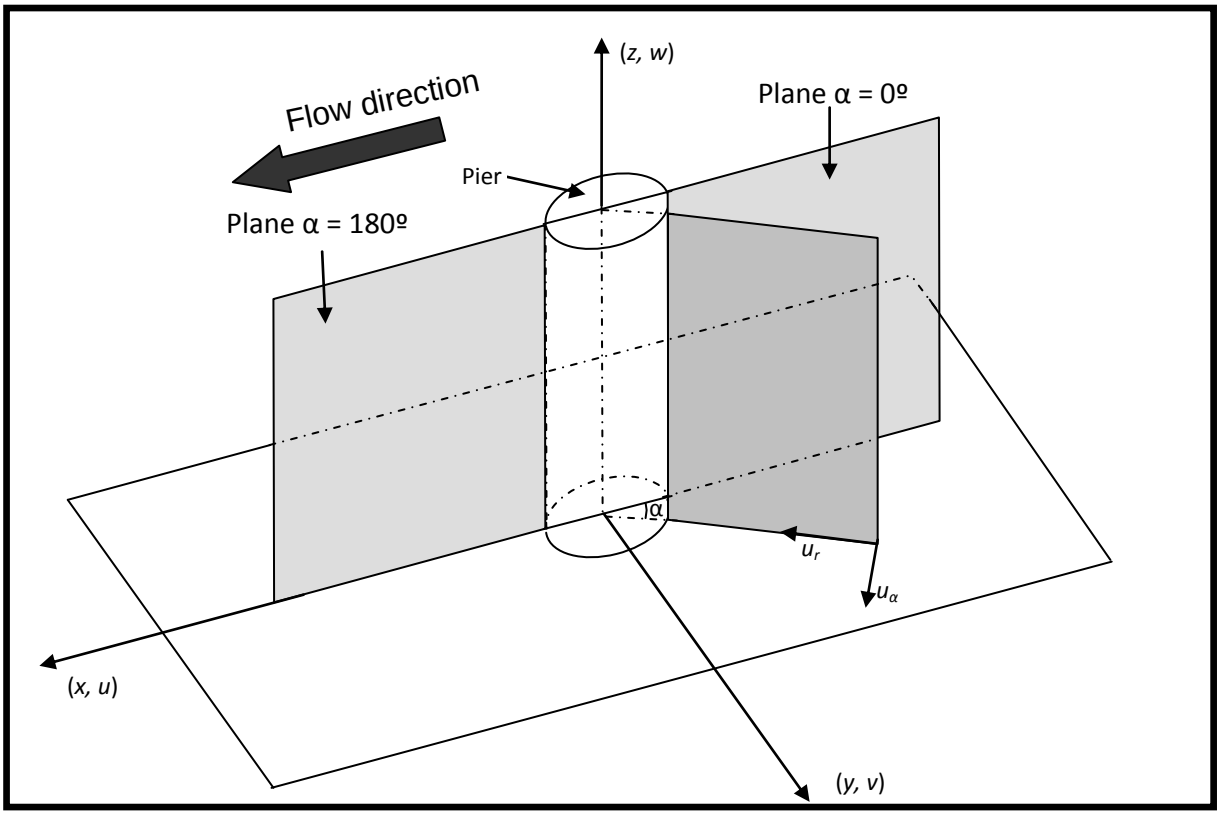

FIG. 3.8 Measurement stations around the pier in (mm) (Kumar, 2007).

CHAPTER 4

RESULTS AND DISCUSSION

4.1 Flow field around vertical circular pier

Measurement for the flow structure at different measuring angles around the circular uniform pier as per experimental details given in Chapter 3. The flow structure comprises vertical distribution of velocity components, turbulence intensities, and Reynolds' stresses .

4.2 Vertical distribution of the velocity

In vertical pier or in setup 1 measurements were taken at seven different vertical planes in radial directions at α = 0º, 30º, 60º, 90º, 120º, 150º and 180º from the flow.

In inclined pier or setup 2 measurements were taken at five different vertical planes in radial directions at α = 0º, 30º, 60º, 90º, and 180º from the flow due to time constrain.

The variation in time averaged components of velocities (longitudinal *u*; transverse *v* and vertical *w*) in the plane at α =0° is shown in fig. 4.1 The velocity components were normalized using upstream flow velocity U_∞ while the vertical distance *z* is normalized using depth of flow *h.* Approaching to the pier *i.e.* while *r* is small and below the level of initial bed in the scour hole region the *u* component shows negative values, which indicates reversal of flow near the pier. The *v* component of the velocity is mostly small in this plane. Approaching to the pier, the *w* component of velocity has larger values in downward direction which is being considered as negative. This means there is dominancy of strong downflow in this region.

In the planes at α = 30º and 60º velocity component are shown in fig. 4.2 & 4.3, a downward flow was obtained near to the pier. The flow pattern in these two planes are similar to that in the plane α = 0º. A little rotating vortex was observed near to the pier and in the scour hole region but with its value less than that observed at 0º plane.

In the plane at α = 90º a small vortex with diminishing strength was observed near the bed of the scour hole. The values of u, v and w are decreasing as compare to 0 degree are shown in fig.4.4.

In plane at α = 120º flow direction is away from the pier and vortex losses its strength on entering in this plane as shown in fig.4.5. Close to the pier downward flow is rather weak however its magnitude is high.

Figure 4.6 & 4.7 shows the measured time averaged velocity components *viz. u, v* and *w* over the vertical plane in the downstream of the pier *i.e.* at α =150°, 180°. In the plane at α = 180°, close to the pier *i.e.* while *r* is small, the *u* component shows a reversal of flow near the water surface also far away from the pier *i.e.* while *r* is larger, the *u* component albeit is larger as compared to its value near the pier but it still has a decreasing tendency nearer the surface of the flow. In the wake region *i.e.* when α = 180°, the *v* component is seen to fluctuate about its mean value. The normalized value of *v* component is seen to vary between –0.50 and 0.2 over this plane. On the contrary to the observations at α = 0° the value of *w* component is always positive at α = 180° revealing that upward flow in the wake region.

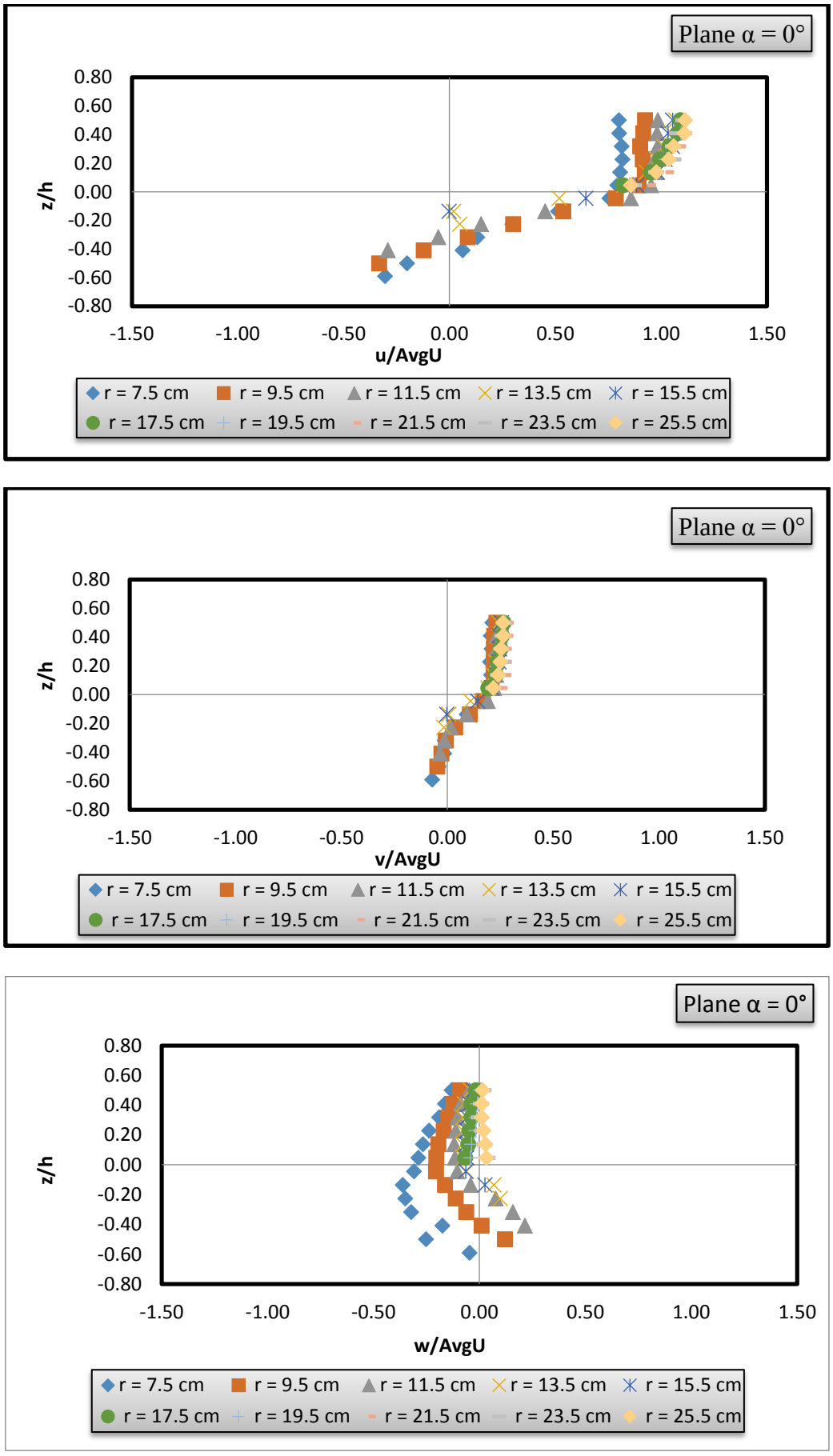

Fig 4.1 Normalized profiles of u, v and w measured in upstream of vertical pier (α = 0°).

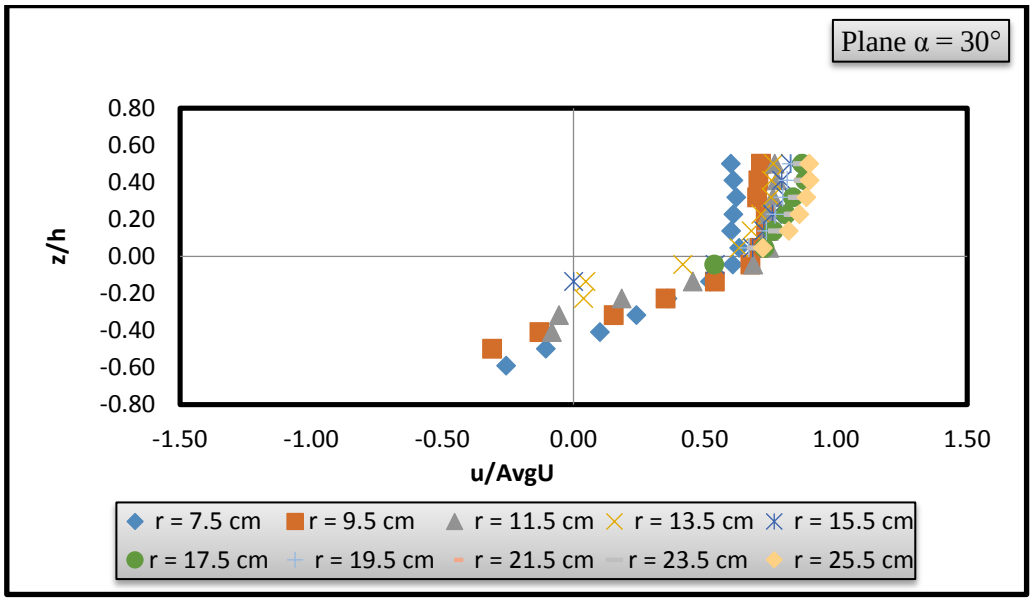

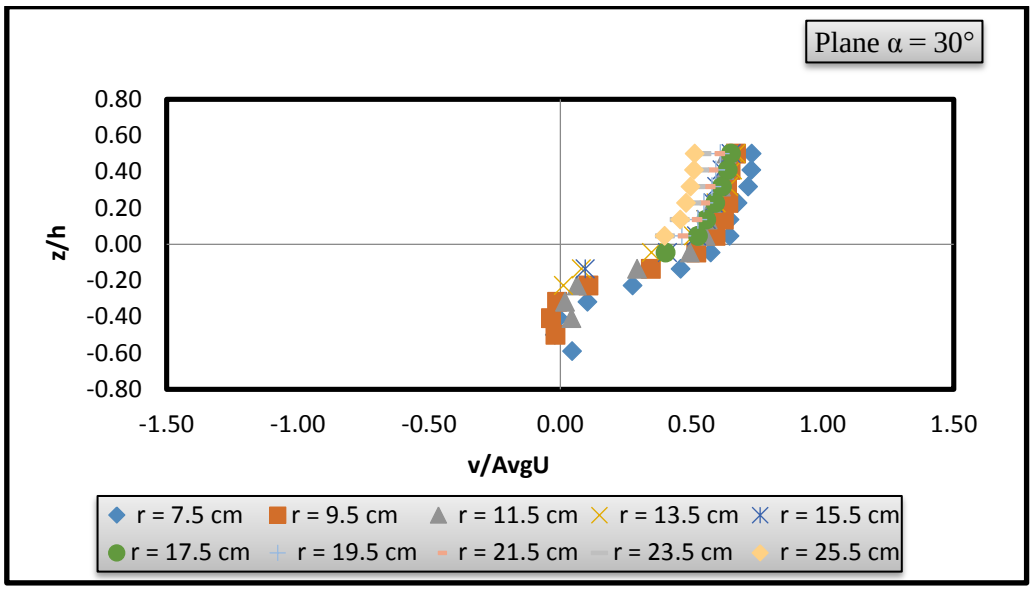

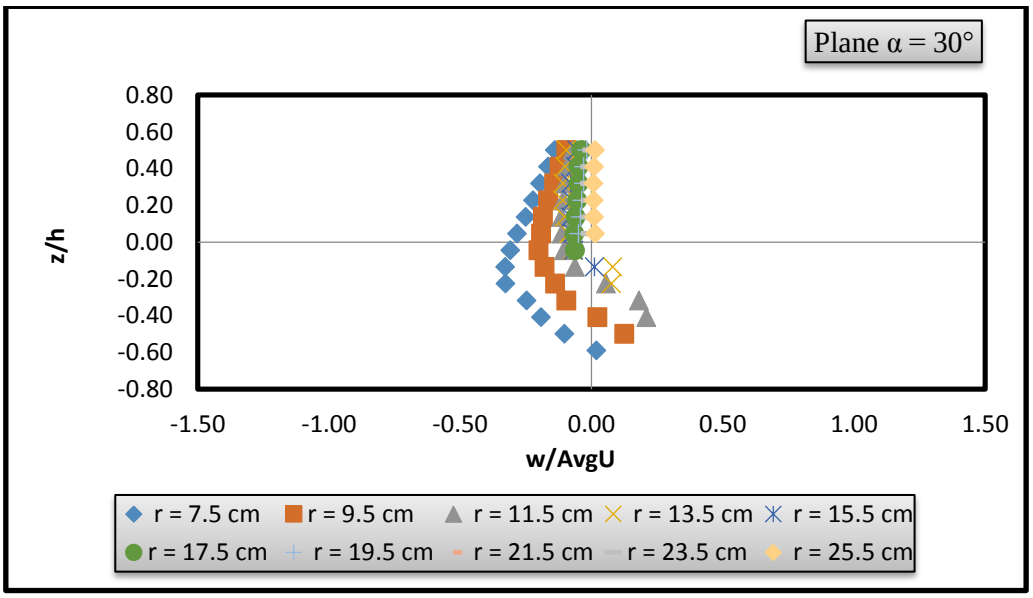

Fig 4.2 Normalized profiles of u, v and w measured in upstream of vertical pier (α = 30°).

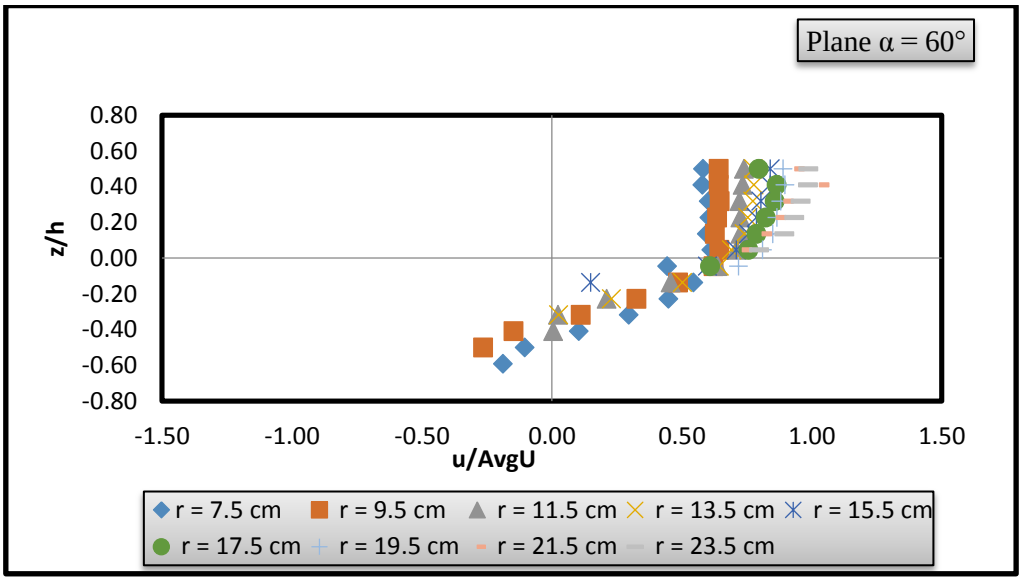

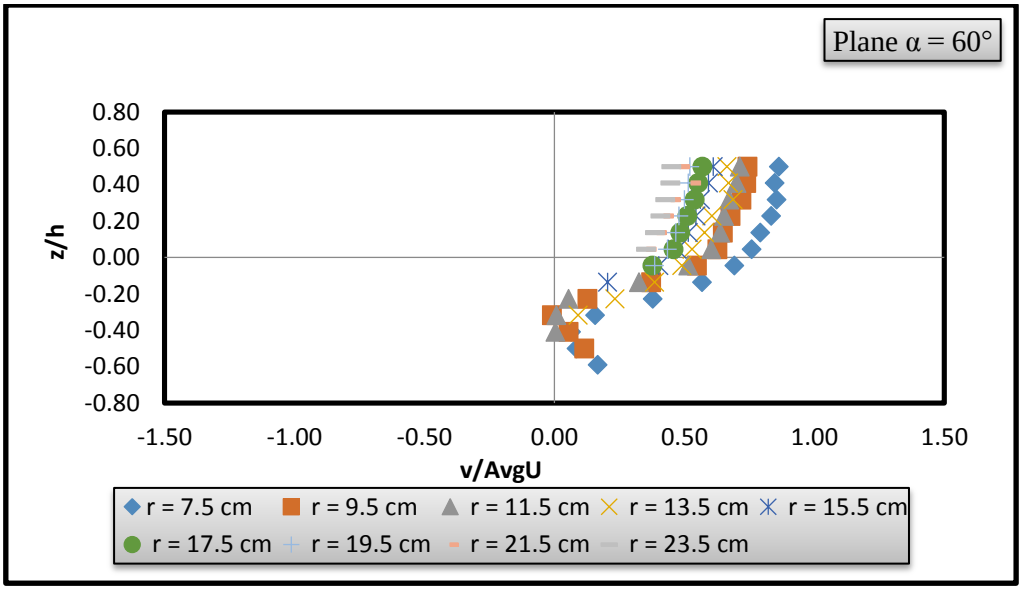

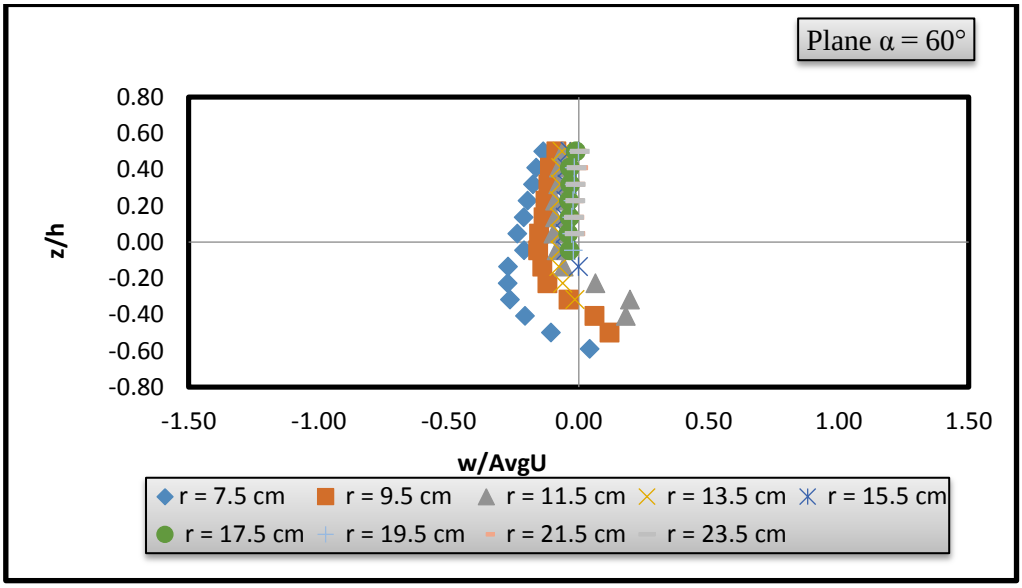

Fig 4.3 Normalized profiles of u, v and w measured in upstream of vertical pier (α = 60°).

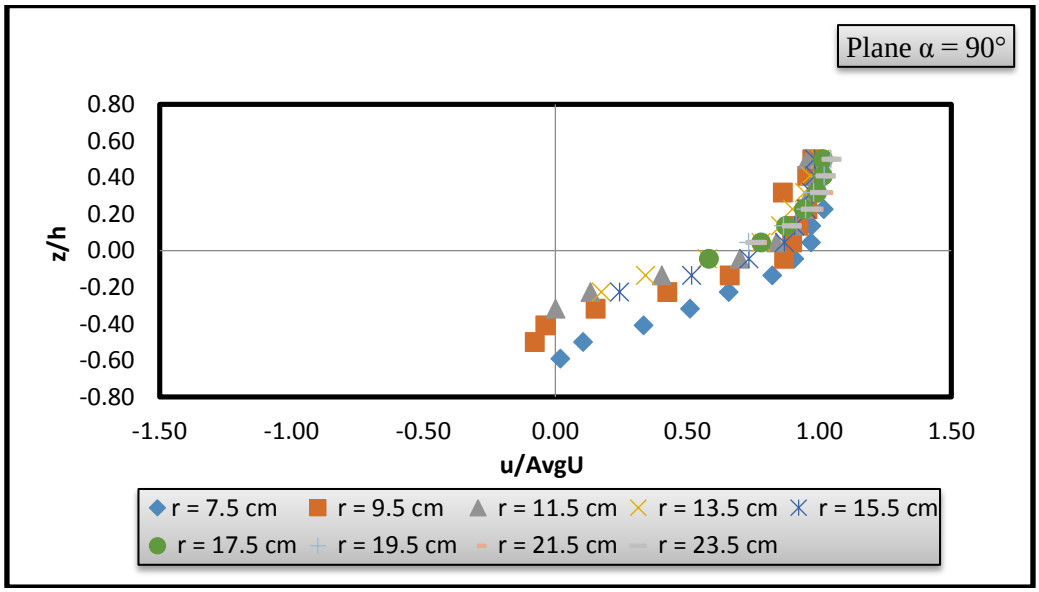

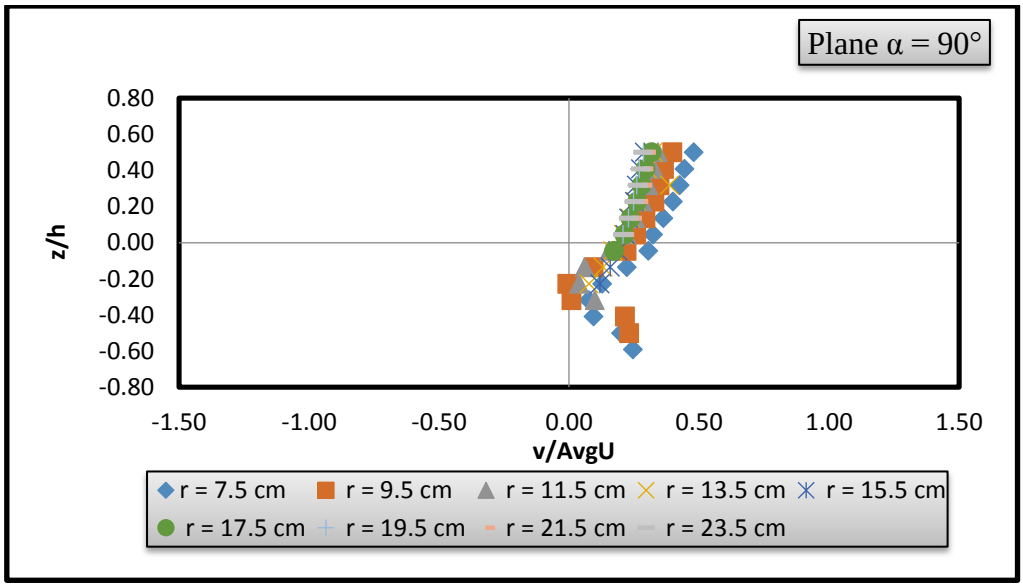

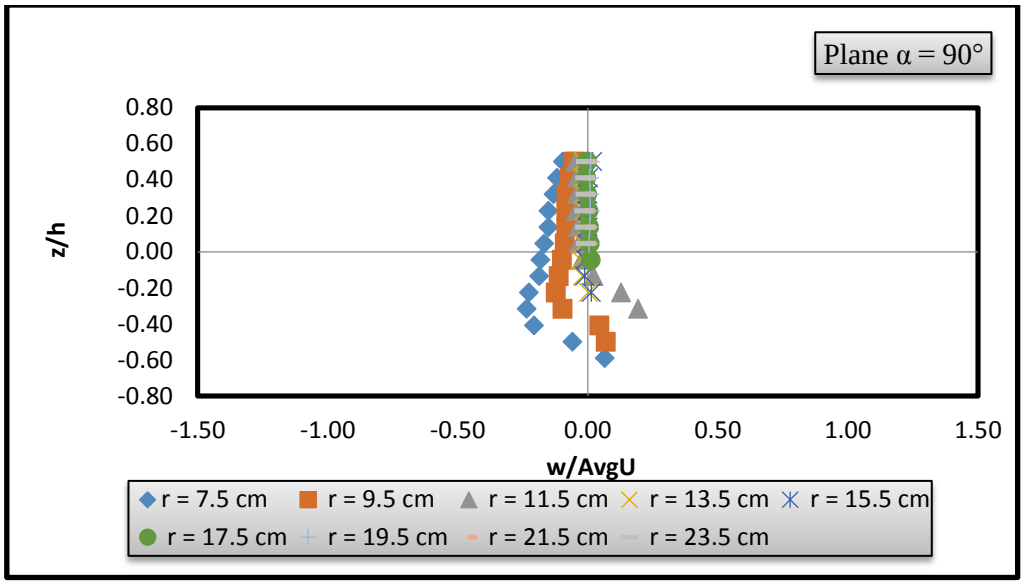

Fig 4.4 Normalized profiles of u, v and w measured in side stream of vertical pier (α = 90°).

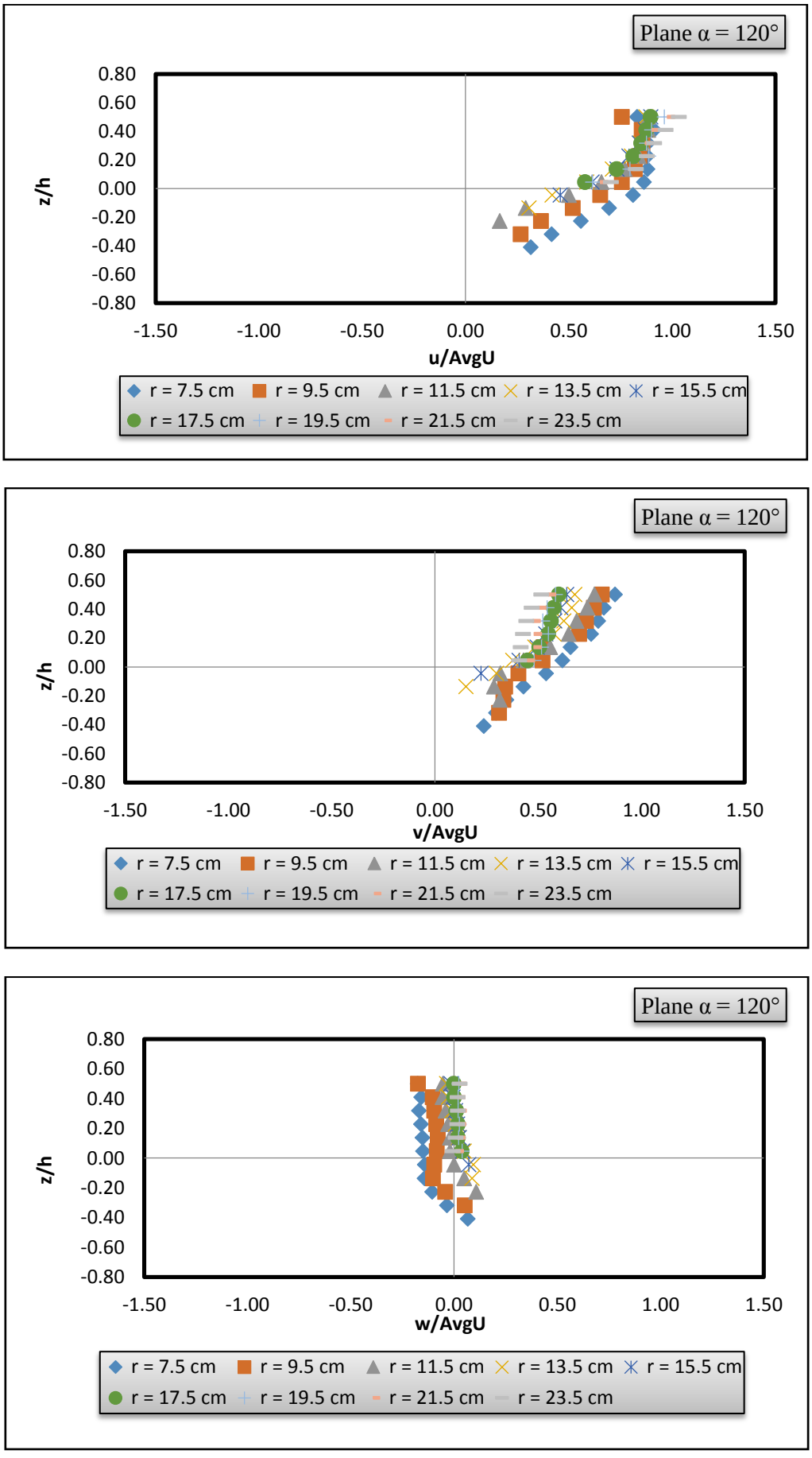

Fig 4.5 Normalized profiles of u, v and w measured in downstream of vertical pier (α = 120°).

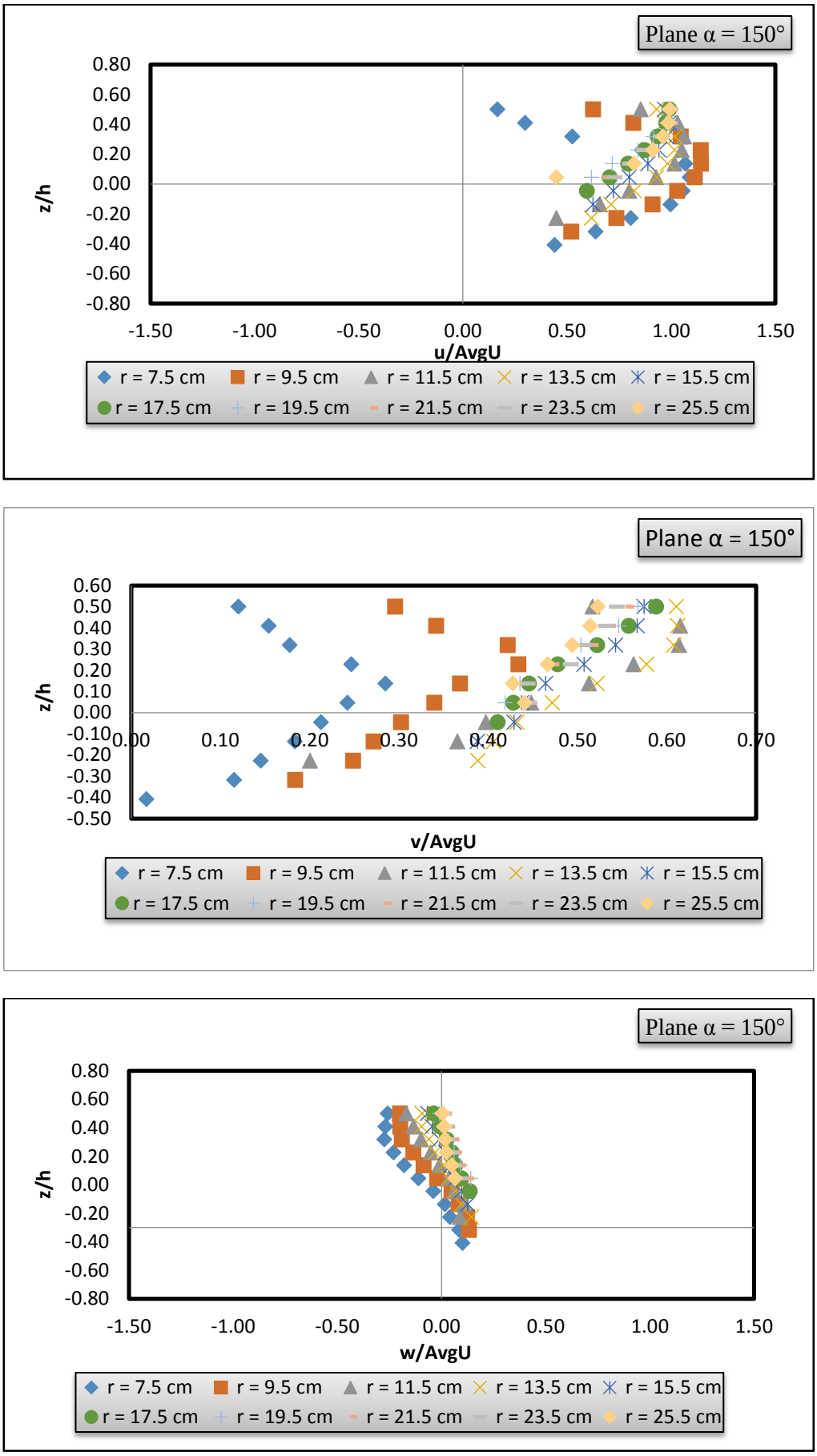

Fig 4.6 Normalized profiles of u, v and w measured in downstream of vertical pier (α = 150°).

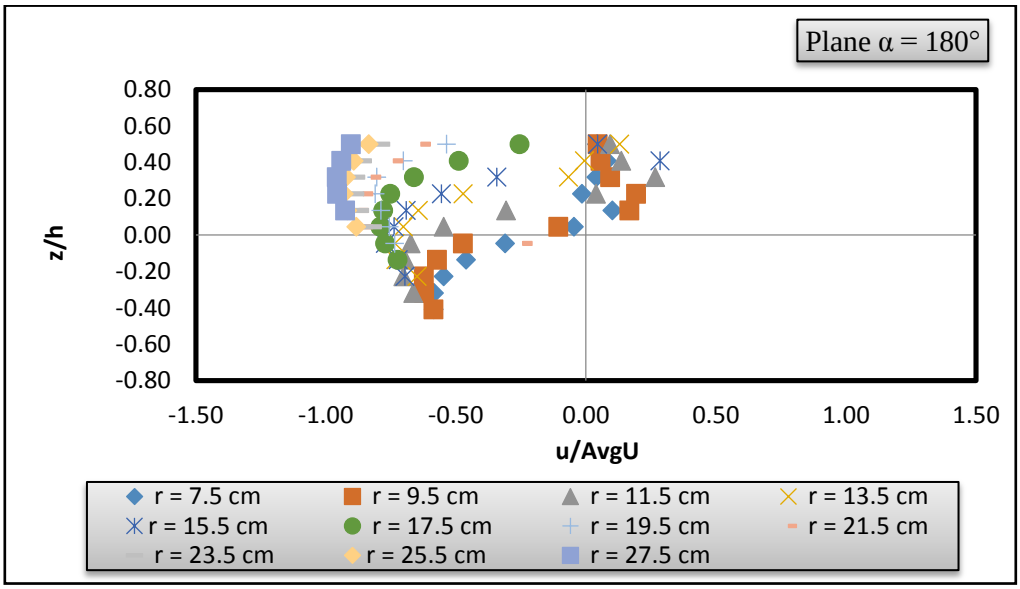

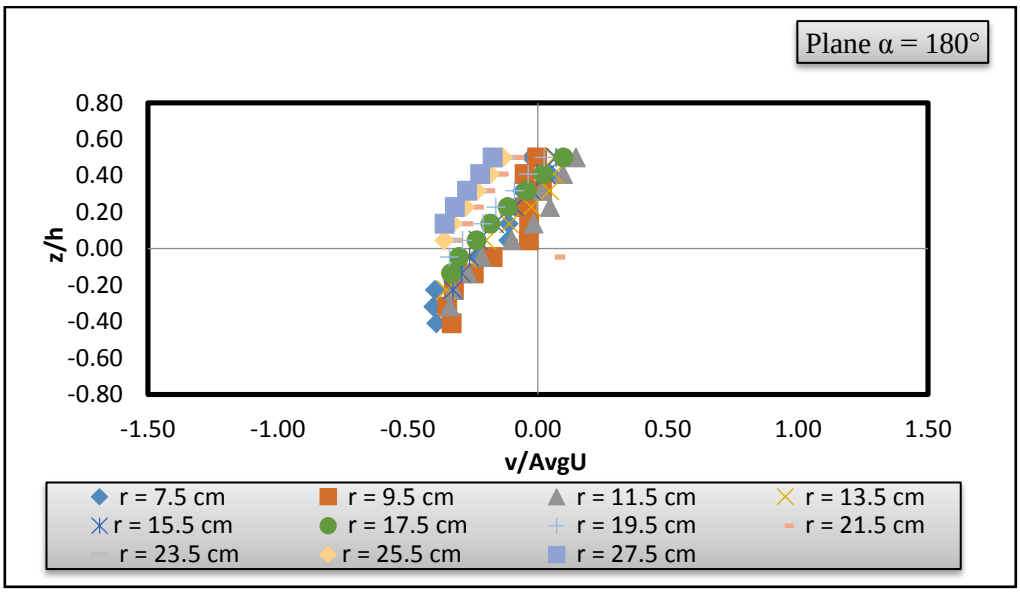

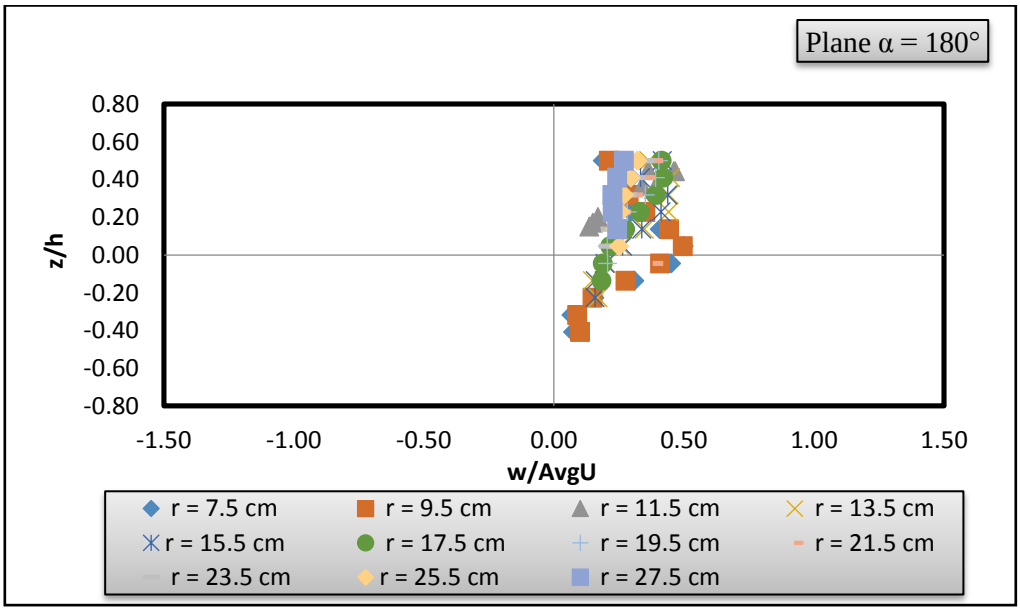

Fig 4.7 Normalized profiles of u, v and w measured in downstream of vertical pier (α = 180°).

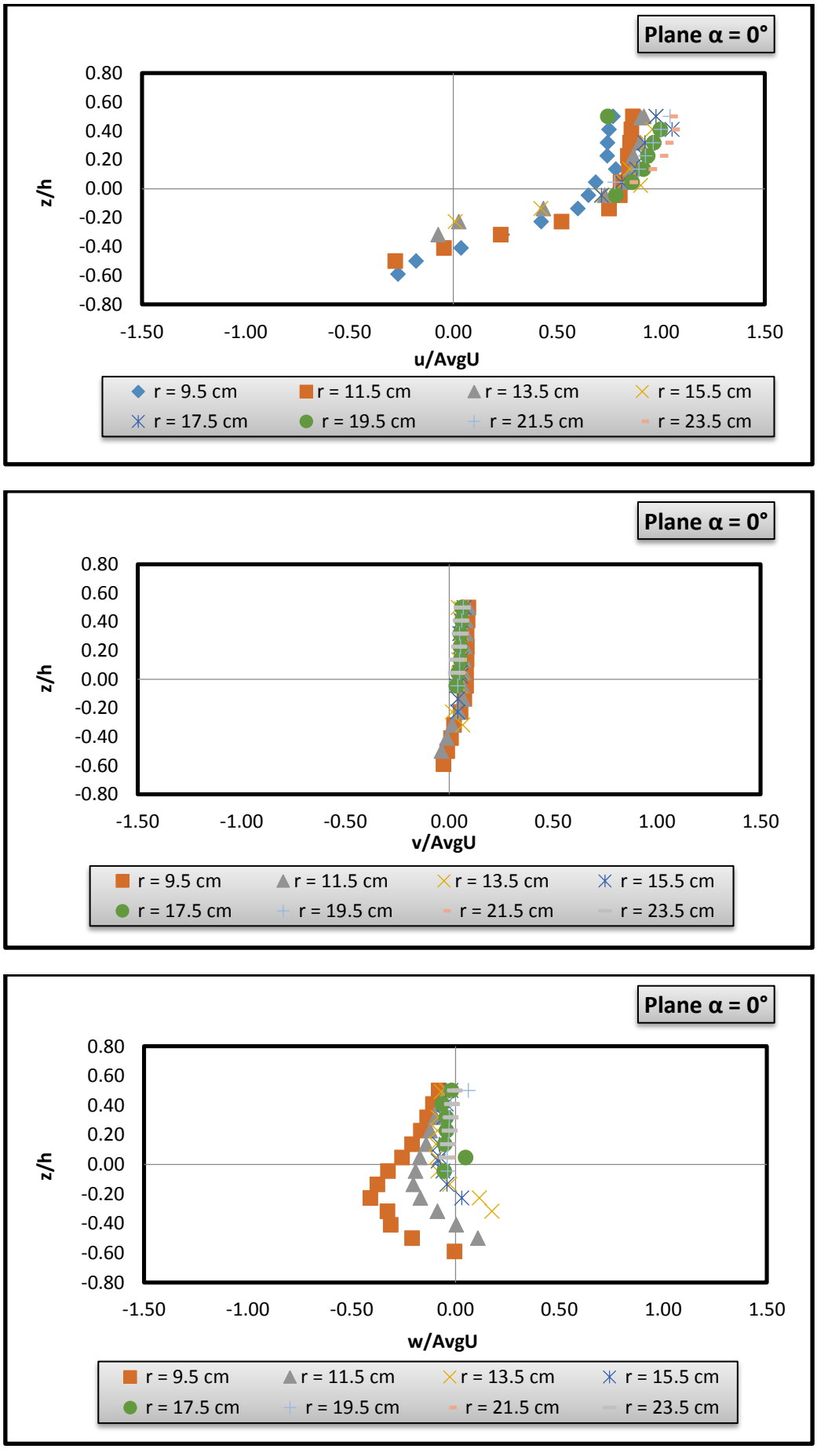

Fig 4.8 Normalized profiles of u, v and w measured in upstream of inclined pier (α =0°).

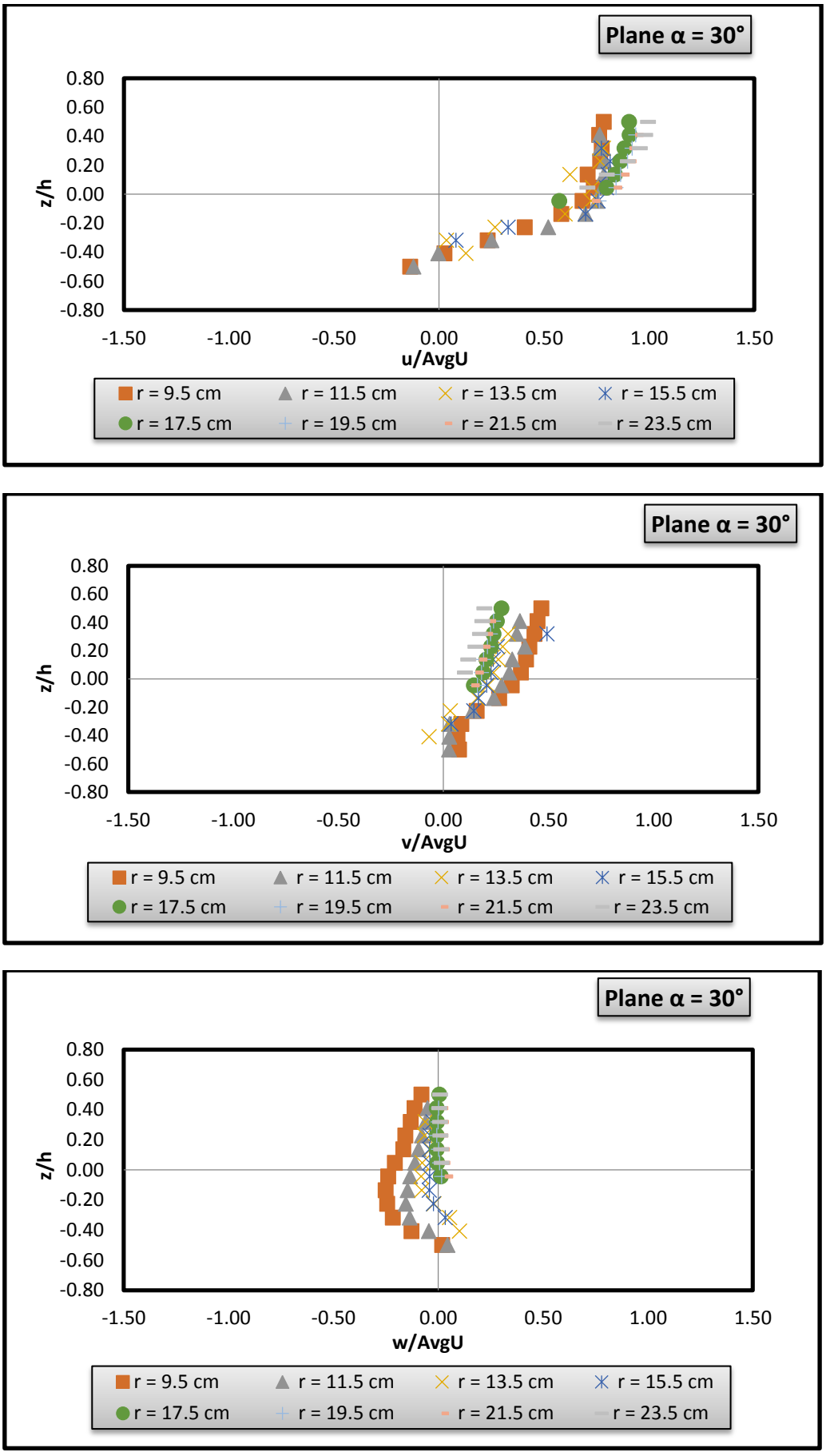

Fig 4.9 Normalized profiles of u, v and w measured in upstream of inclined pier (α = 30°).

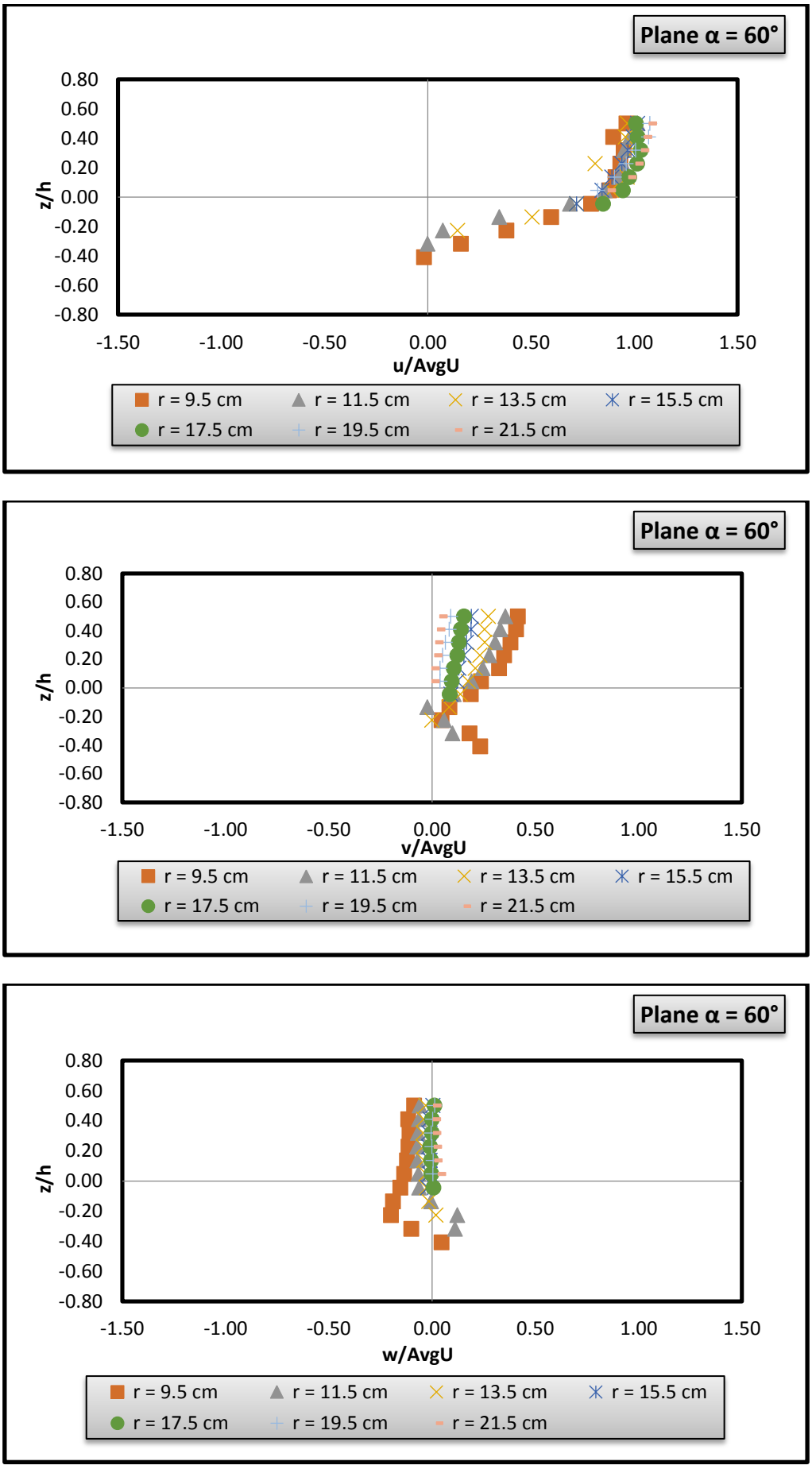

Fig 4.10 Normalized profiles of u, v and w measured in upstream of inclined pier (α = 60°).

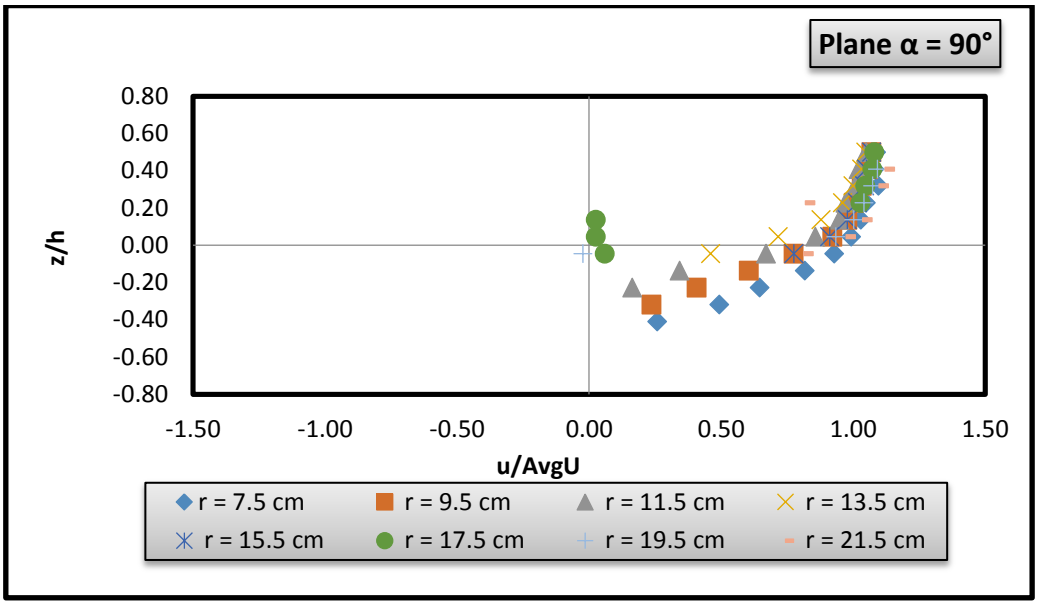

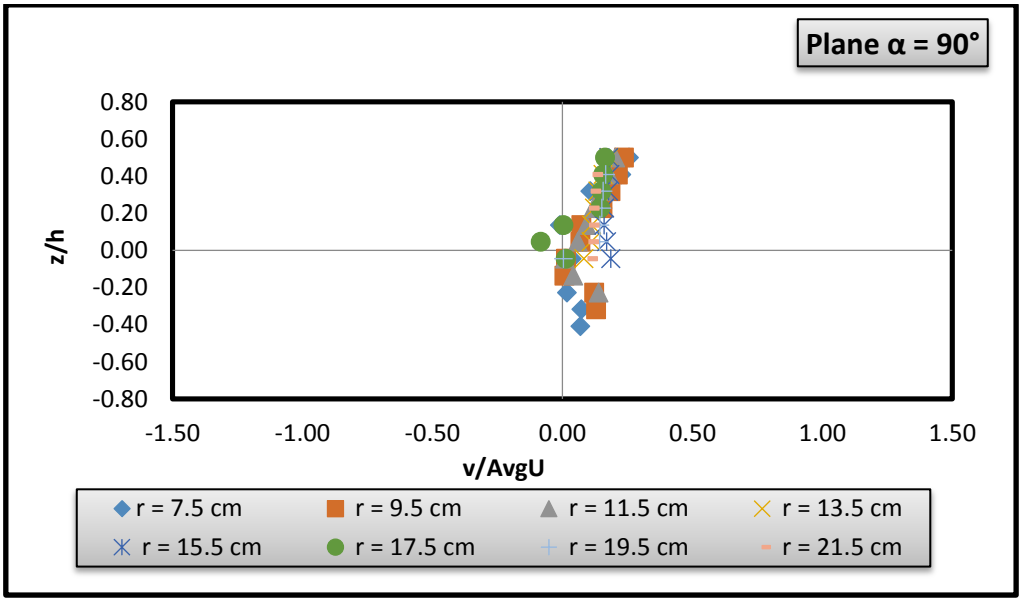

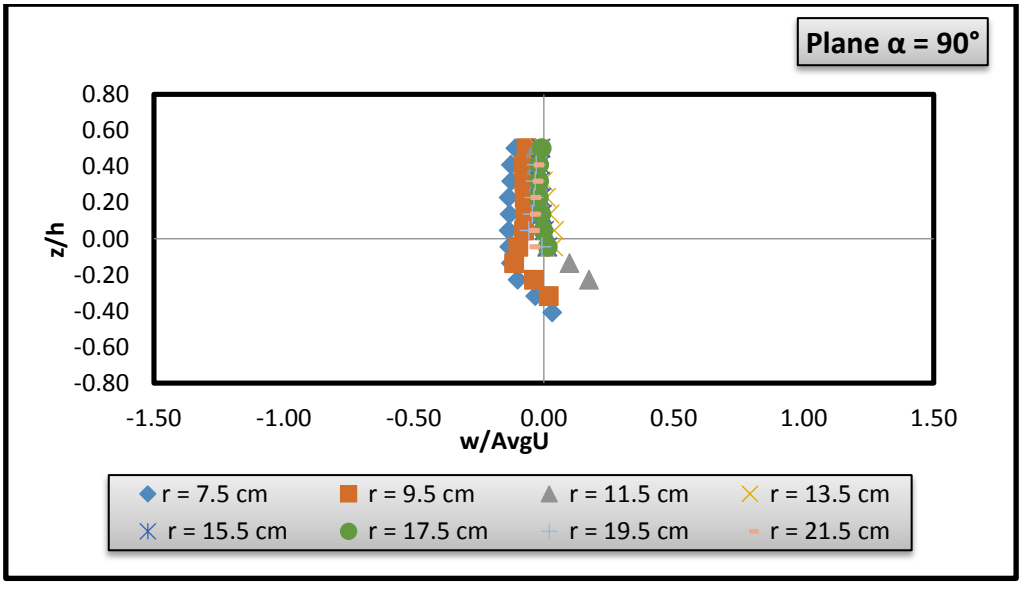

Fig 4.11 Normalized profiles of u, v and w measured in side stream of inclined pier (α = 90°).

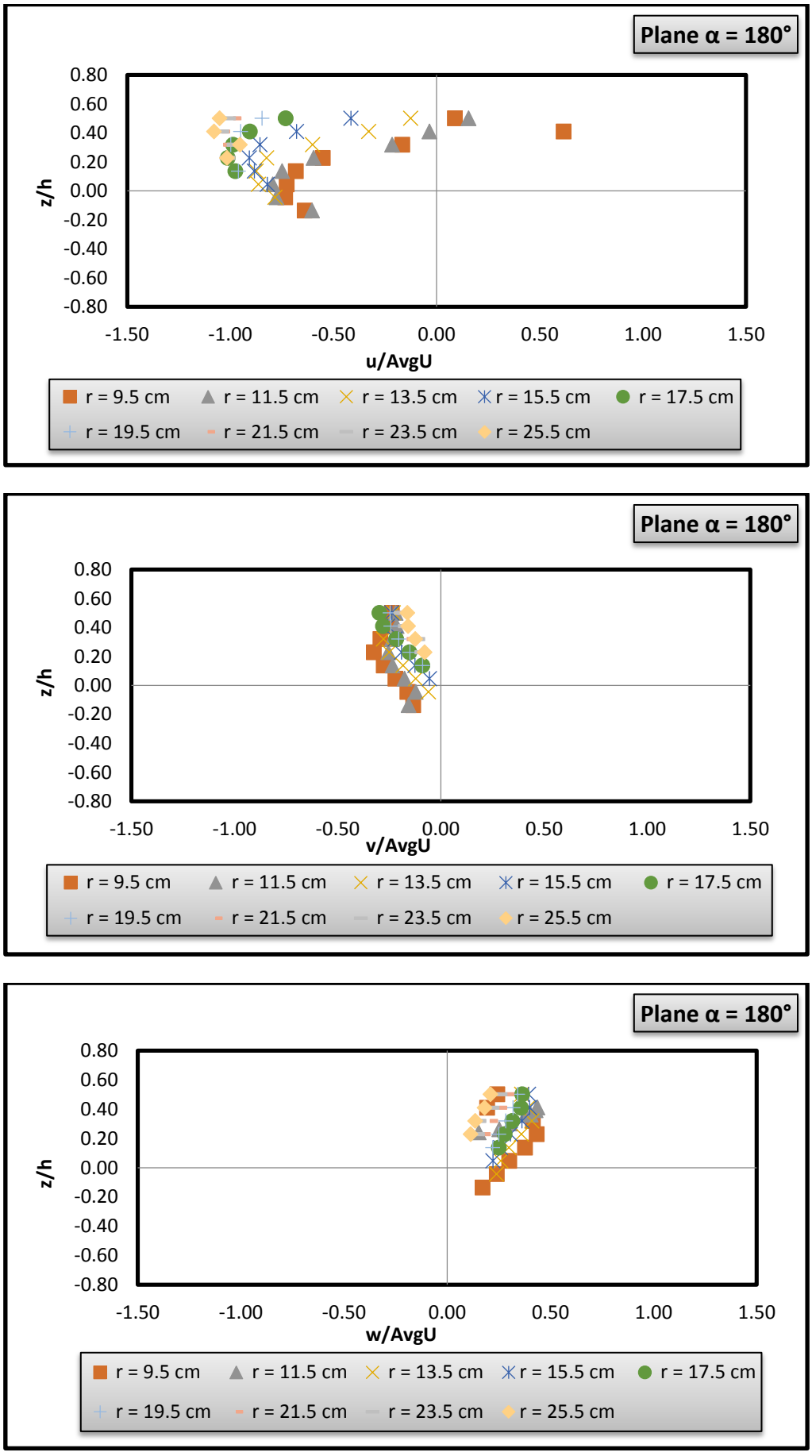

Fig 4.12 Normalized profiles of u, v and w measured in downstream of inclined pier (α = 180°).

4.3 Comparative study of velocity components

Here we have concerned with the comparative study of velocity components of vertical pier (setup 1) with the inclined pier (setup 2), in upstream of the piers(0°),in side stream of the piers (90°) and in downstream of the piers (180°) at various radial locations of 9.5 cm, 11.5 cm, 13.5 cm, and 15.5 cm. After comparison we come up with following points.

- **In upstream of piers**

1. Longitudinal component of velocity or u component has value approx. 90 % of avg.U at bed level or at the surface in setup 1 while in setup 2 it is around 70 % of avg.U.
2. It does not showing negative value or reversal of flow because we start taking readings at 9.5 cm due to inclination of pier, soffit of pier get touched with ADV sensors.
3. The maximum negative value of u is about 0.3 times of avg.U at the bottom of scour which get vanishes as we move away from the pier.
4. Latitude component of velocity or v component has very low value around 0.04 times of avg.U in setup 1 while in setup 2 it is upto 0.09 times of avg.U.
5. Vertical component of velocity or w component has maximum value at -0.3 depth of flow depth and it is strong in case of setup 2.

- **In side stream of piers**

1. u component of velocity in setup 2 with in scour is less than in setup 1.
2. v component of velocity in setup 1 is around 0.40 times avg.U and in setup 2 it is 0.24 times of avg.U.
3. w component of velocity is negative above bed level and positive in the bottom of scour hole in both setups and having greater value in setup 1.

- **In downstream of piers**

1. u component shows a reversal of flow near the water surface also far away from the pier and having its value greater in setup 2, normalized value around 0.88.
2. Far away from the pier u component is large as compared to its value near the pier but it still has a decreasing pattern close to the surface of flow.
3. v component in setup 1 is negative in scour hole and positive near to the surface of water while in setup 2 it has negative value everywhere.
4. w component is always positive showing upward flow in the wake region and having its greater value in setup 1 upto 0.50 times avg.U.

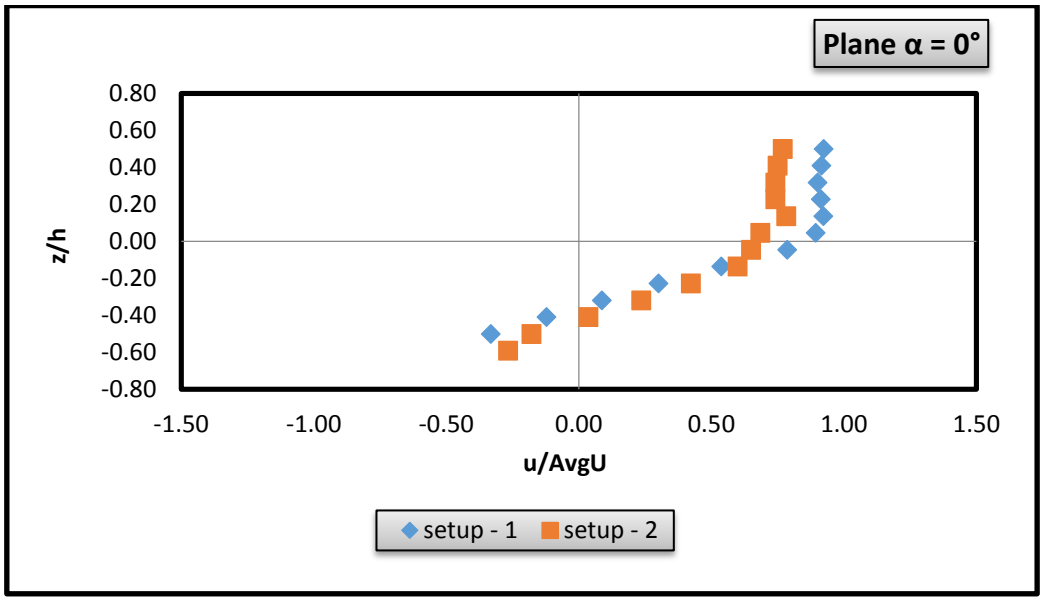

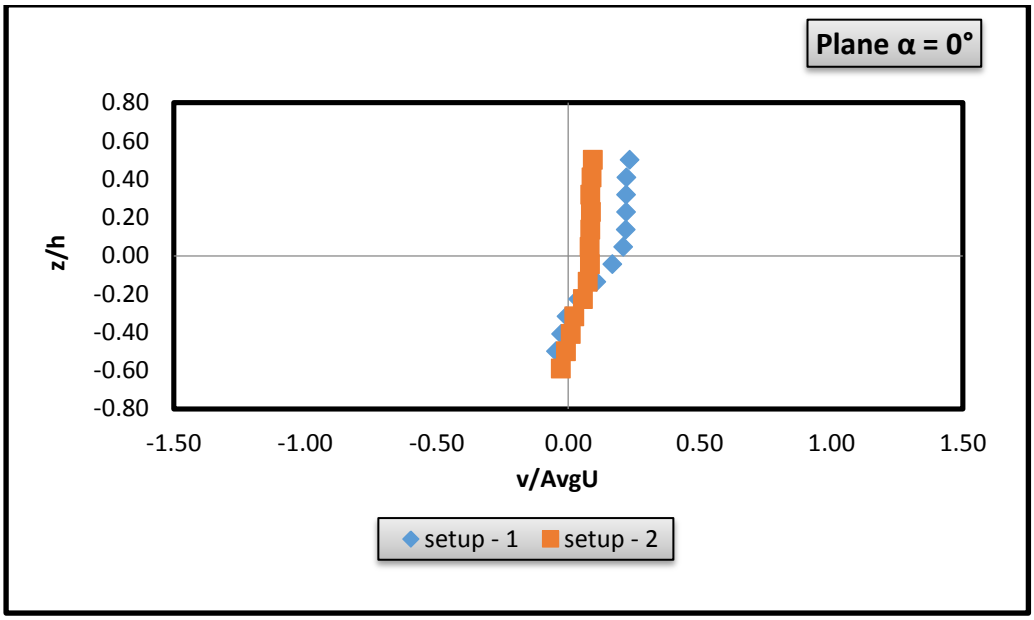

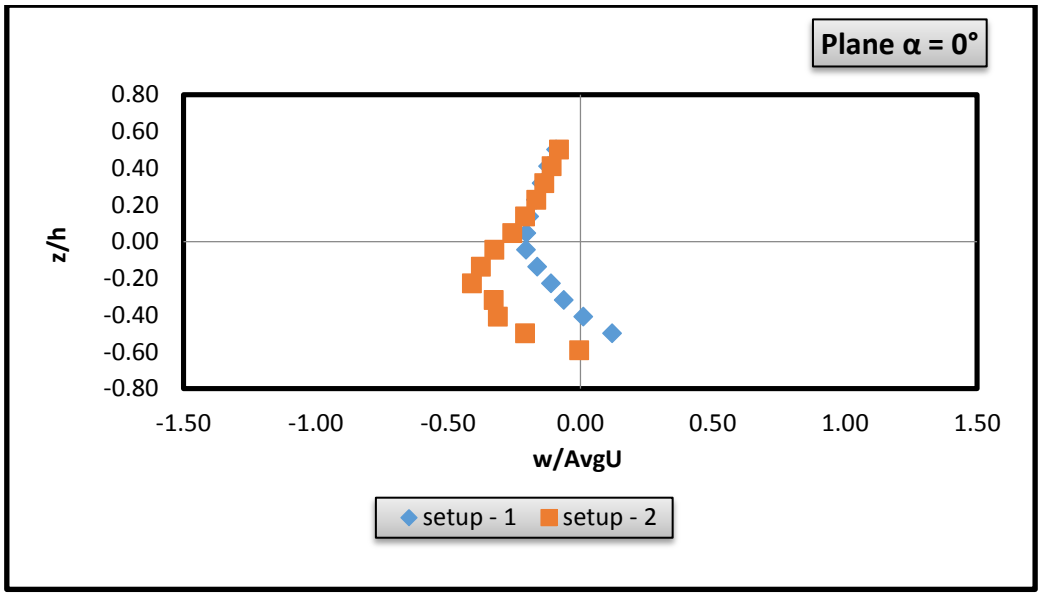

Fig 4.13 Comparison of normalized profiles of u, v and w measured in upstream of vertical and inclined pier (α = 0°) at r = 9.5 cm.

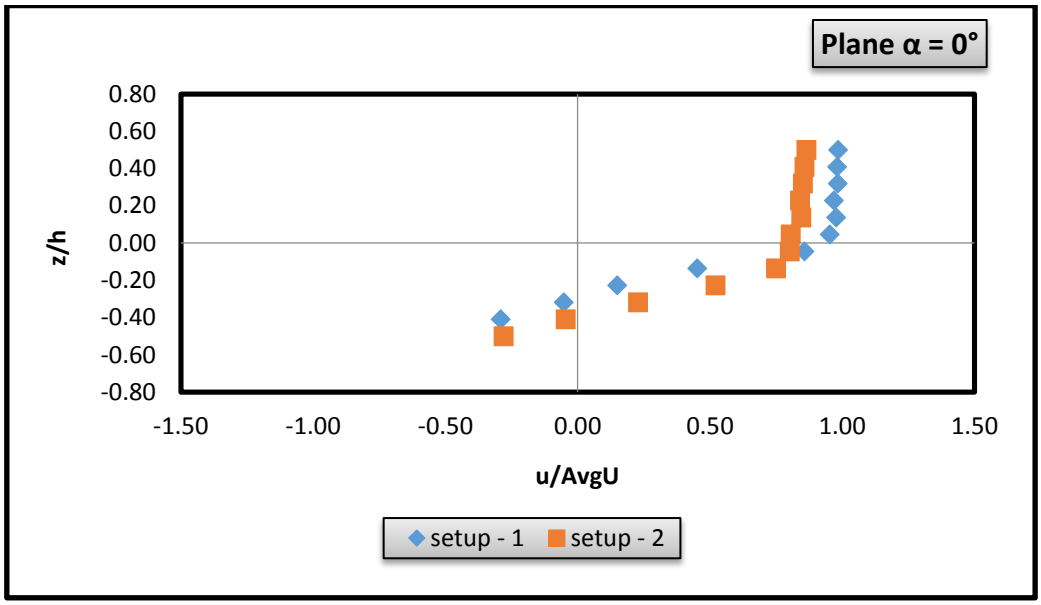

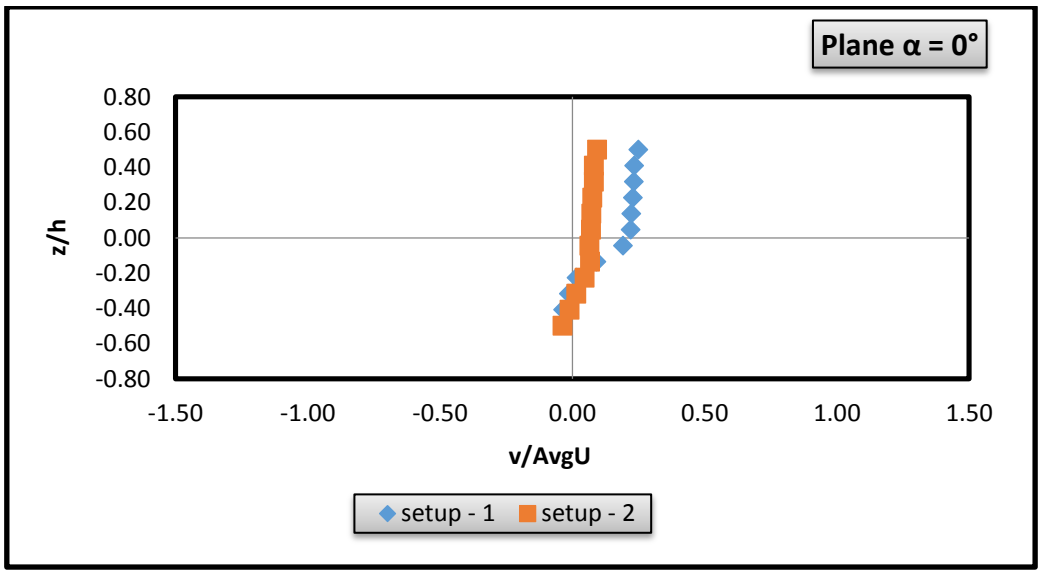

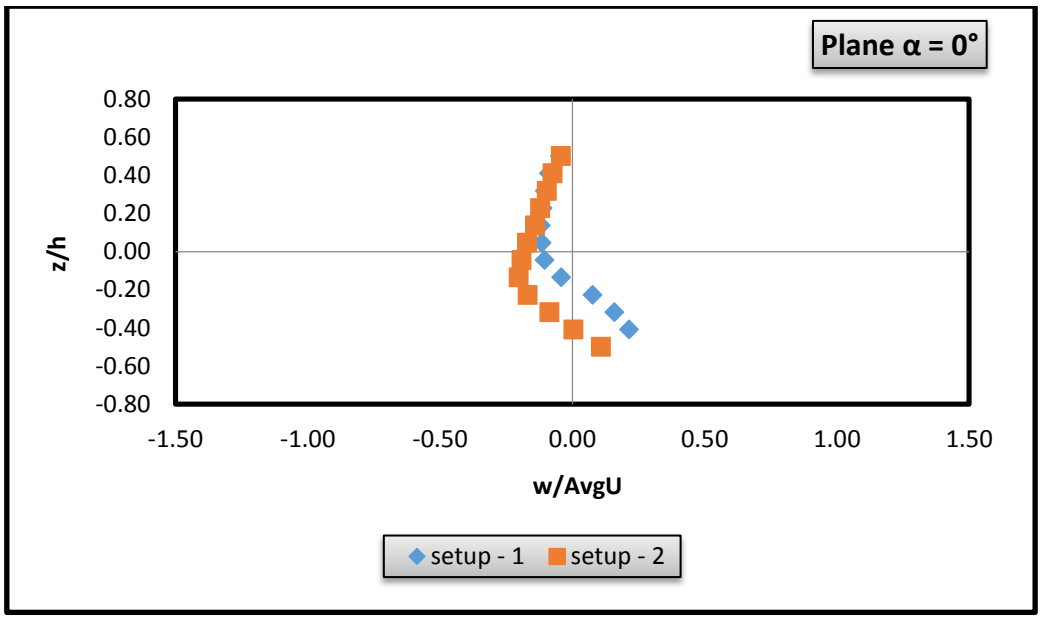

Fig 4.14 Comparison of normalized profiles of u, v and w measured in upstream of vertical and inclined pier (α = 0°) at r = 11.5 cm.

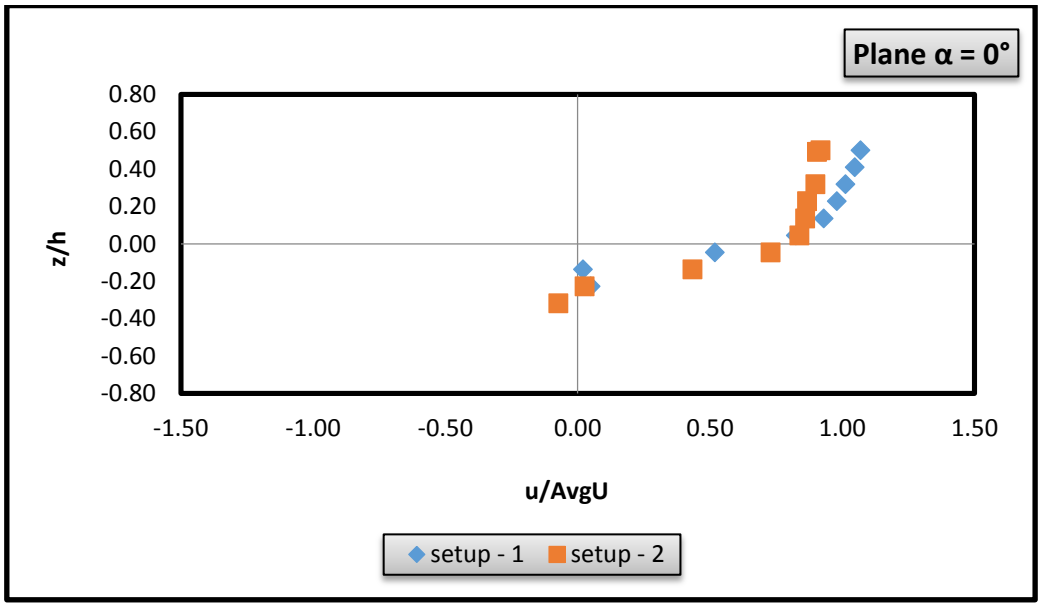

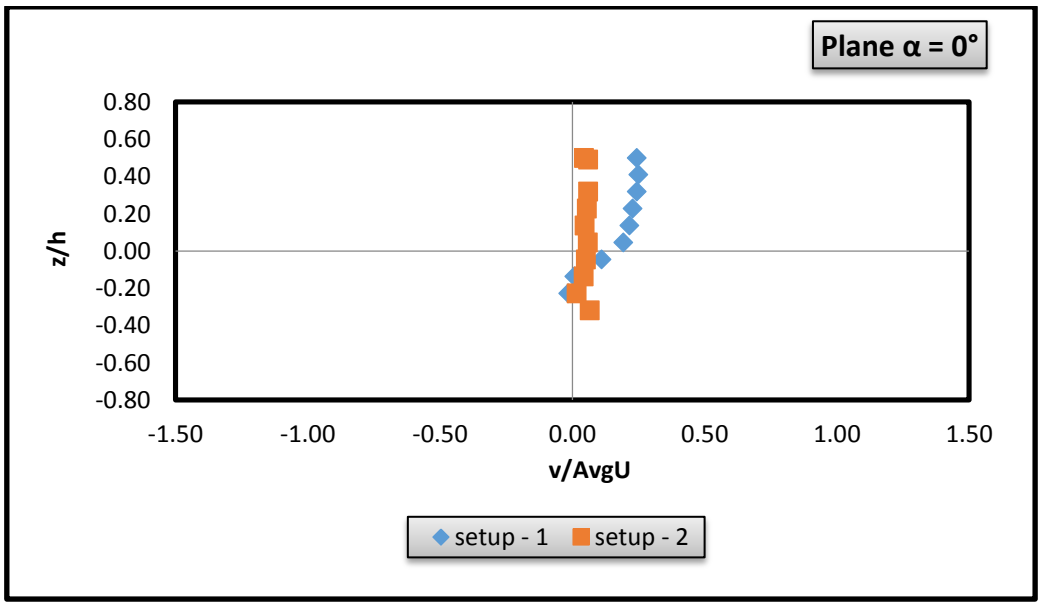

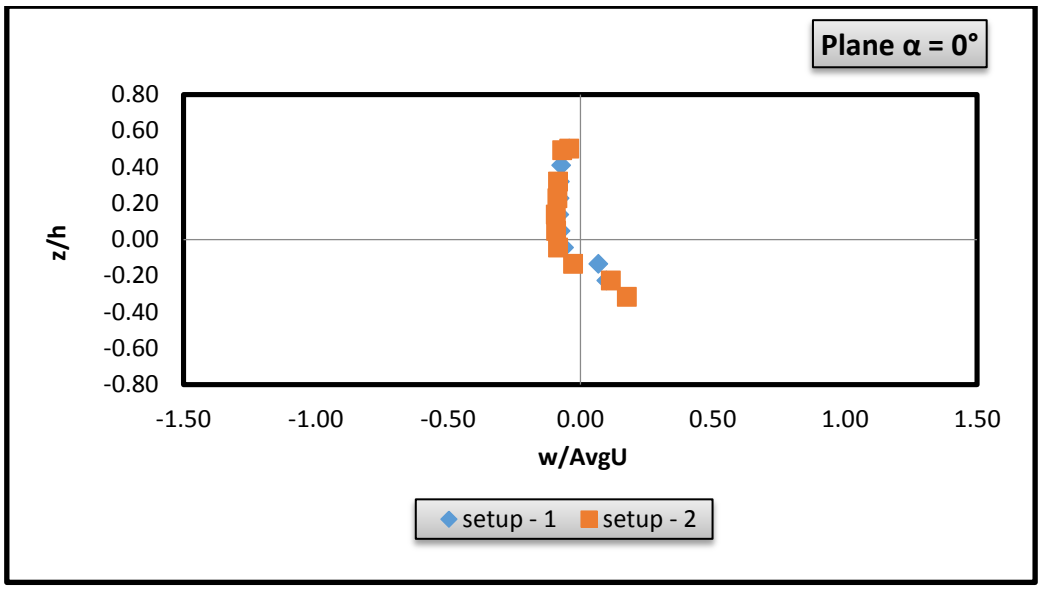

Fig 4.15 Comparison of normalized profiles of u, v and w measured in upstream of vertical and inclined pier (α = 0°) at r = 13.5 cm.

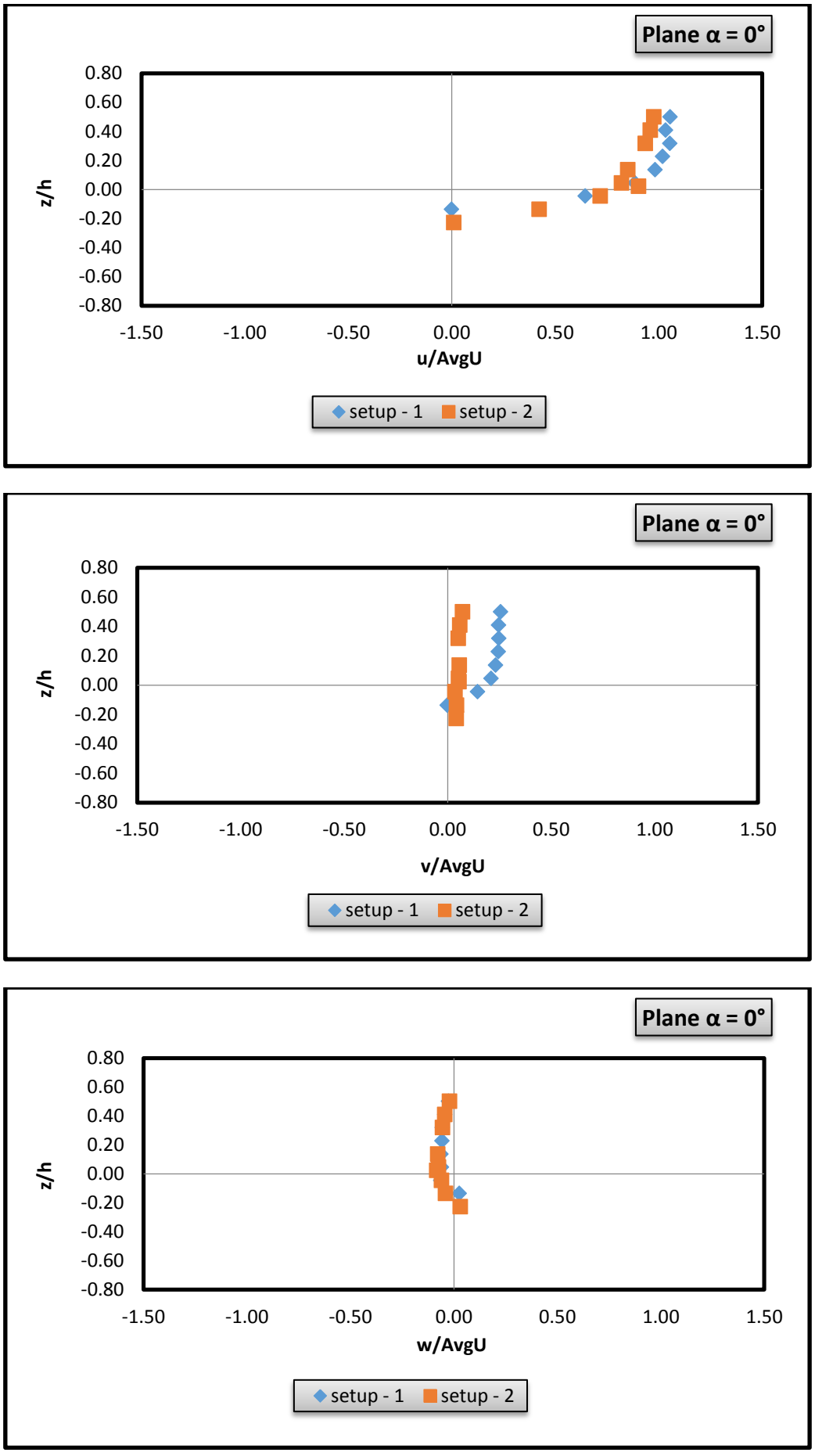

Fig 4.16 Comparison of normalized profiles of u, v and w measured in upstream of vertical and inclined pier (α = 0°) at r = 15.5 cm.

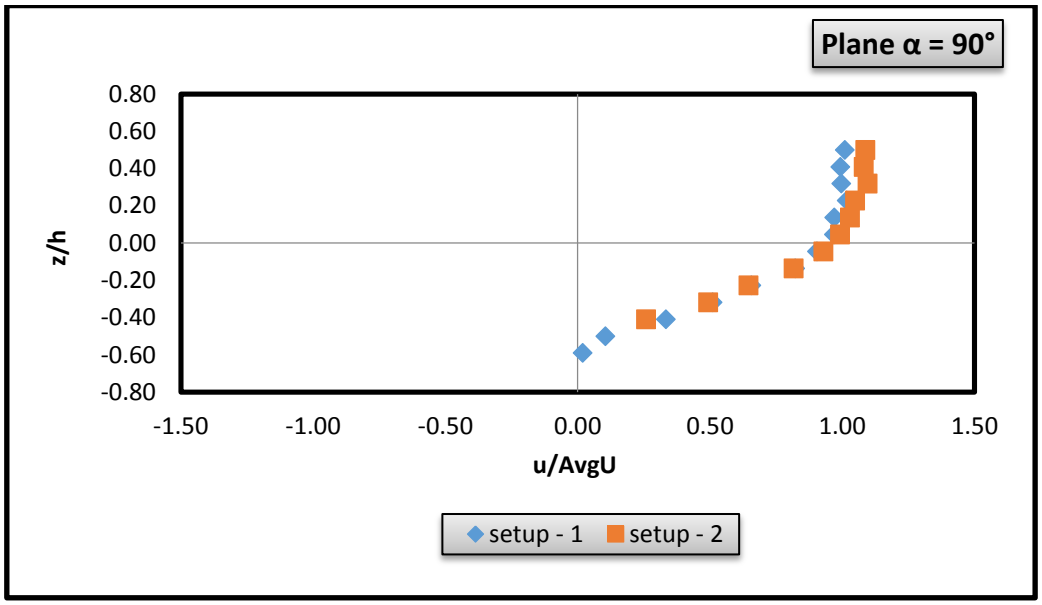

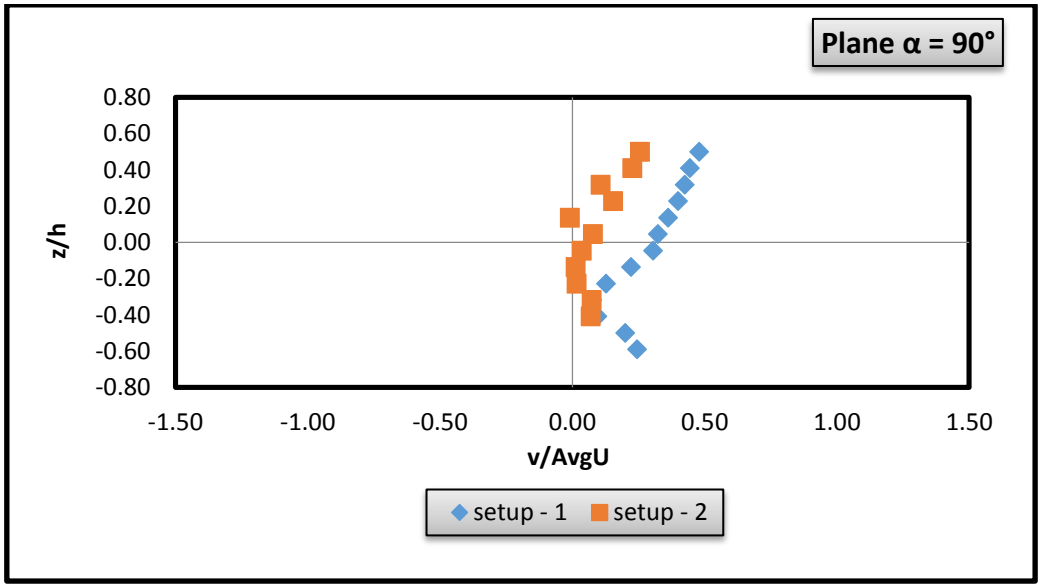

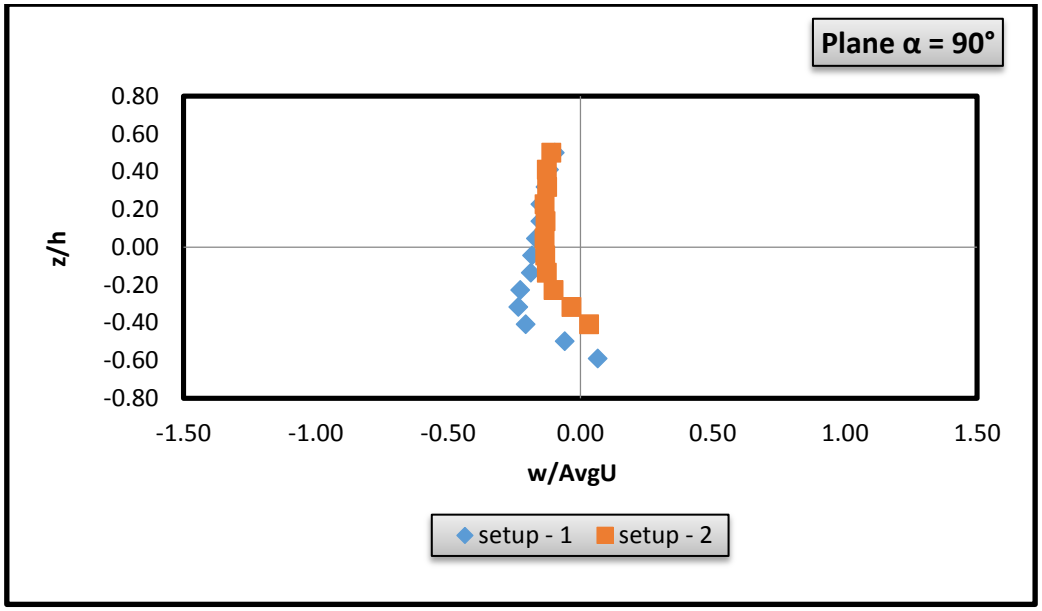

Fig 4.17 Comparison of normalized profiles of u, v and w measured in side stream of vertical and inclined pier (α = 90°) at r = 7.5 cm.

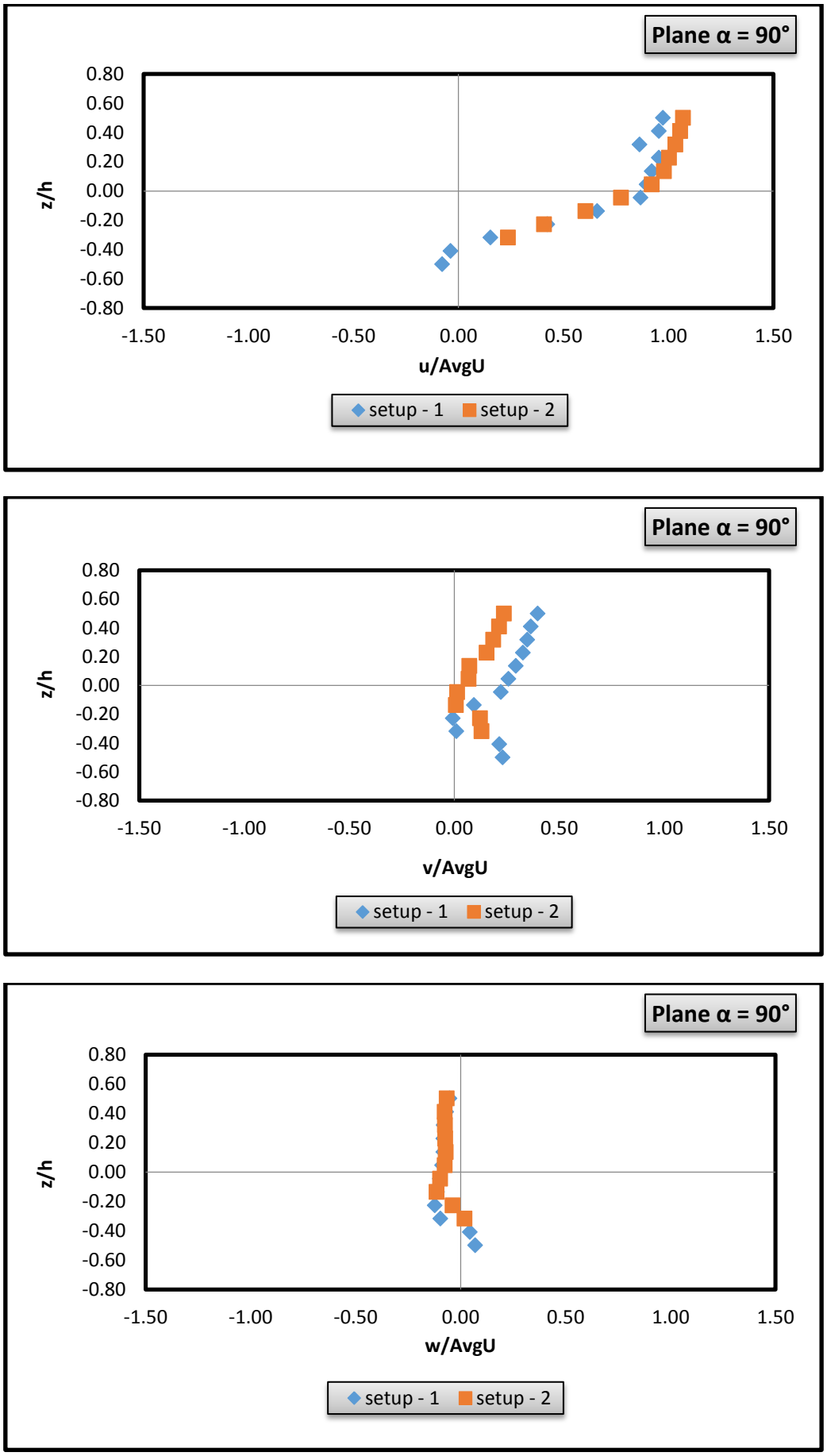

Fig 4.18 Comparison of normalized profiles of u, v and w measured in side stream of vertical and inclined pier (α = 90°) at r = 9.5 cm.

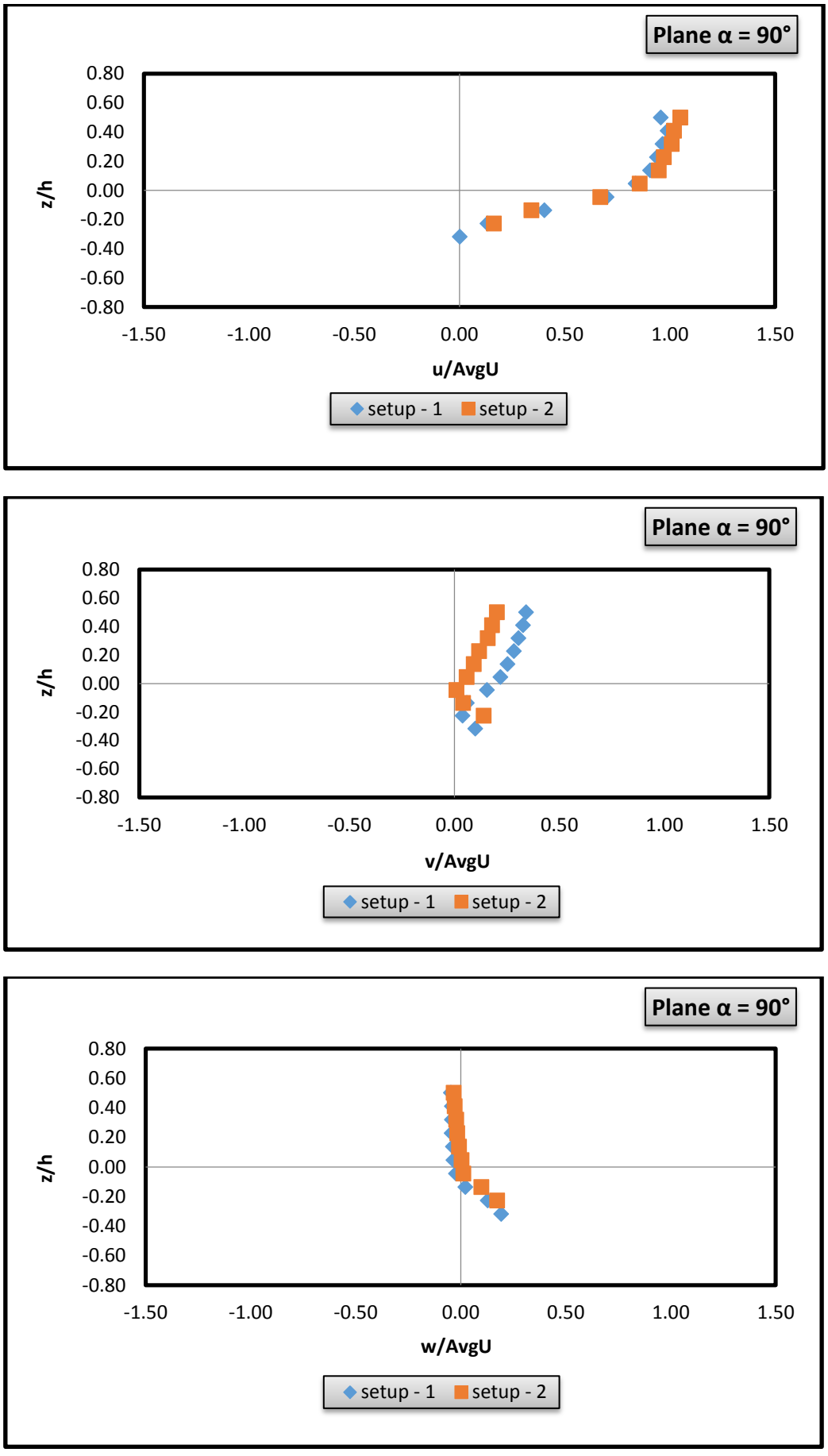

Fig 4.19 Comparison of normalized profiles of u, v and w measured in side stream of vertical and inclined pier (α = 90°) at r = 11.5 cm.

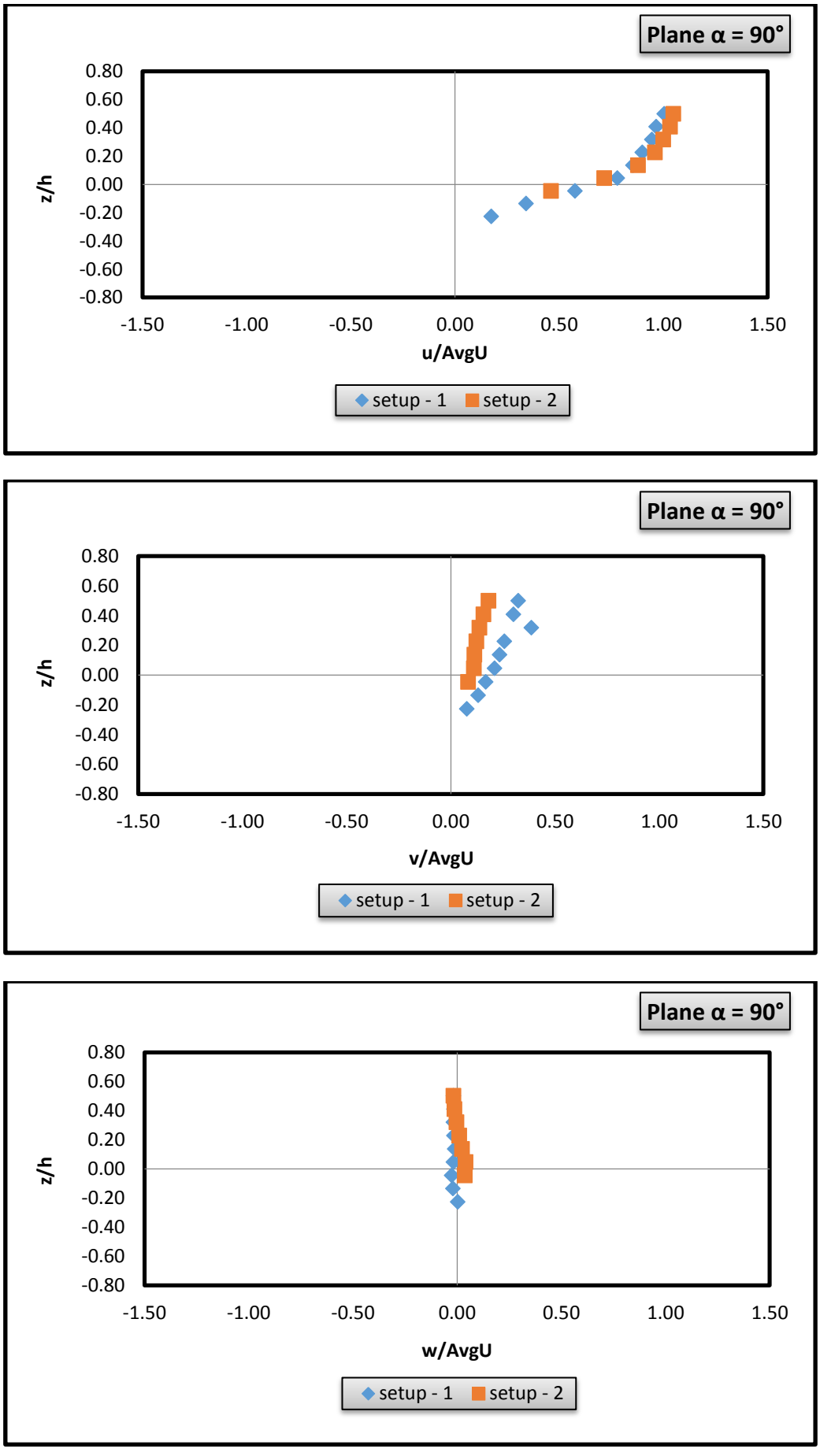

Fig 4.20 Comparison of normalized profiles of u, v and w measured in side stream of vertical and inclined pier (α = 90°) at r = 13.5 cm.

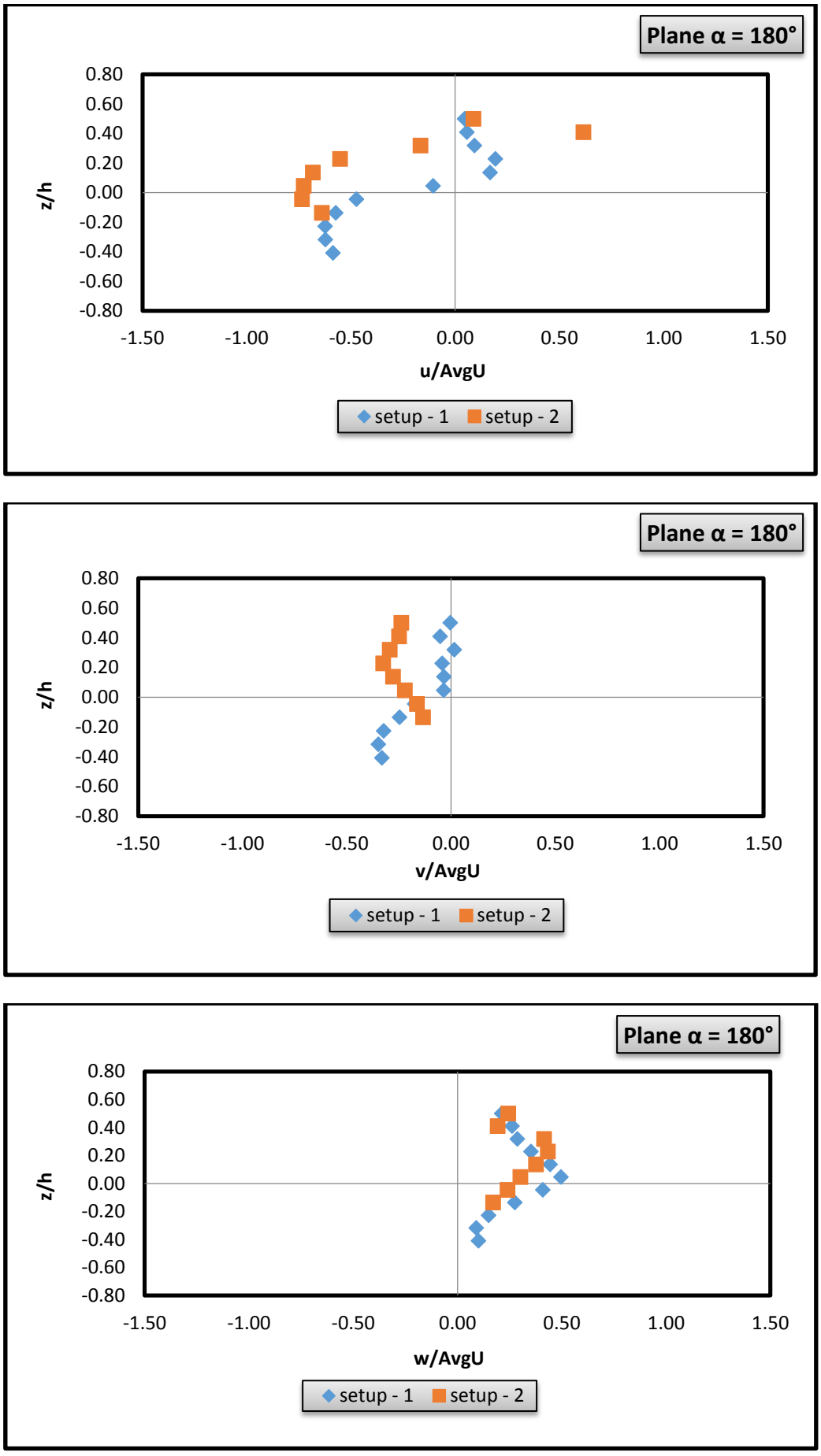

Fig 4.21 Comparison of normalized profiles of u, v and w measured in downstream of vertical and inclined pier (α = 180°) at r = 9.5 cm.

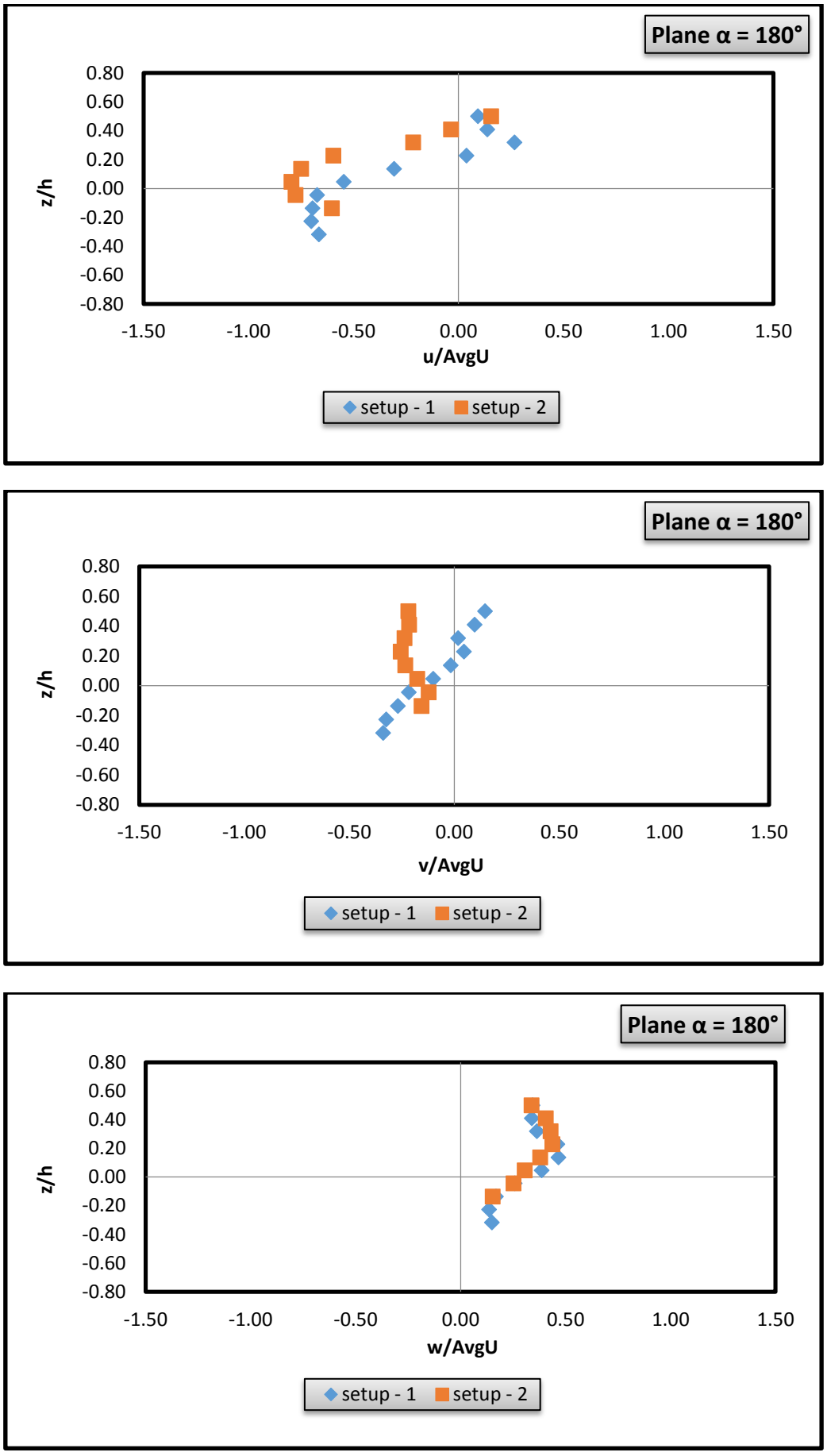

Fig 4.22 Comparison of normalized profiles of u, v and w measured in downstream of vertical and inclined pier (α = 180°) at r = 11.5 cm.

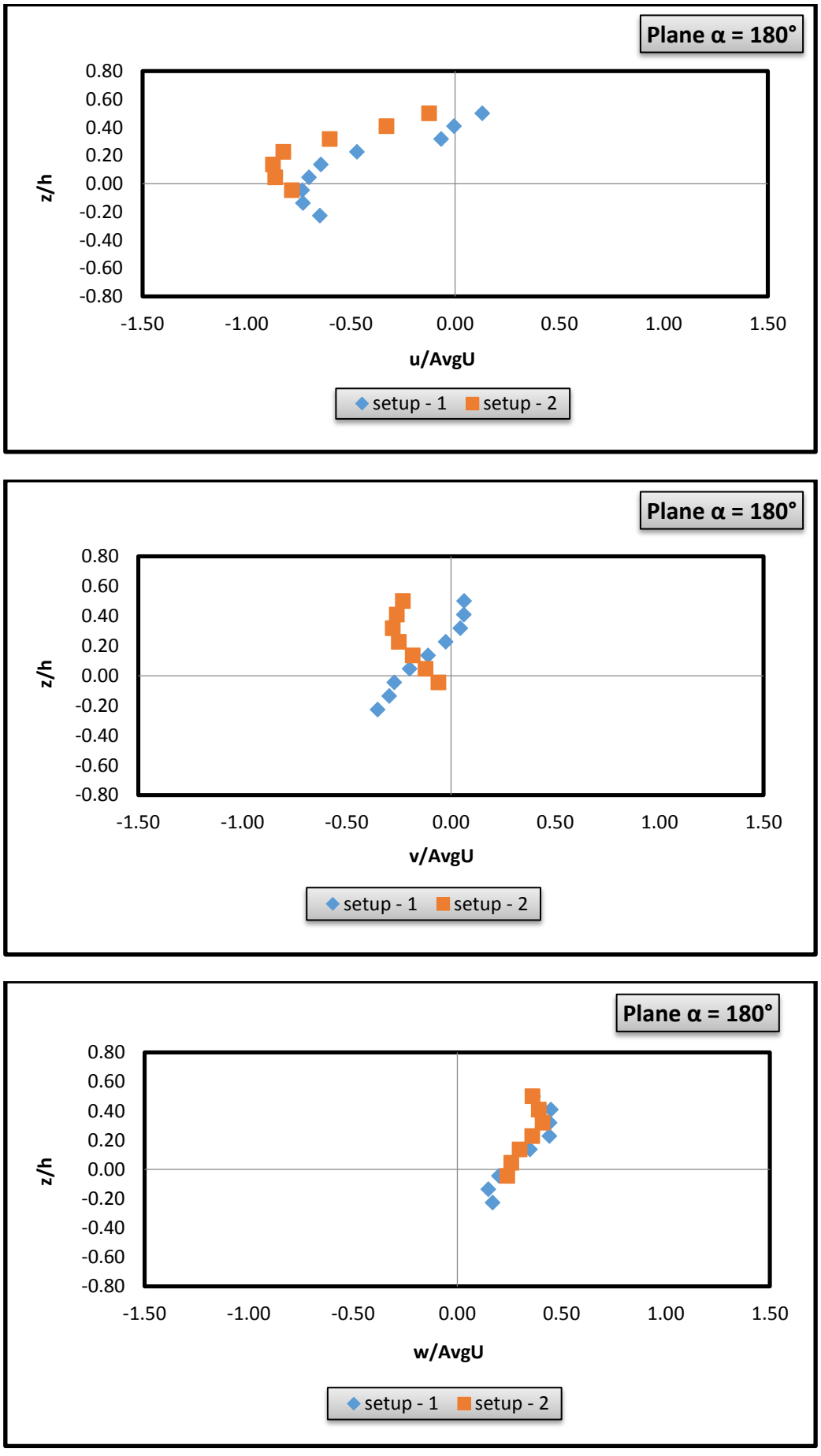

Fig 4.23 Comparison of normalized profiles of u, v and w measured in downstream of vertical and inclined pier (α = 180°) at r = 13.5 cm.

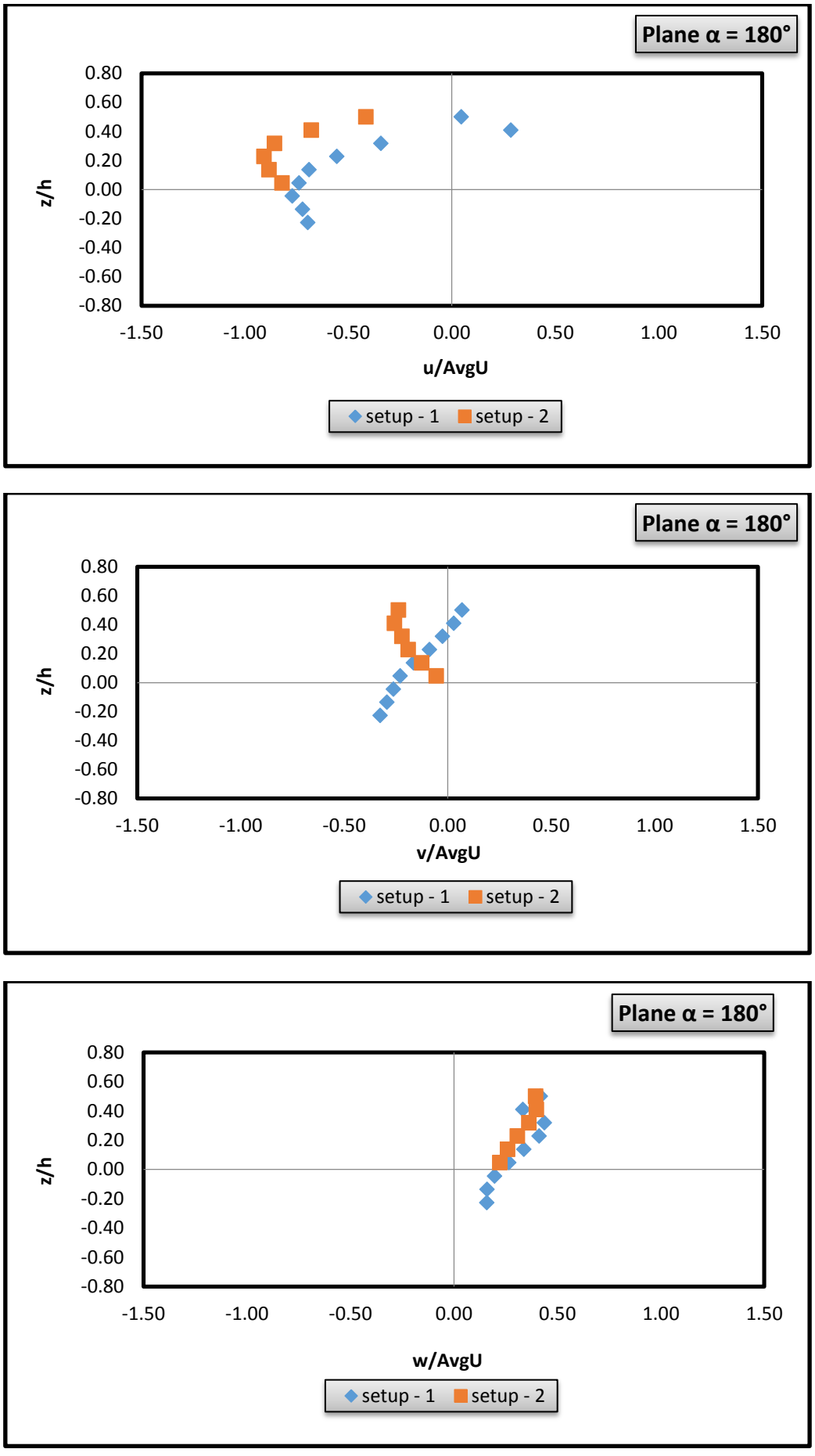

Fig 4.24 Comparison of normalized profiles of u, v and w measured in downstream of vertical and inclined pier (α = 180°) at r = 15.5 cm.

4.4 Turbulence Characteristics

The turbulence characteristics are represented by turbulence intensities ($\sqrt{\overline{u'u'}}$, $\sqrt{\overline{v'v'}}$, $\sqrt{\overline{w'w'}}$), Reynolds' stresses ($\overline{u'w'}$, $\overline{v'w'}$)of the flow. Where u' is the fluctuation of u component, v' is fluctuation of v component and w' is fluctuation of w component. The turbulence characteristics represented by turbulence intensities and Reynolds stresses of the flow in the upstream plane. The turbulence intensities are normalized using shear velocity u_* in the approach flow.

In the plane at α = 0° the turbulence intensities (particularly the vertical component $\sqrt{\overline{w'w'}}$ of turbulence intensity) show no significant change in the upper zone *i.e.* when $z > 0$ and their values decrease towards the water surface. However, there is an increase with z/h in the values of turbulence intensities within the scour hole. The longitudinal component of Reynolds' stress ($-\overline{u'w'}$) has positive values within the scour hole and near the bed. Also the longitudinal component $-\overline{u'w'}$ is dominant over transverse component $-\overline{v'w'}$ of Reynolds' stress.

In the planes at α = 30° and 60° the distribution of all the three components of turbulence intensity is similar as it was in the plane α = 0°. The magnitude of longitudinal component $-\overline{u'w'}$ of Reynolds' stress is slightly higher than the previous plane.

In the plane at α = 90°, all the three components of turbulence intensity show higher magnitude. Within the scoured region and below the general bed level the $-\overline{u'w'}$ component has large values in comparison to $-\overline{v'w'}$. Both components of Reynolds' stress have higher magnitude than that observed in other planes.

In the plane at α = 120° approaching to the pier, within the scoured region and below the general bed level ($z < 0$), the magnitudes of all the components of turbulence intensity are higher than those in the planes upstream to this. However trend of the variation is similar. Above the general bed level and far away from the scoured region, the profile of turbulence intensity and Reynolds' stress components exhibit similar magnitudes.

In the downstream plane when α = 180°, the turbulence is seen to be more strong as compared to that in the plane upstream of the pier. Close to the pier, the magnitudes of the three components of turbulence intensity are almost two times of the corresponding values in the plane at α = 0°. As the flow moves away from the pier, the turbulence intensities are seen to decrease. The stress components $\overline{u'w'}$ and $\overline{v'w'}$ however show no conclusive trend, still their magnitudes are much higher than those in the plane at α = 0°. The direction of stress components is opposite to that in the plane at α = 0° and these are more staggered here indicating the presence of larger turbulence in the wake region.

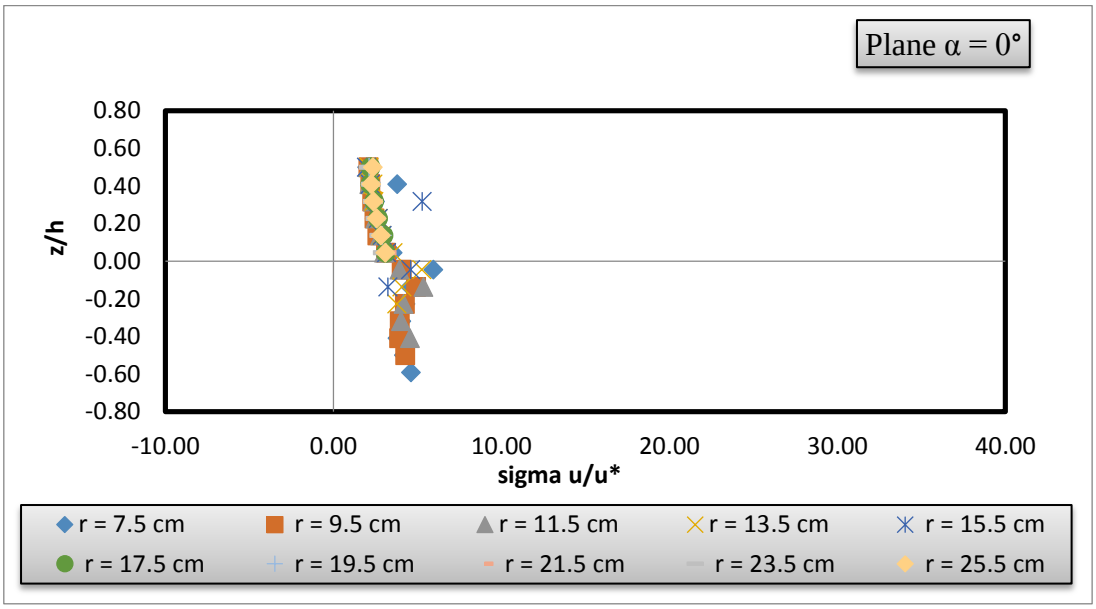
Plane α = 0°
0.80
0.60
0.40
0.20
0.00
-0.20
-0.40
-0.60
-0.80
z/h
-10.00
0.00
10.00
20.00
30.00
40.00
sigma u/u*
r = 7.5 cm
r = 9.5 cm
r = 11.5 cm
r = 13.5 cm
r = 15.5 cm
r = 17.5 cm
r = 19.5 cm
r = 21.5 cm
r = 23.5 cm
r = 25.5 cm

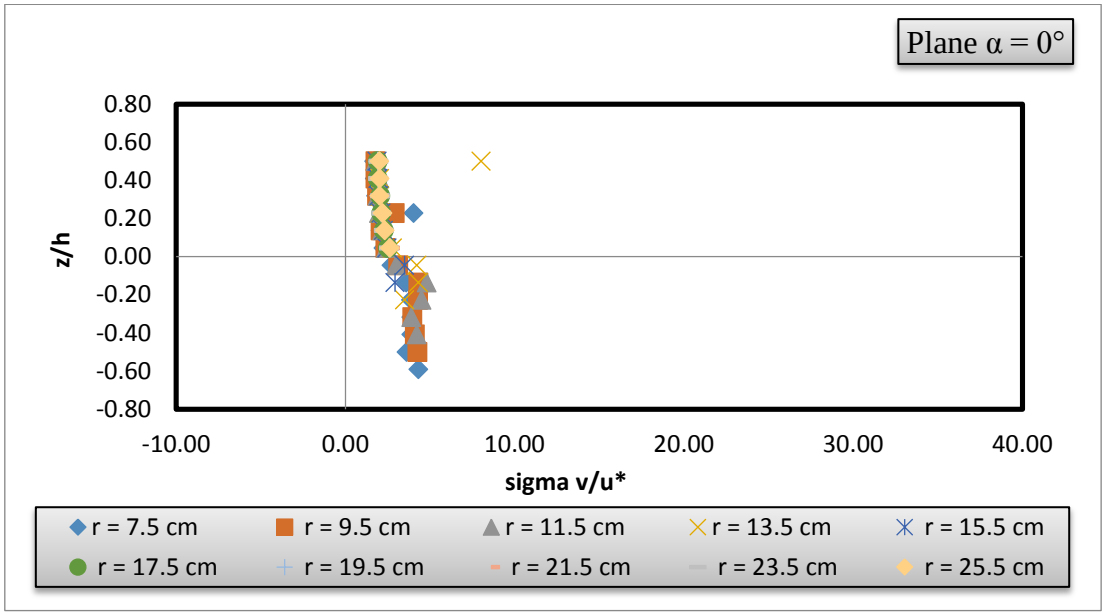
Plane α = 0°
0.80
0.60
0.40
0.20
0.00
-0.20
-0.40
-0.60
-0.80
z/h
-10.00
0.00
10.00
20.00
30.00
40.00
sigma v/u*
r = 7.5 cm
r = 9.5 cm
r = 11.5 cm
r = 13.5 cm
r = 15.5 cm
r = 17.5 cm
r = 19.5 cm
r = 21.5 cm
r = 23.5 cm
r = 25.5 cm

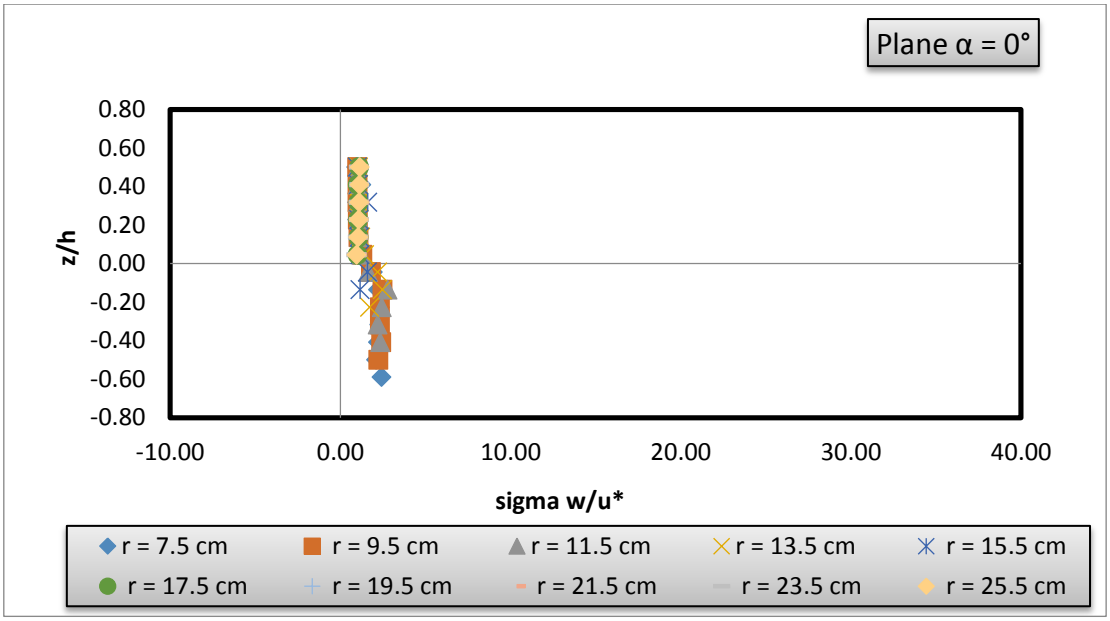
Plane α = 0°
0.80
0.60
0.40
0.20
0.00
-0.20
-0.40
-0.60
-0.80
z/h
-10.00
0.00
10.00
20.00
30.00
40.00
sigma w/u*
r = 7.5 cm
r = 9.5 cm
r = 11.5 cm
r = 13.5 cm
r = 15.5 cm
r = 17.5 cm
r = 19.5 cm
r = 21.5 cm
r = 23.5 cm
r = 25.5 cm

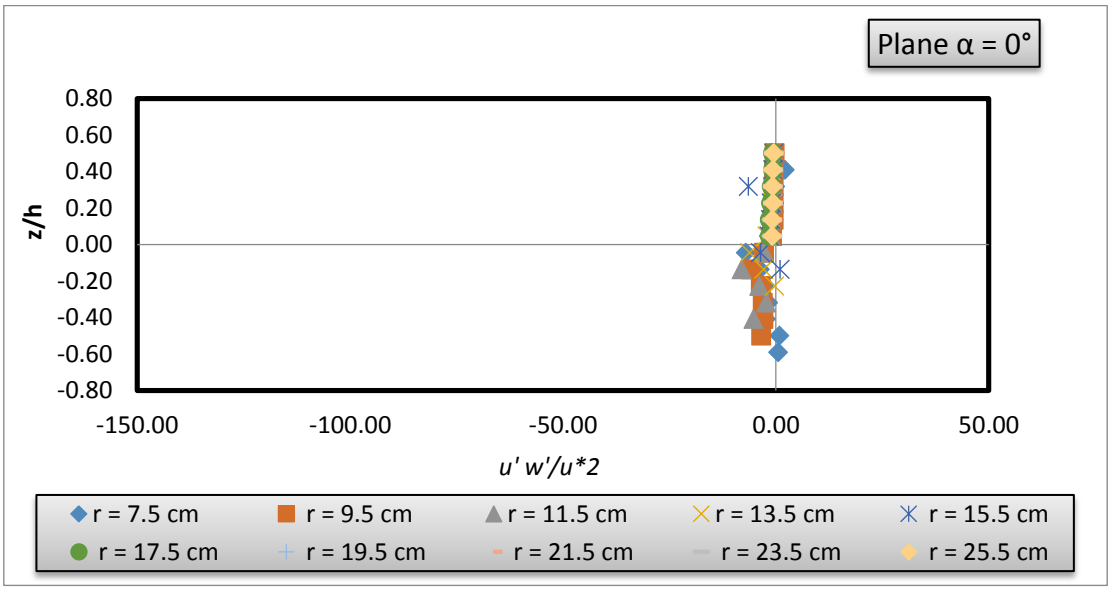

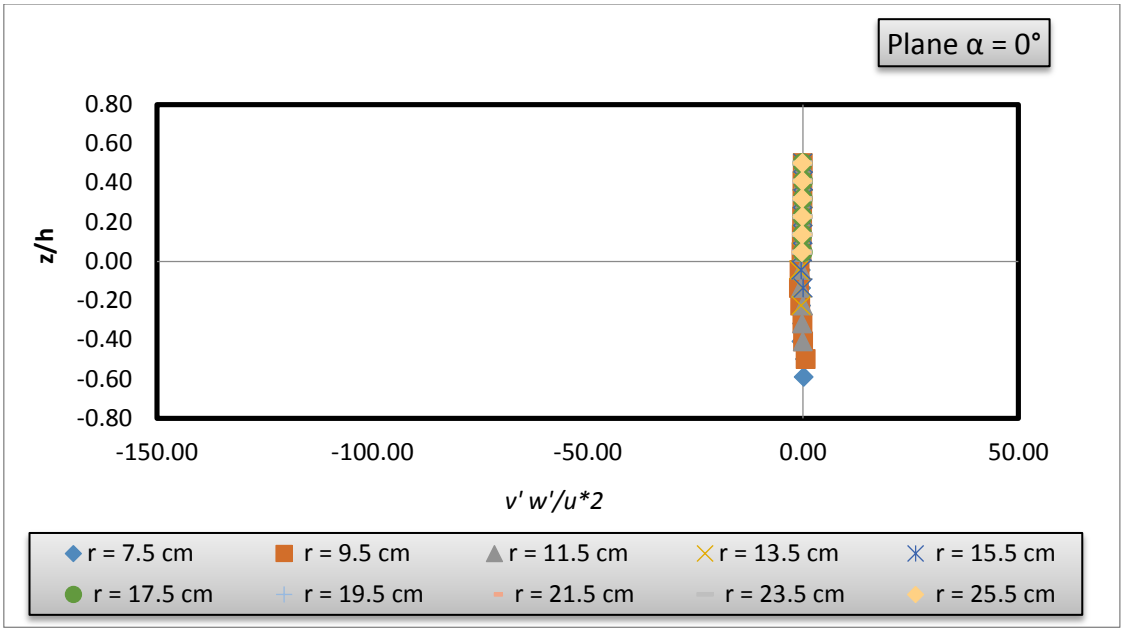

Fig 4.25 Distribution of normalized turbulence intensities and Reynolds stresses in upstream of vertical pier (α = 0°).

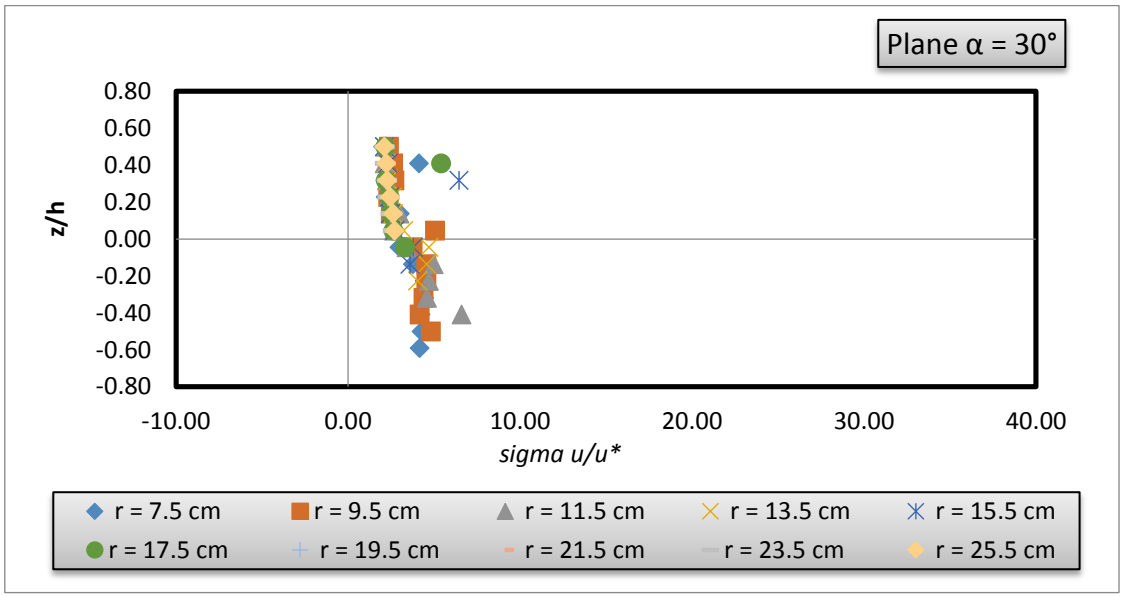
Plane α = 30°
0.80
0.60
0.40
0.20
0.00
-0.20
-0.40
-0.60
-0.80
z/h
-10.00
0.00
10.00
20.00
30.00
40.00
sigma u/u*
r = 7.5 cm
r = 9.5 cm
r = 11.5 cm
r = 13.5 cm
r = 15.5 cm
r = 17.5 cm
r = 19.5 cm
r = 21.5 cm
r = 23.5 cm
r = 25.5 cm

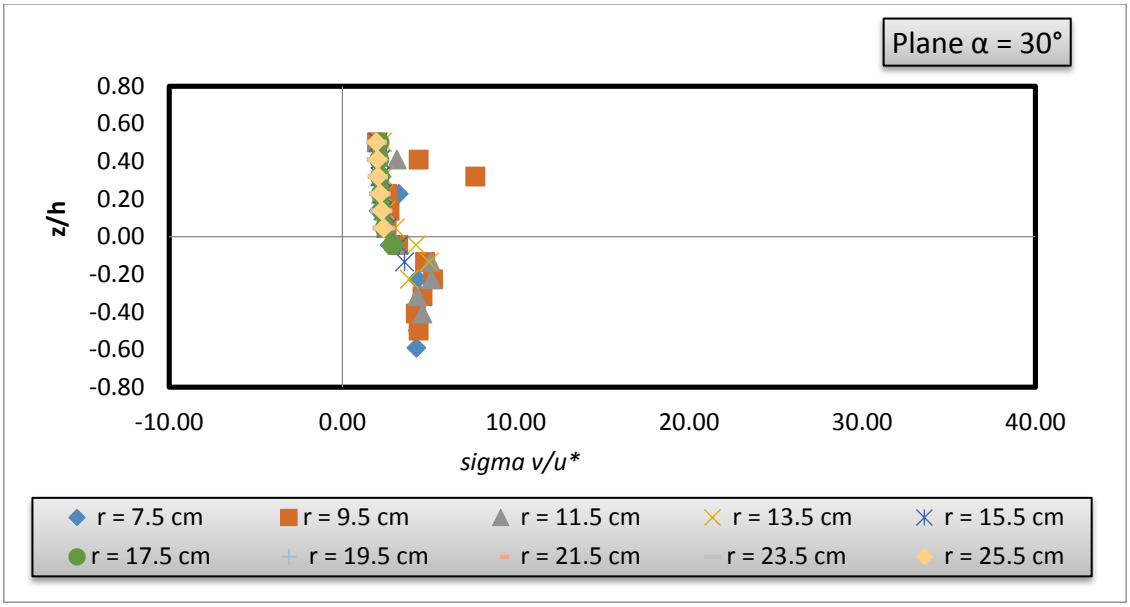
Plane α = 30°
0.80
0.60
0.40
0.20
0.00
-0.20
-0.40
-0.60
-0.80
z/h
-10.00
0.00
10.00
20.00
30.00
40.00
sigma v/u*
r = 7.5 cm
r = 9.5 cm
r = 11.5 cm
r = 13.5 cm
r = 15.5 cm
r = 17.5 cm
r = 19.5 cm
r = 21.5 cm
r = 23.5 cm
r = 25.5 cm

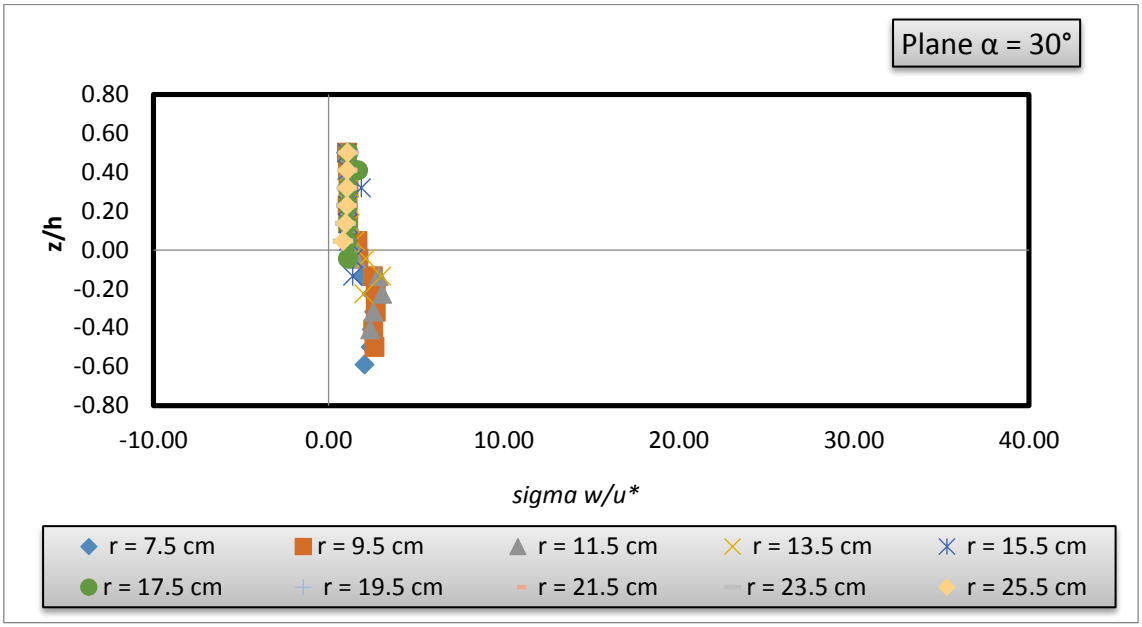
Plane α = 30°
0.80
0.60
0.40
0.20
0.00
-0.20
-0.40
-0.60
-0.80
z/h
-10.00
0.00
10.00
20.00
30.00
40.00
sigma w/u*
r = 7.5 cm
r = 9.5 cm
r = 11.5 cm
r = 13.5 cm
r = 15.5 cm
r = 17.5 cm
r = 19.5 cm
r = 21.5 cm
r = 23.5 cm
r = 25.5 cm

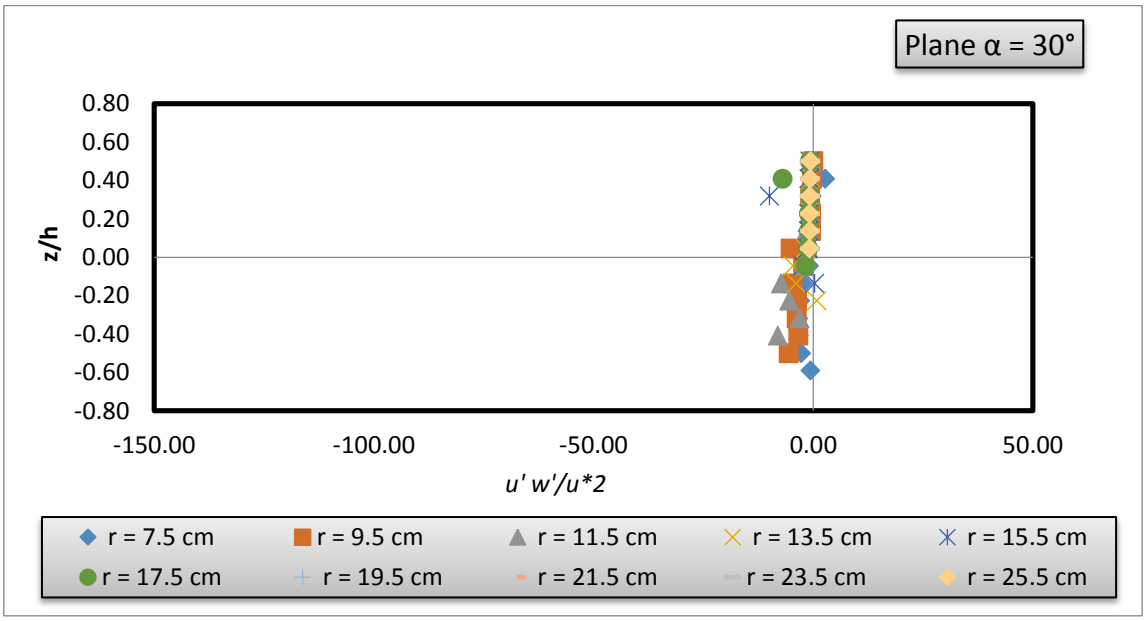

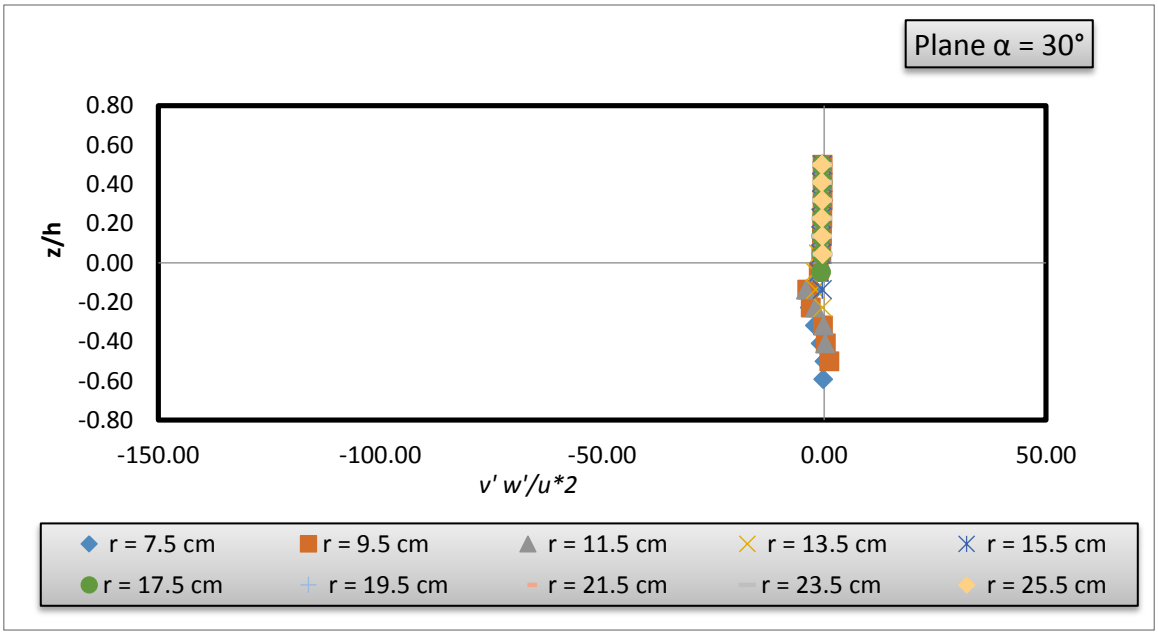

Fig 4.26 Distribution of normalized turbulence intensities and Reynolds stresses in upstream of vertical pier (α =30°).

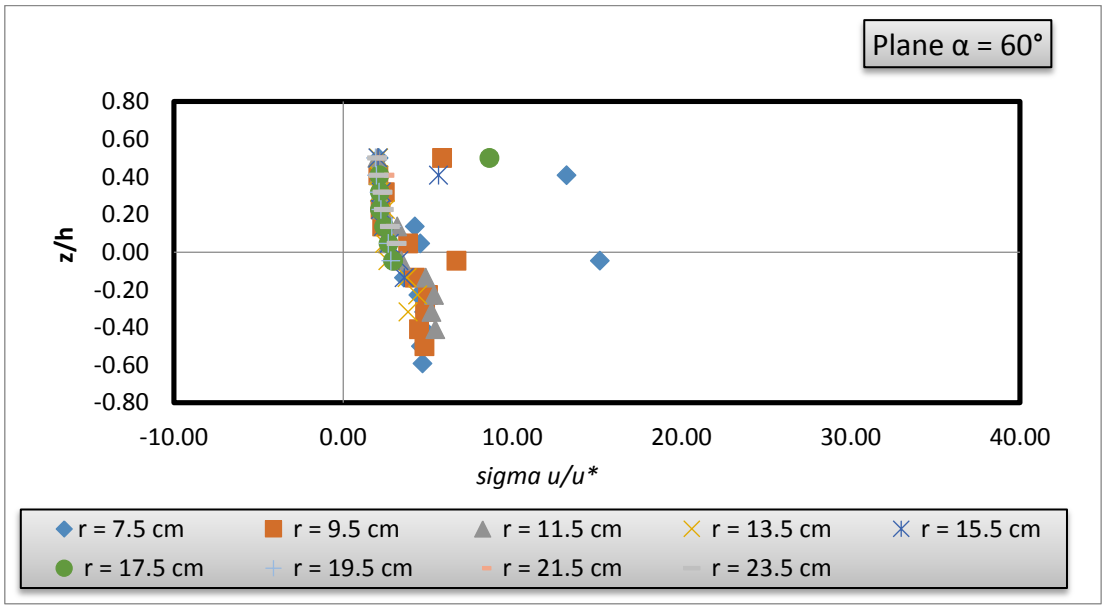
Plane α = 60°
0.80
0.60
0.40
0.20
0.00
-0.20
-0.40
-0.60
-0.80
z/h
-10.00
0.00
10.00
20.00
30.00
40.00
sigma u/u*
r = 7.5 cm
r = 9.5 cm
r = 11.5 cm
r = 13.5 cm
r = 15.5 cm
r = 17.5 cm
r = 19.5 cm
r = 21.5 cm
r = 23.5 cm

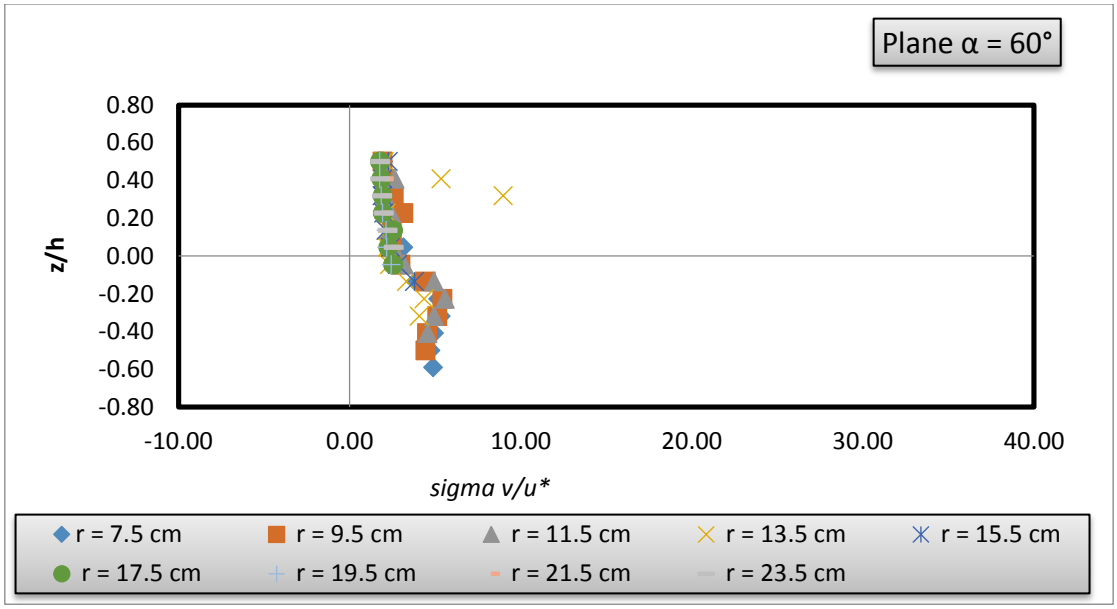
Plane α = 60°
0.80
0.60
0.40
0.20
0.00
-0.20
-0.40
-0.60
-0.80
z/h
-10.00
0.00
10.00
20.00
30.00
40.00
sigma v/u*
r = 7.5 cm
r = 9.5 cm
r = 11.5 cm
r = 13.5 cm
r = 15.5 cm
r = 17.5 cm
r = 19.5 cm
r = 21.5 cm
r = 23.5 cm

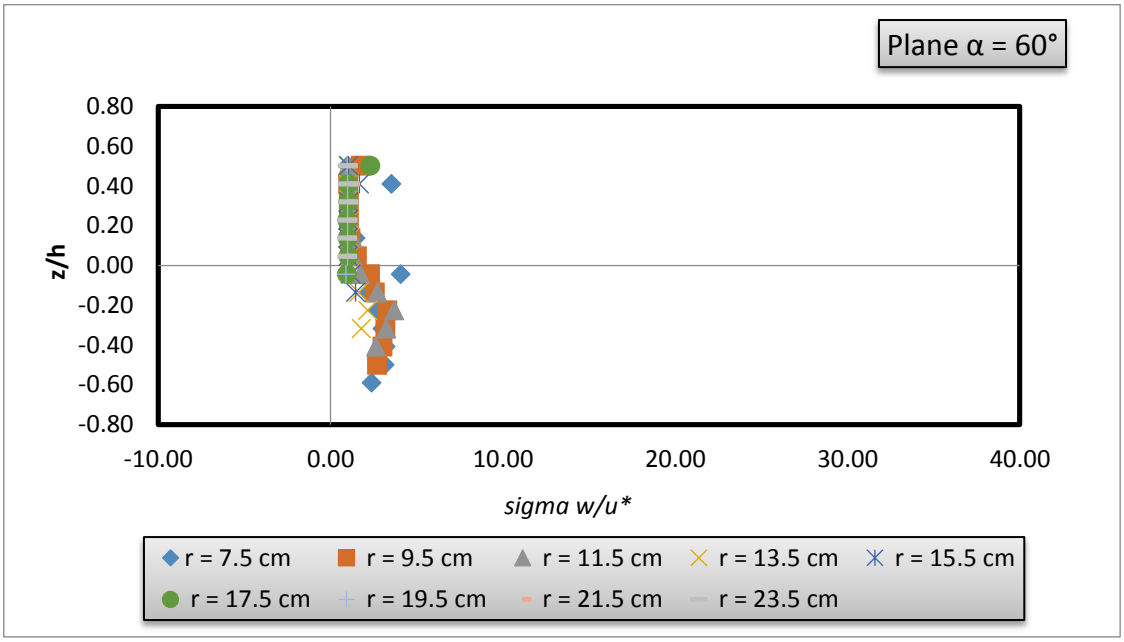
Plane α = 60°
0.80
0.60
0.40
0.20
0.00
-0.20
-0.40
-0.60
-0.80
z/h
-10.00
0.00
10.00
20.00
30.00
40.00
sigma w/u*
r = 7.5 cm
r = 9.5 cm
r = 11.5 cm
r = 13.5 cm
r = 15.5 cm
r = 17.5 cm
r = 19.5 cm
r = 21.5 cm
r = 23.5 cm

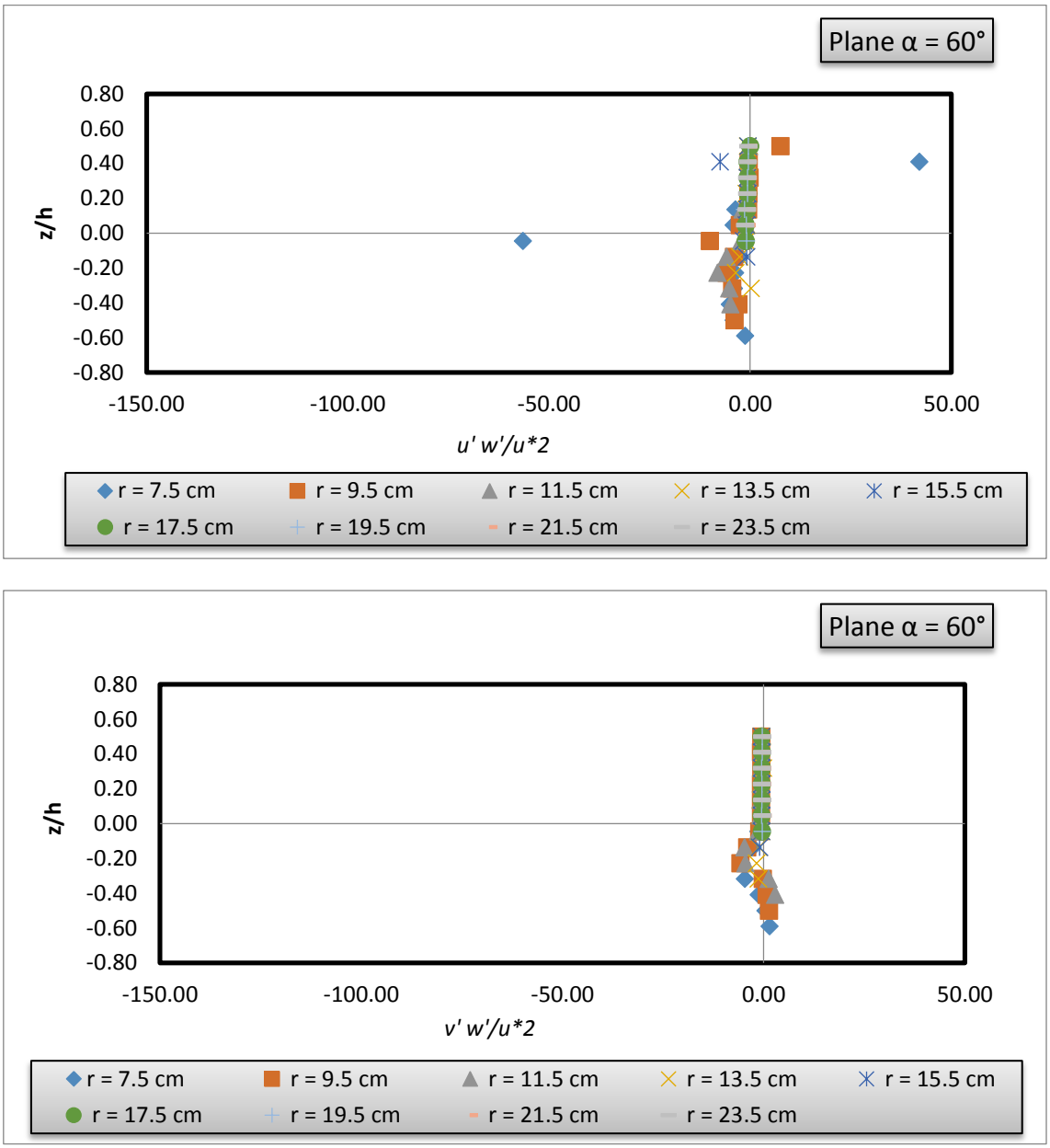

Fig 4.27 Distribution of normalized turbulence intensities and Reynolds stresses in upstream of vertical pier (α =60°).

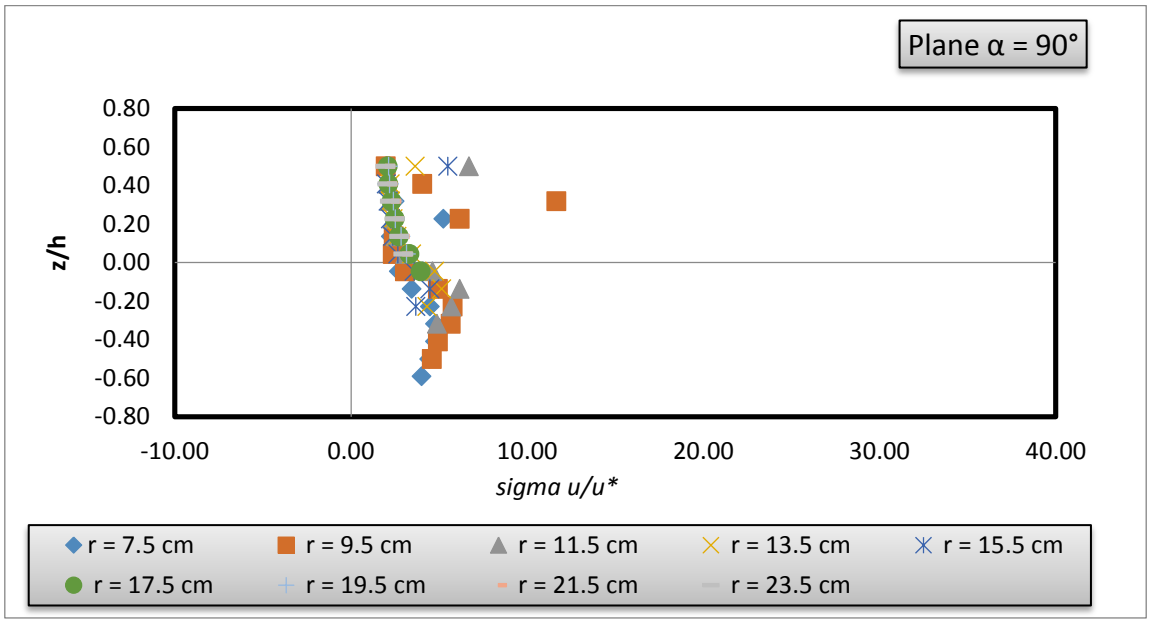
Plane α = 90°
0.80
0.60
0.40
0.20
0.00
-0.20
-0.40
-0.60
-0.80
z/h
-10.00
0.00
10.00
20.00
30.00
40.00
sigma u/u*
r = 7.5 cm
r = 9.5 cm
r = 11.5 cm
r = 13.5 cm
r = 15.5 cm
r = 17.5 cm
r = 19.5 cm
r = 21.5 cm
r = 23.5 cm

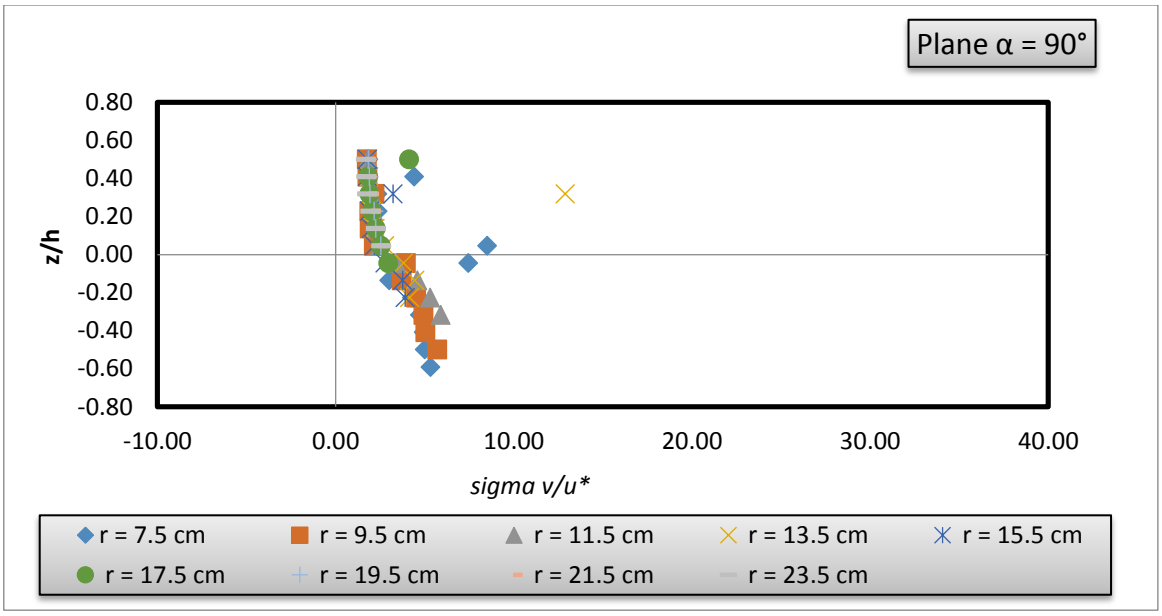
Plane α = 90°
0.80
0.60
0.40
0.20
0.00
-0.20
-0.40
-0.60
-0.80
z/h
-10.00
0.00
10.00
20.00
30.00
40.00
sigma v/u*
r = 7.5 cm
r = 9.5 cm
r = 11.5 cm
r = 13.5 cm
r = 15.5 cm
r = 17.5 cm
r = 19.5 cm
r = 21.5 cm
r = 23.5 cm

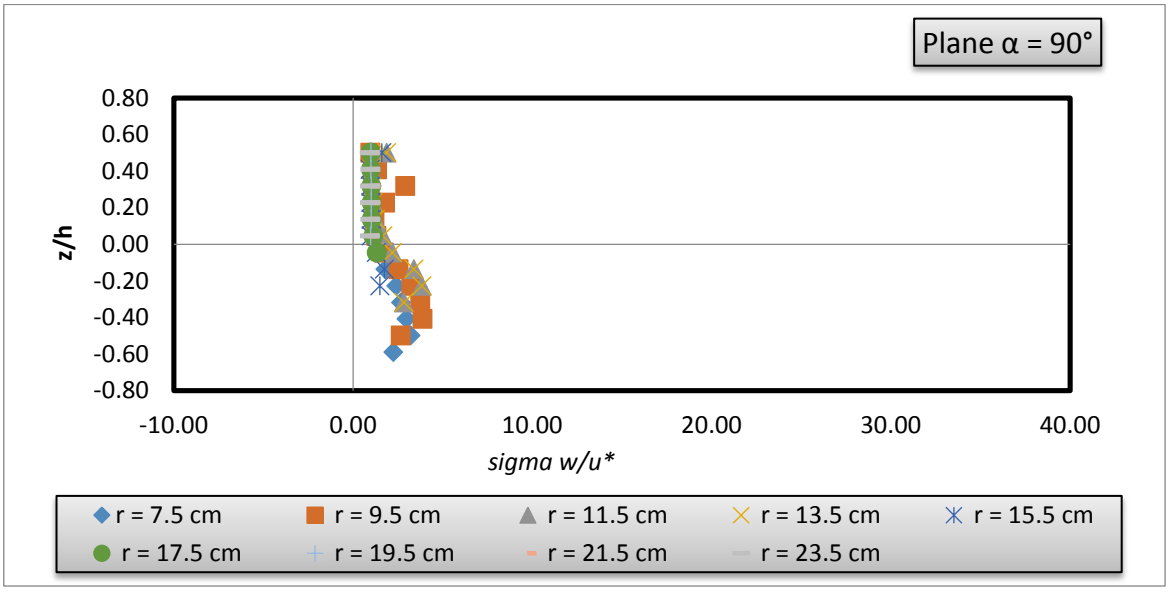
Plane α = 90°
0.80
0.60
0.40
0.20
0.00
-0.20
-0.40
-0.60
-0.80
z/h
-10.00
0.00
10.00
20.00
30.00
40.00
sigma w/u*
r = 7.5 cm
r = 9.5 cm
r = 11.5 cm
r = 13.5 cm
r = 15.5 cm
r = 17.5 cm
r = 19.5 cm
r = 21.5 cm
r = 23.5 cm

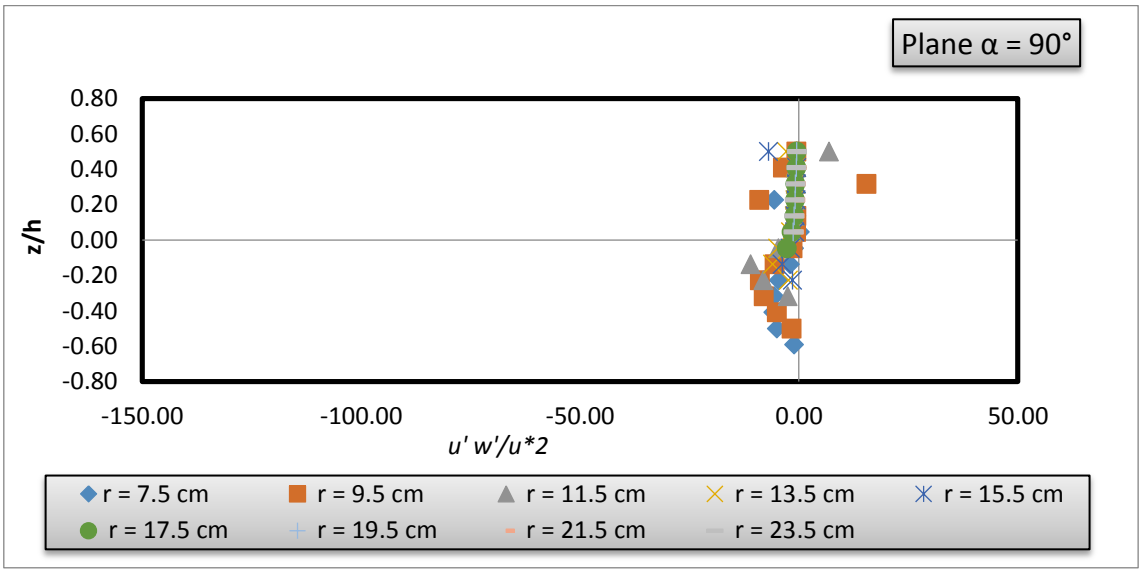

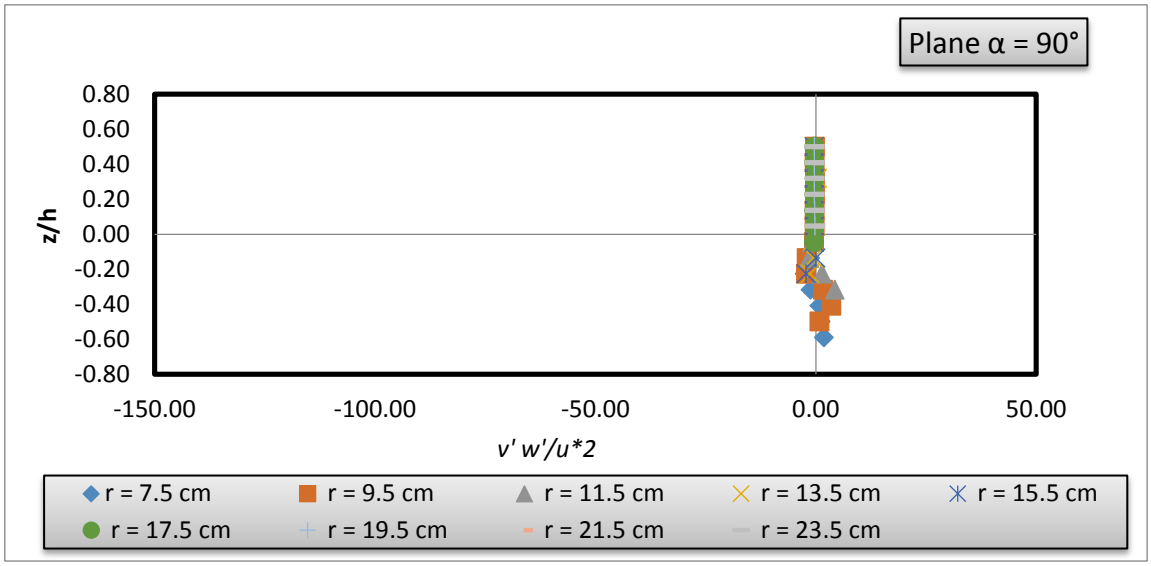

Fig 4.28 Distribution of normalized turbulence intensities and Reynolds stresses in side stream of vertical pier (α =90°).

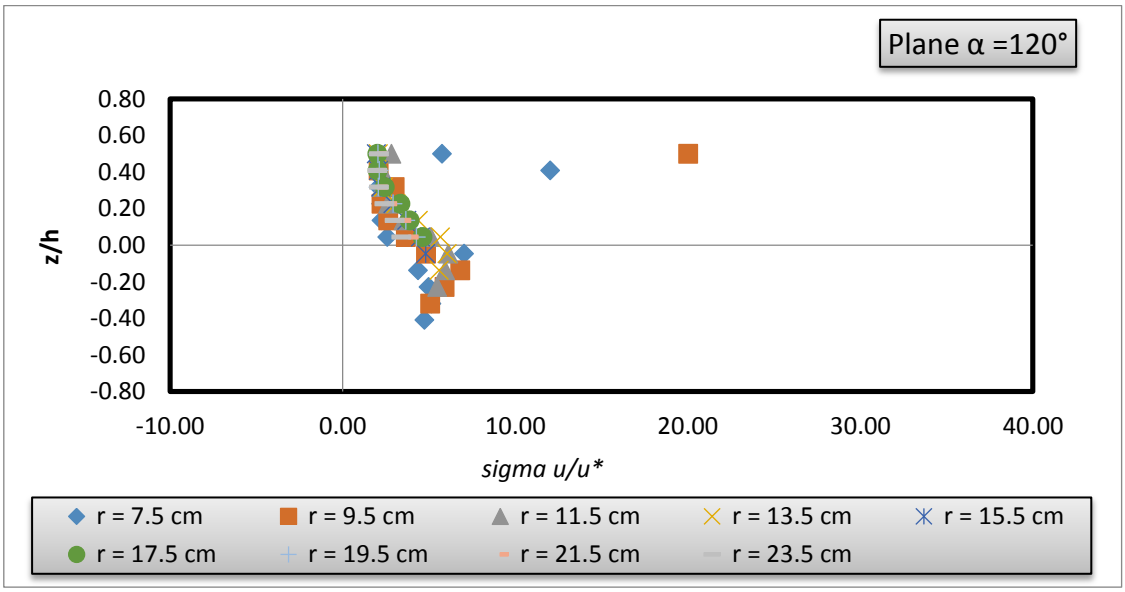
Plane α =120°
0.80
0.60
0.40
0.20
0.00
-0.20
-0.40
-0.60
-0.80
z/h
-10.00
0.00
10.00
20.00
30.00
40.00
sigma u/u*
r = 7.5 cm
r = 9.5 cm
r = 11.5 cm
r = 13.5 cm
r = 15.5 cm
r = 17.5 cm
r = 19.5 cm
r = 21.5 cm
r = 23.5 cm

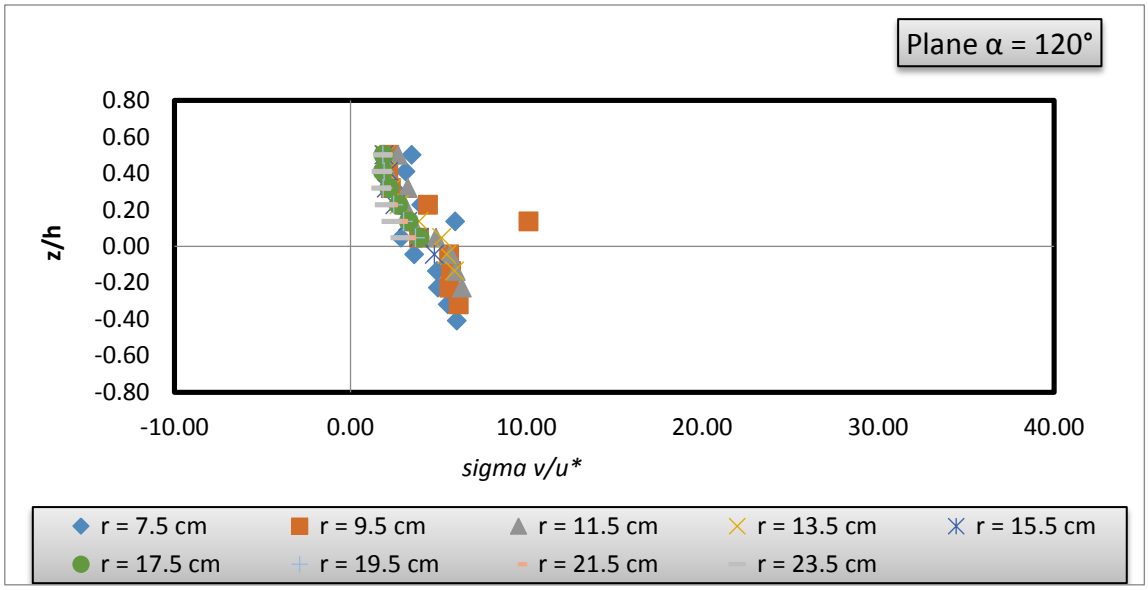
Plane α = 120°
0.80
0.60
0.40
0.20
0.00
-0.20
-0.40
-0.60
-0.80
z/h
-10.00
0.00
10.00
20.00
30.00
40.00
sigma v/u*
r = 7.5 cm
r = 9.5 cm
r = 11.5 cm
r = 13.5 cm
r = 15.5 cm
r = 17.5 cm
r = 19.5 cm
r = 21.5 cm
r = 23.5 cm

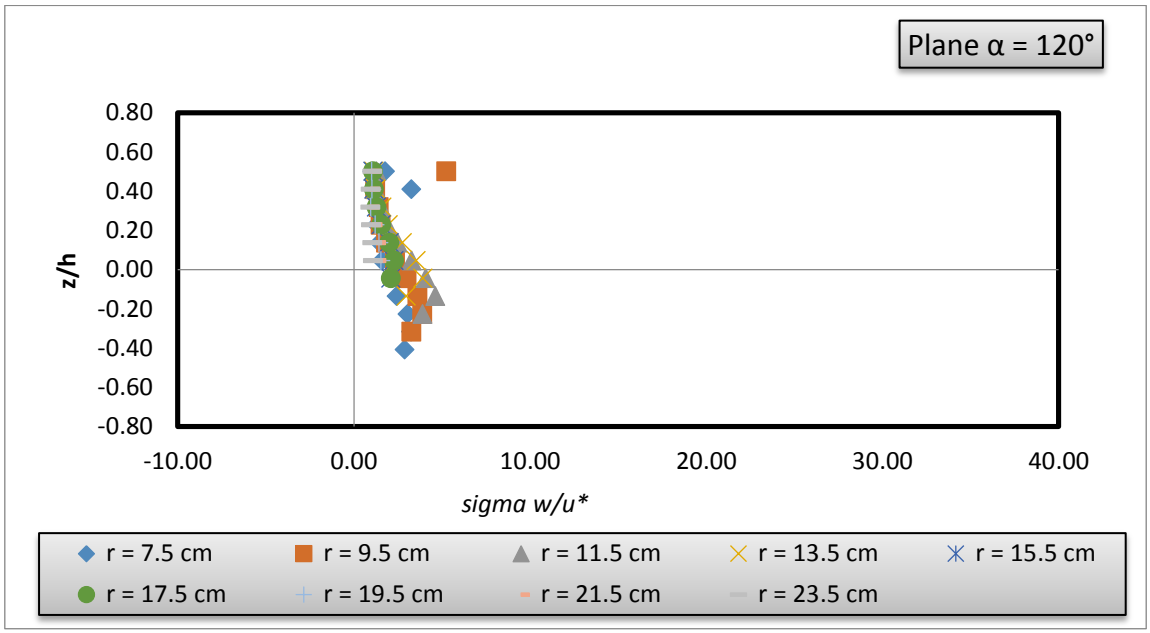
Plane α = 120°
0.80
0.60
0.40
0.20
0.00
-0.20
-0.40
-0.60
-0.80
z/h
-10.00
0.00
10.00
20.00
30.00
40.00
sigma w/u*
r = 7.5 cm
r = 9.5 cm
r = 11.5 cm
r = 13.5 cm
r = 15.5 cm
r = 17.5 cm
r = 19.5 cm
r = 21.5 cm
r = 23.5 cm

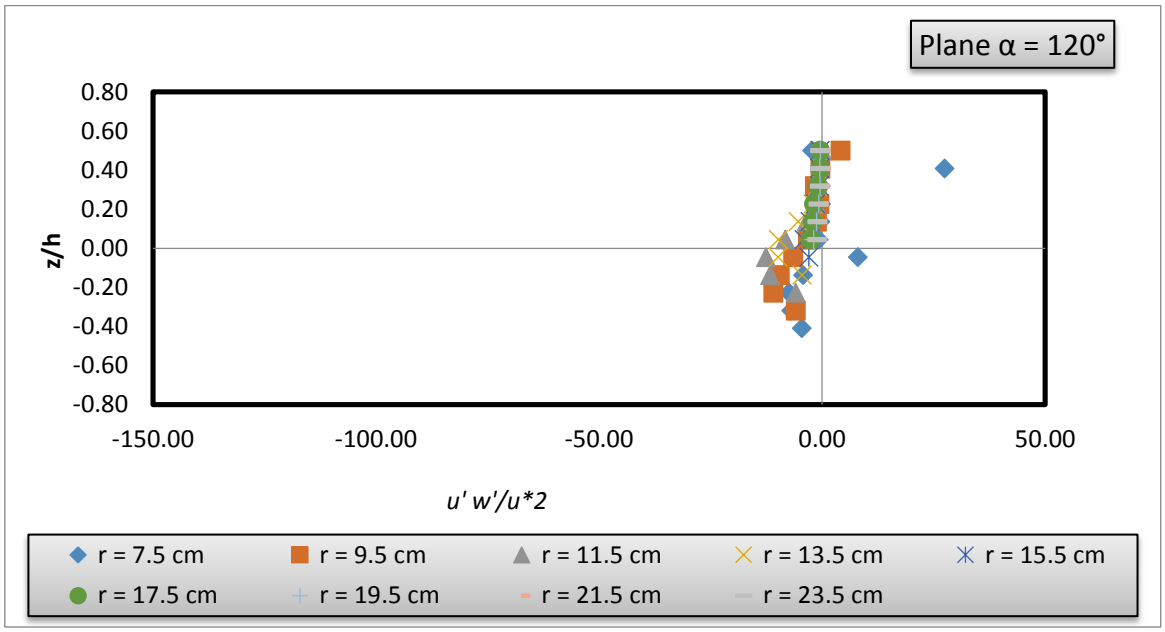

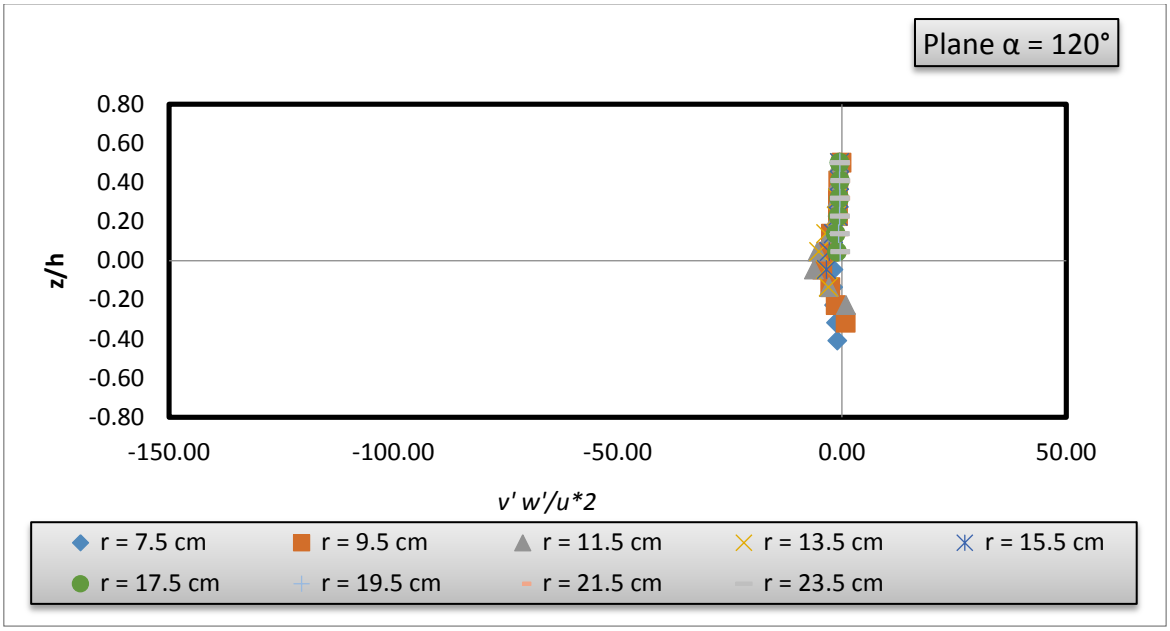

Fig 4.29 Distribution of normalized turbulence intensities and Reynolds stresses in downstream of vertical pier (α =120°).

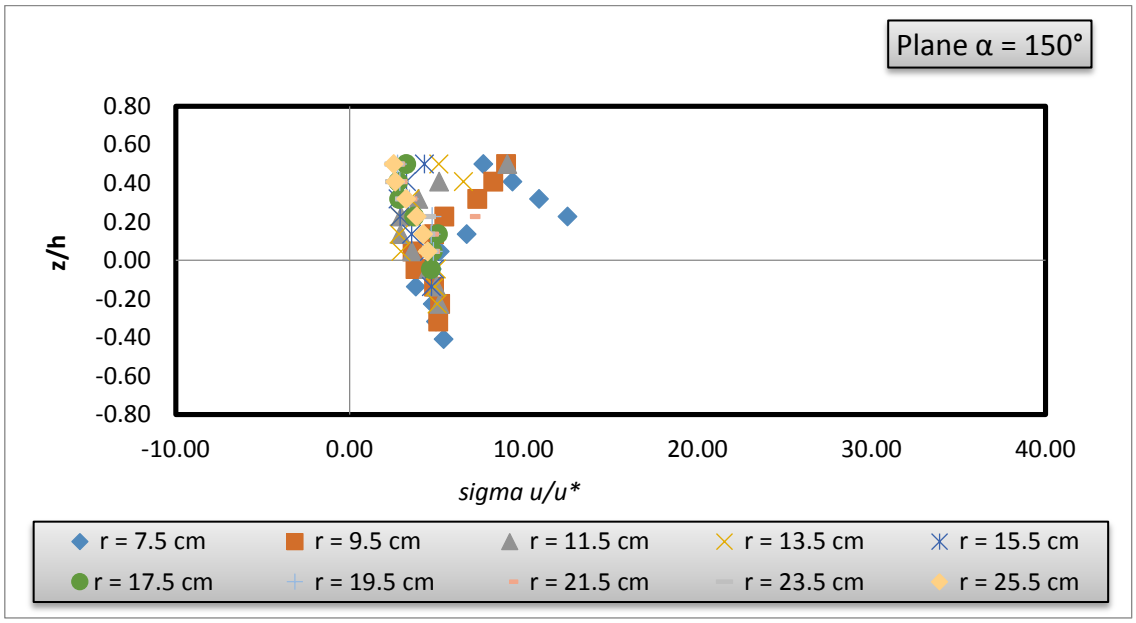
Plane α = 150°
0.80
0.60
0.40
0.20
0.00
-0.20
-0.40
-0.60
-0.80
z/h
-10.00
0.00
10.00
20.00
30.00
40.00
sigma u/u*
r = 7.5 cm
r = 9.5 cm
r = 11.5 cm
r = 13.5 cm
r = 15.5 cm
r = 17.5 cm
r = 19.5 cm
r = 21.5 cm
r = 23.5 cm
r = 25.5 cm

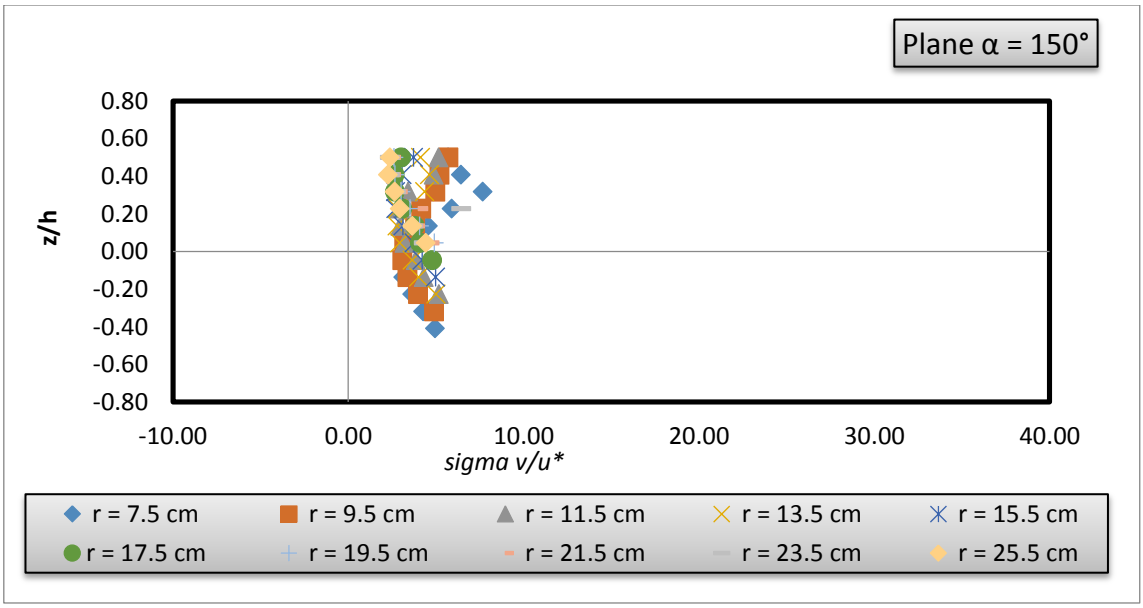
Plane α = 150°
0.80
0.60
0.40
0.20
0.00
-0.20
-0.40
-0.60
-0.80
z/h
-10.00
0.00
10.00
20.00
30.00
40.00
sigma v/u*
r = 7.5 cm
r = 9.5 cm
r = 11.5 cm
r = 13.5 cm
r = 15.5 cm
r = 17.5 cm
r = 19.5 cm
r = 21.5 cm
r = 23.5 cm
r = 25.5 cm

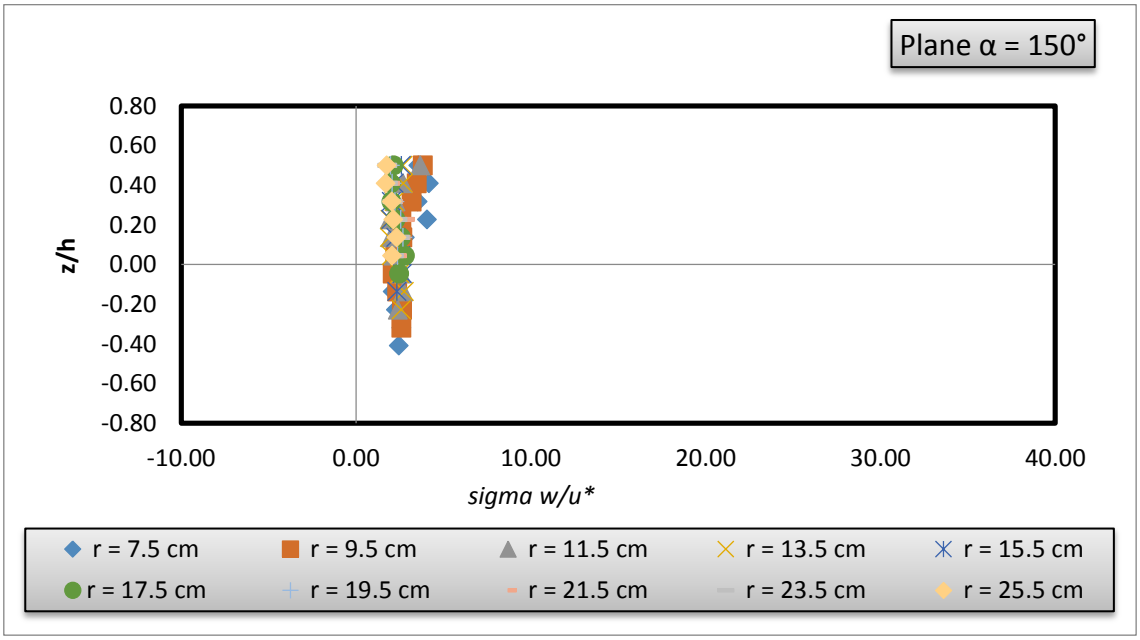
Plane α = 150°
0.80
0.60
0.40
0.20
0.00
-0.20
-0.40
-0.60
-0.80
z/h
-10.00
0.00
10.00
20.00
30.00
40.00
sigma w/u*
r = 7.5 cm
r = 9.5 cm
r = 11.5 cm
r = 13.5 cm
r = 15.5 cm
r = 17.5 cm
r = 19.5 cm
r = 21.5 cm
r = 23.5 cm
r = 25.5 cm

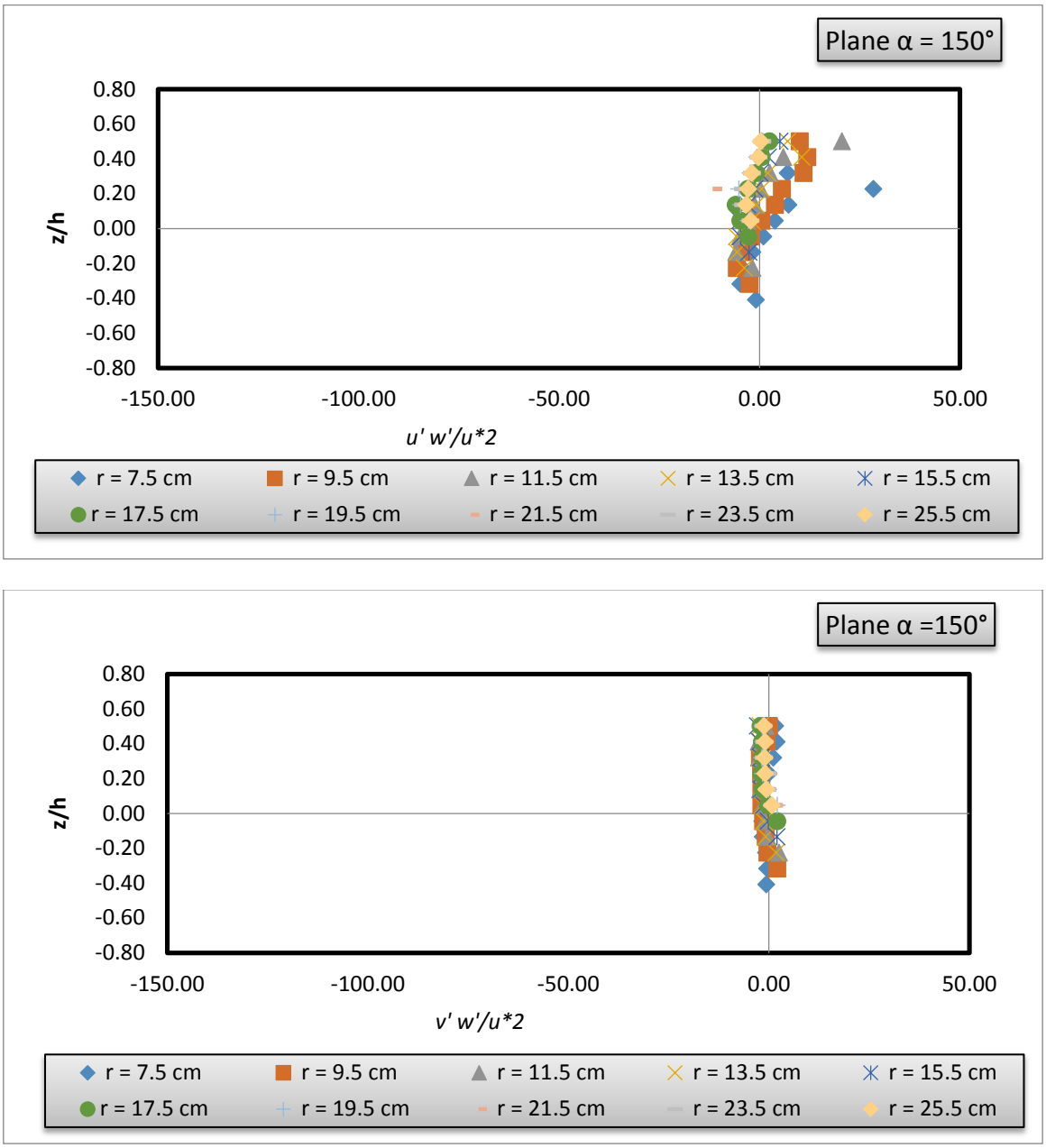

Fig 4.30 Distribution of normalized turbulence intensities and Reynolds stresses in downstream of vertical pier (α =150°).

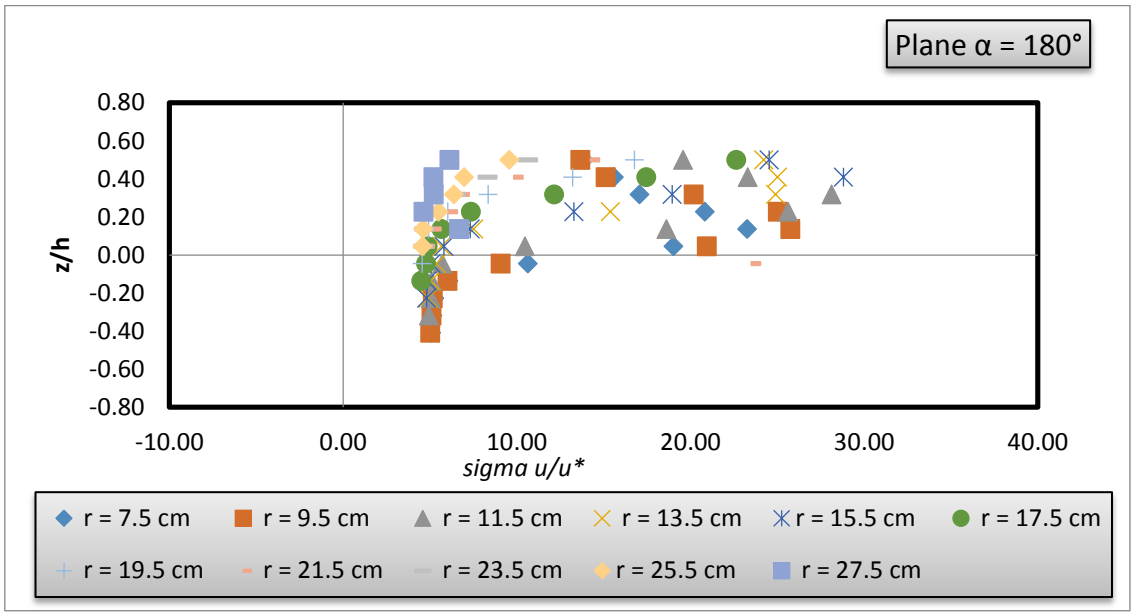
Plane α = 180°
0.80
0.60
0.40
0.20
0.00
-0.20
-0.40
-0.60
-0.80
z/h
-10.00
0.00
10.00
20.00
30.00
40.00
sigma u/u*
r = 7.5 cm
r = 9.5 cm
r = 11.5 cm
r = 13.5 cm
r = 15.5 cm
r = 17.5 cm
r = 19.5 cm
r = 21.5 cm
r = 23.5 cm
r = 25.5 cm
r = 27.5 cm

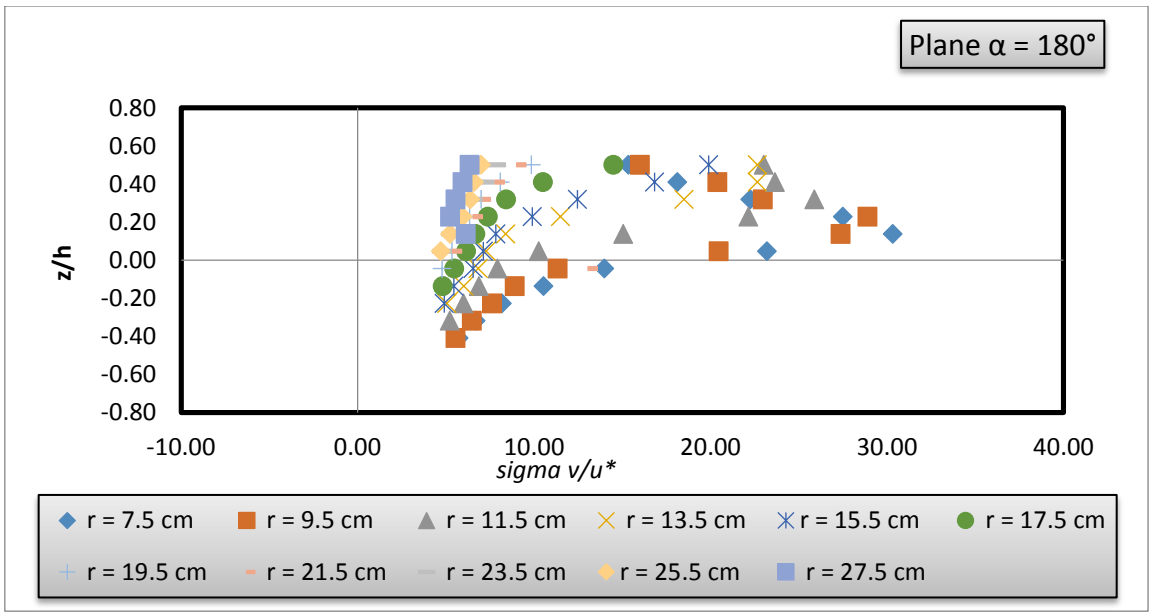
Plane α = 180°
0.80
0.60
0.40
0.20
0.00
-0.20
-0.40
-0.60
-0.80
z/h
-10.00
0.00
10.00
20.00
30.00
40.00
sigma v/u*
r = 7.5 cm
r = 9.5 cm
r = 11.5 cm
r = 13.5 cm
r = 15.5 cm
r = 17.5 cm
r = 19.5 cm
r = 21.5 cm
r = 23.5 cm
r = 25.5 cm
r = 27.5 cm

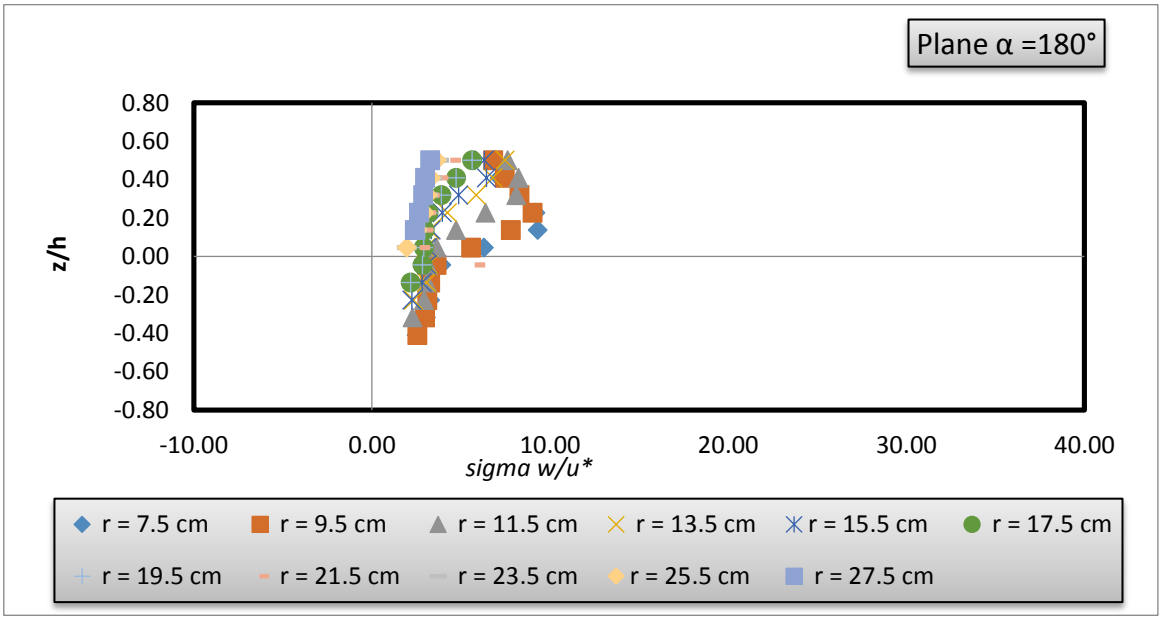
Plane α =180°
0.80
0.60
0.40
0.20
0.00
-0.20
-0.40
-0.60
-0.80
z/h
-10.00
0.00
10.00
20.00
30.00
40.00
sigma w/u*
r = 7.5 cm
r = 9.5 cm
r = 11.5 cm
r = 13.5 cm
r = 15.5 cm
r = 17.5 cm
r = 19.5 cm
r = 21.5 cm
r = 23.5 cm
r = 25.5 cm
r = 27.5 cm

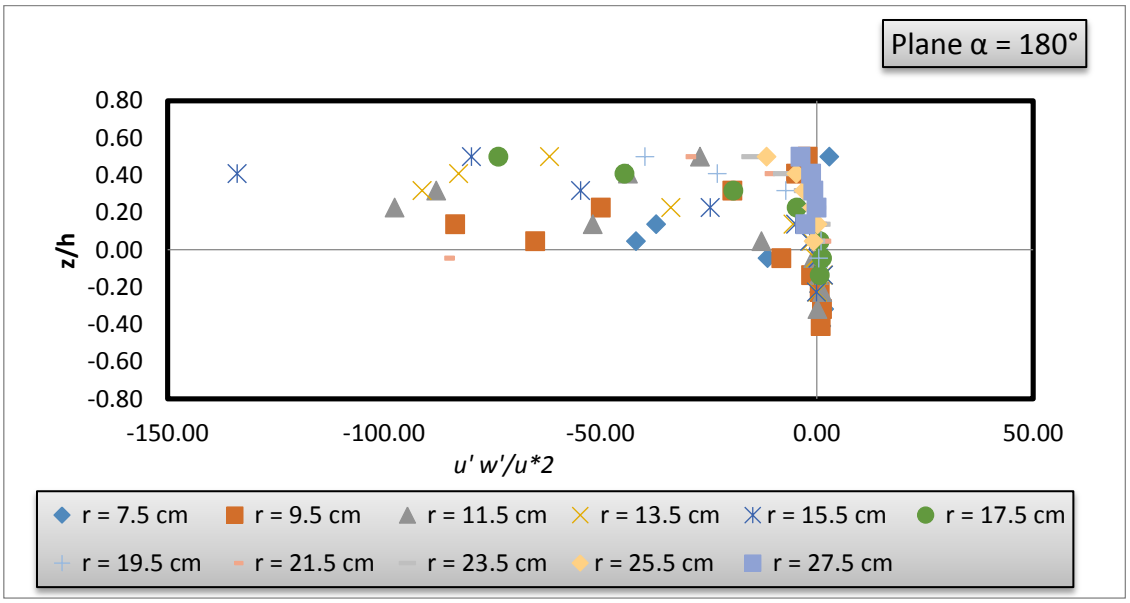

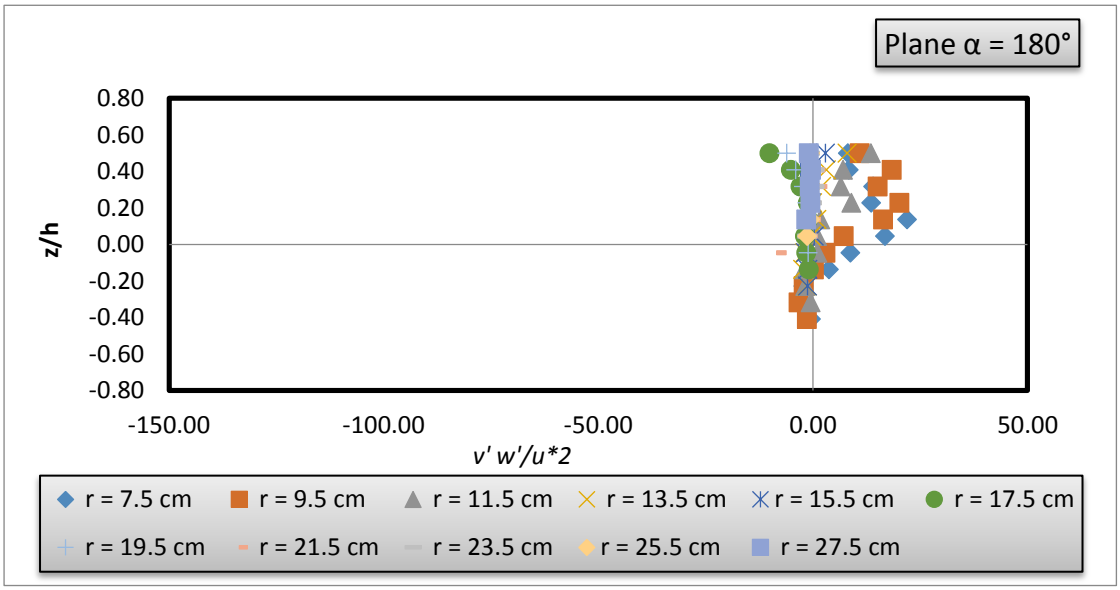

Fig 4.31 Distribution of normalized turbulence intensities and Reynolds stresses in downstream of vertical pier (α =180°).

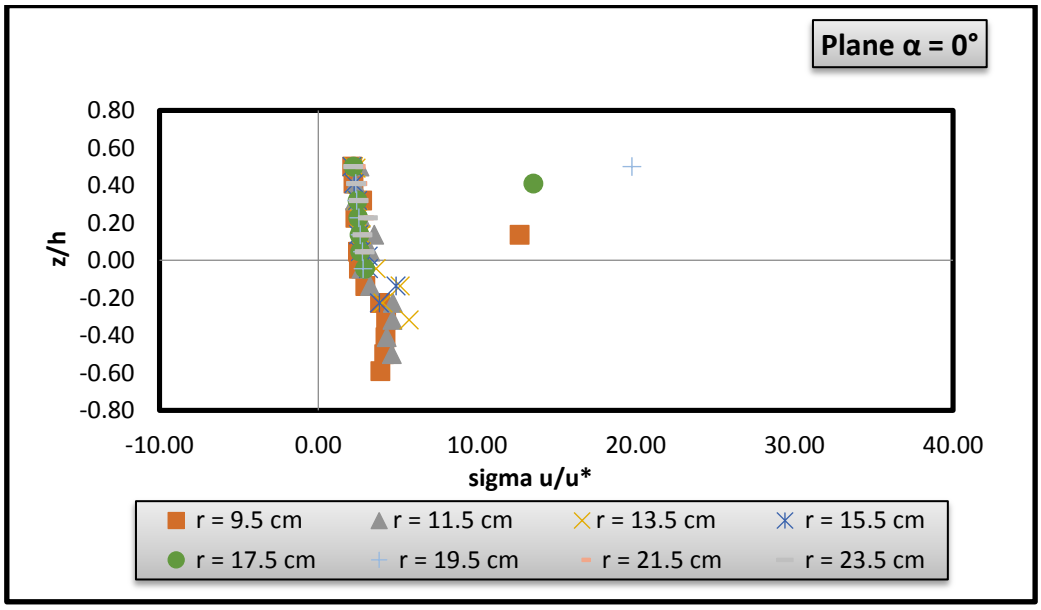
Plane α = 0°
0.80
0.60
0.40
0.20
0.00
-0.20
-0.40
-0.60
-0.80
z/h
-10.00
0.00
10.00
20.00
30.00
40.00
sigma u/u*
r = 9.5 cm
r = 11.5 cm
r = 13.5 cm
r = 15.5 cm
r = 17.5 cm
r = 19.5 cm
r = 21.5 cm
r = 23.5 cm

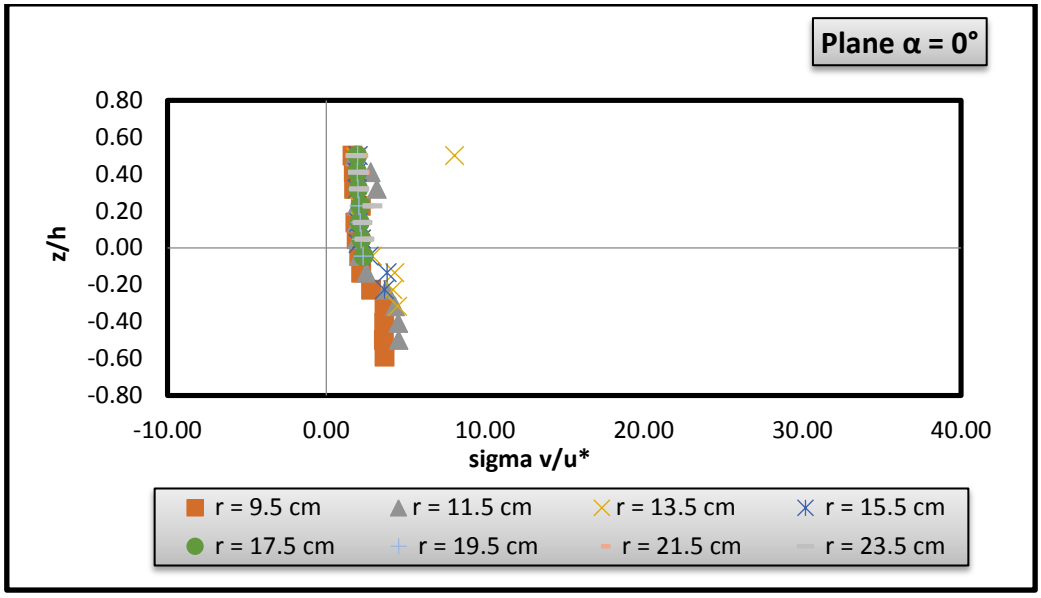
Plane α = 0°
0.80
0.60
0.40
0.20
0.00
-0.20
-0.40
-0.60
-0.80
z/h
-10.00
0.00
10.00
20.00
30.00
40.00
sigma v/u*
r = 9.5 cm
r = 11.5 cm
r = 13.5 cm
r = 15.5 cm
r = 17.5 cm
r = 19.5 cm
r = 21.5 cm
r = 23.5 cm

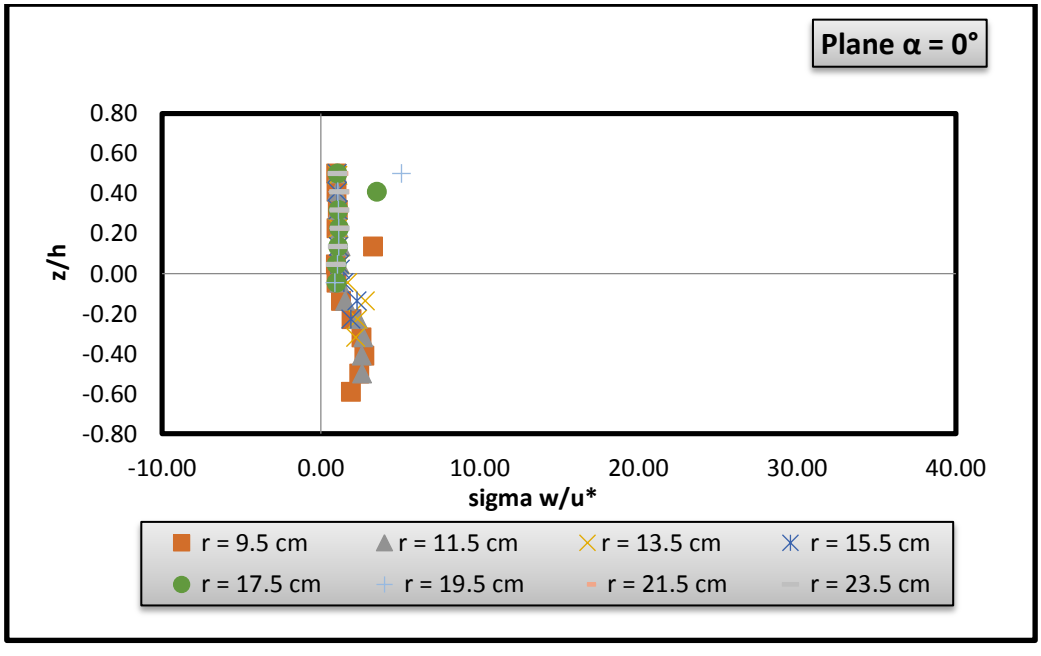
Plane α = 0°
0.80
0.60
0.40
0.20
0.00
-0.20
-0.40
-0.60
-0.80
z/h
-10.00
0.00
10.00
20.00
30.00
40.00
sigma w/u*
r = 9.5 cm
r = 11.5 cm
r = 13.5 cm
r = 15.5 cm
r = 17.5 cm
r = 19.5 cm
r = 21.5 cm
r = 23.5 cm

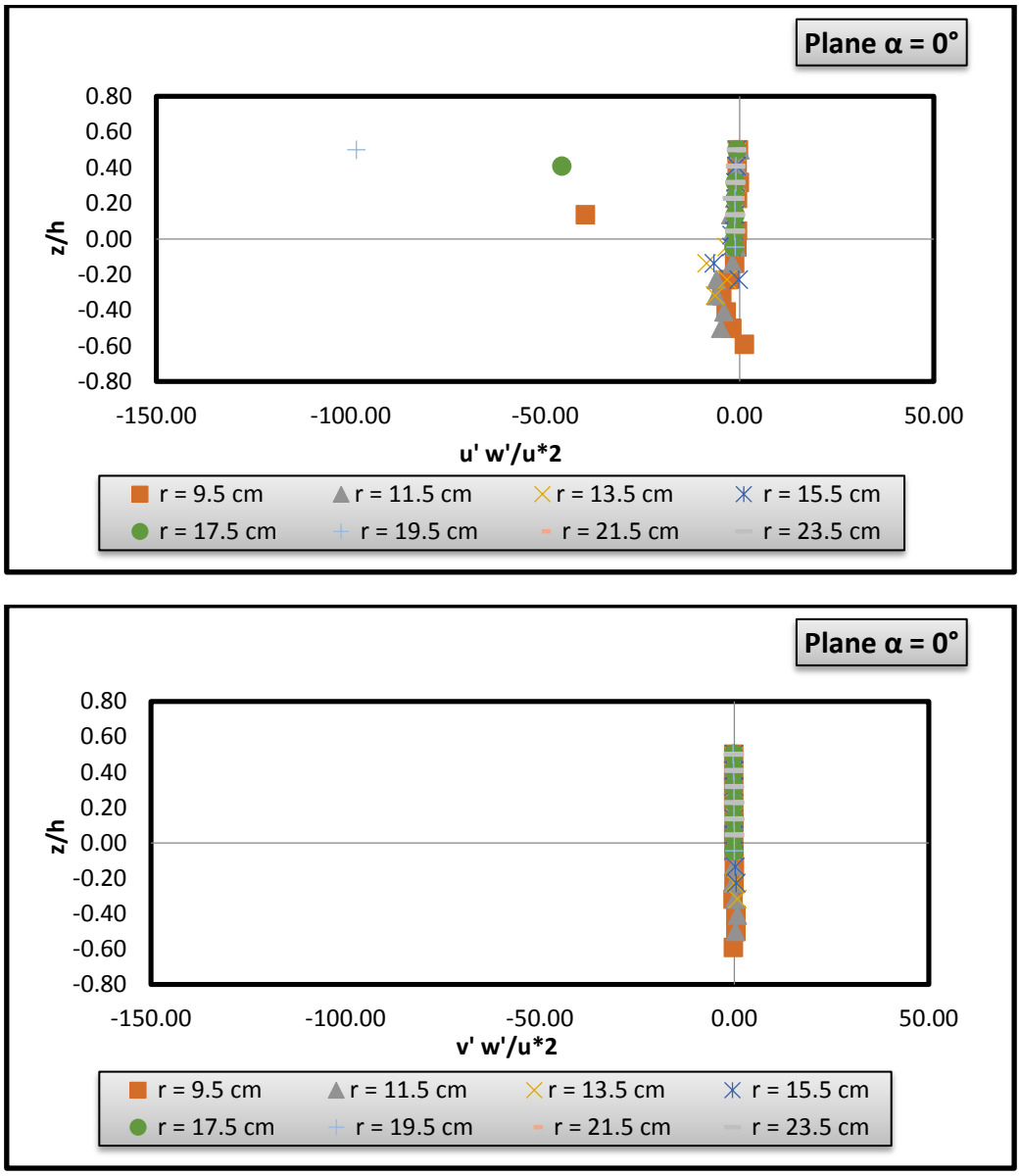

Fig 4.32 Distribution of normalized turbulence intensities and Reynolds stresses in upstream of inclined pier (α =0°).

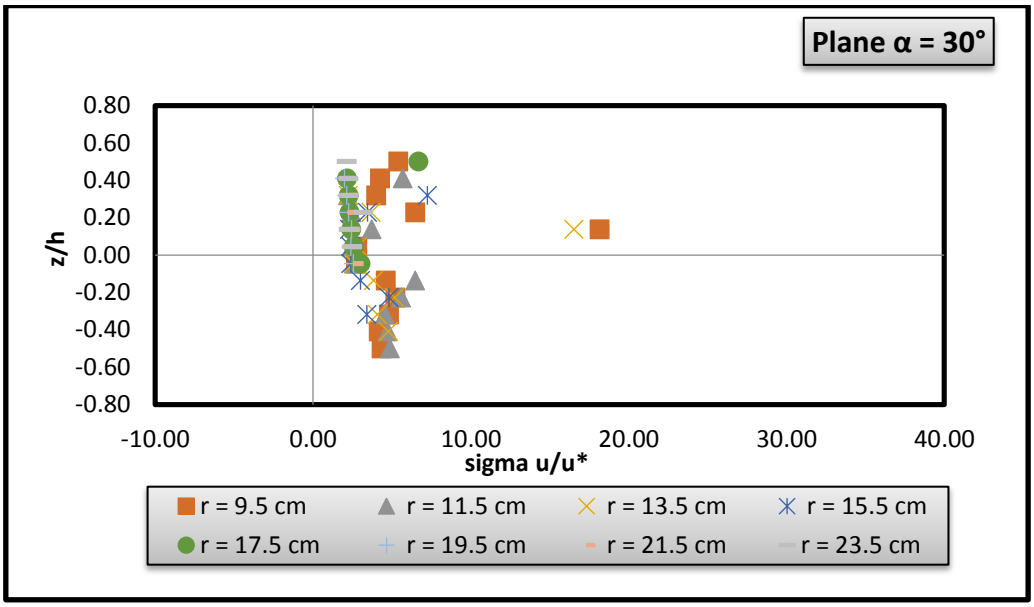
Plane α = 30°
0.80
0.60
0.40
0.20
0.00
-0.20
-0.40
-0.60
-0.80
z/h
-10.00
0.00
10.00
20.00
30.00
40.00
sigma u/u*
r = 9.5 cm
r = 11.5 cm
r = 13.5 cm
r = 15.5 cm
r = 17.5 cm
r = 19.5 cm
r = 21.5 cm
r = 23.5 cm

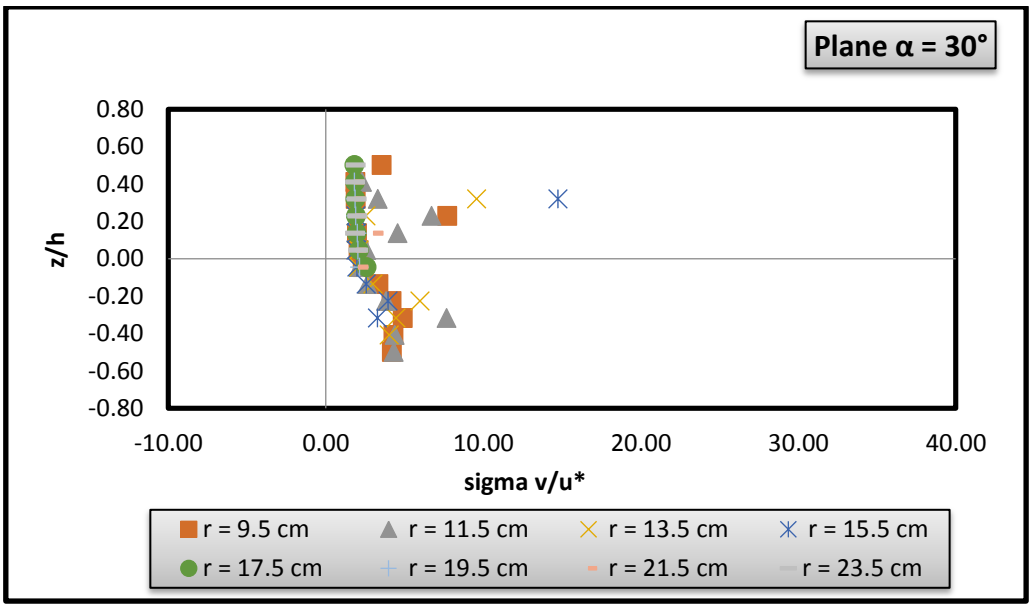
Plane α = 30°
0.80
0.60
0.40
0.20
0.00
-0.20
-0.40
-0.60
-0.80
z/h
-10.00
0.00
10.00
20.00
30.00
40.00
sigma v/u*
r = 9.5 cm
r = 11.5 cm
r = 13.5 cm
r = 15.5 cm
r = 17.5 cm
r = 19.5 cm
r = 21.5 cm
r = 23.5 cm

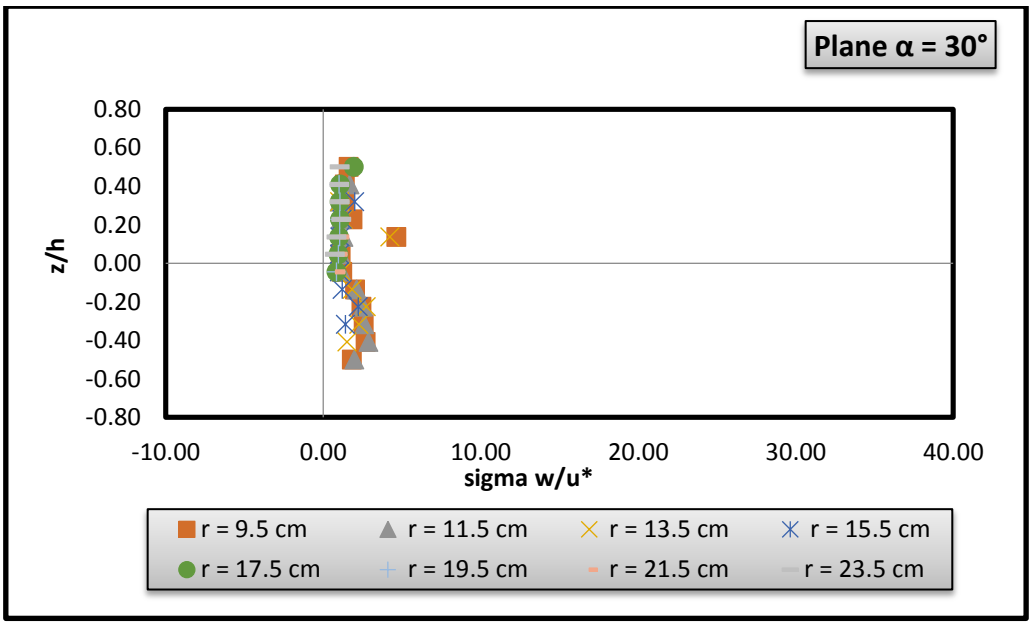
Plane α = 30°
0.80
0.60
0.40
0.20
0.00
-0.20
-0.40
-0.60
-0.80
z/h
-10.00
0.00
10.00
20.00
30.00
40.00
sigma w/u*
r = 9.5 cm
r = 11.5 cm
r = 13.5 cm
r = 15.5 cm
r = 17.5 cm
r = 19.5 cm
r = 21.5 cm
r = 23.5 cm

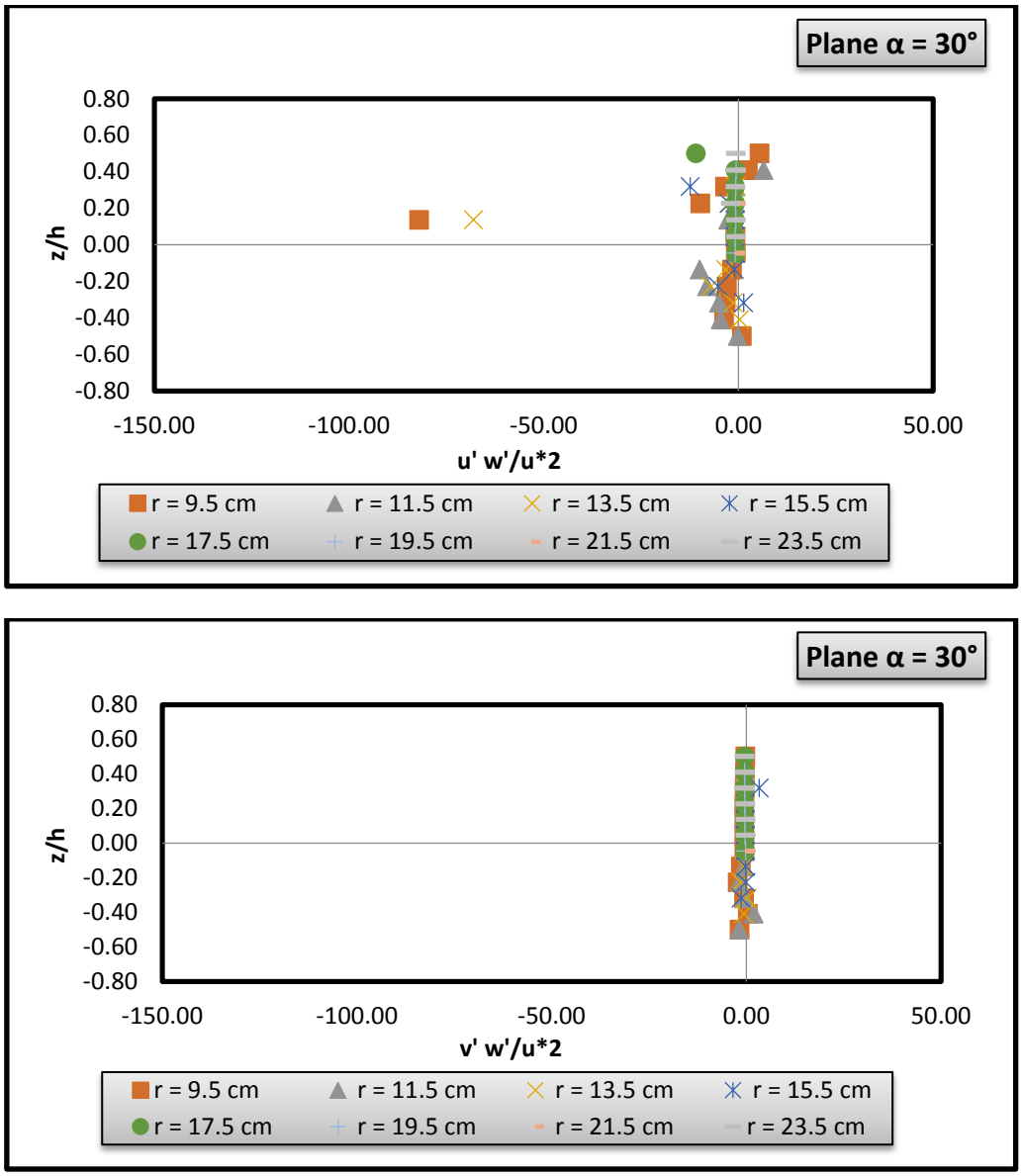

Fig 4.33 Distribution of normalized turbulence intensities and Reynolds stresses in upstream of inclined pier (α =30°).

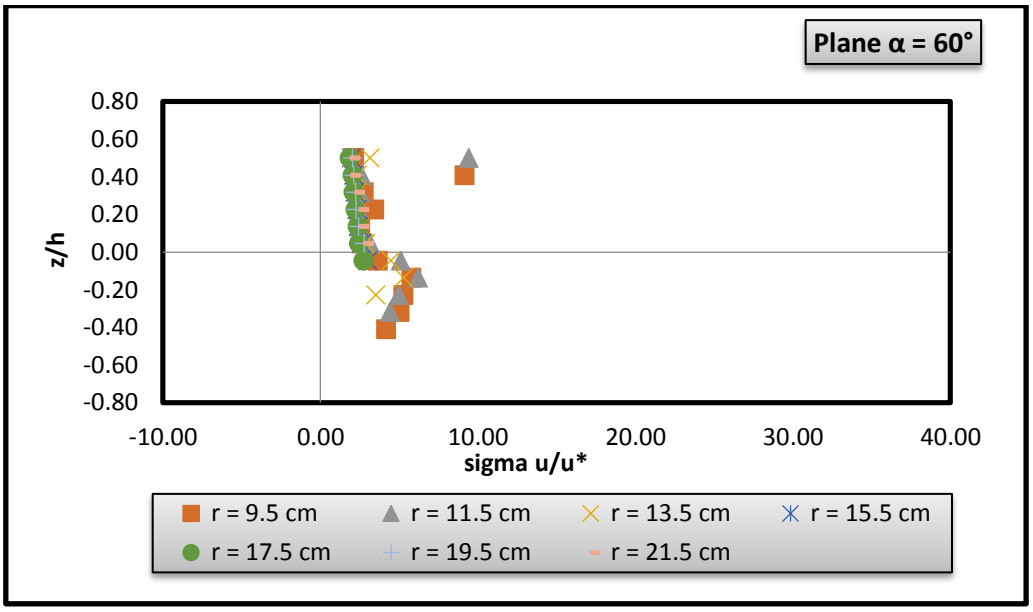
Plane α = 60°
0.80
0.60
0.40
0.20
0.00
-0.20
-0.40
-0.60
-0.80
z/h
-10.00
0.00
10.00
20.00
30.00
40.00
sigma u/u*
r = 9.5 cm
r = 11.5 cm
r = 13.5 cm
r = 15.5 cm
r = 17.5 cm
r = 19.5 cm
r = 21.5 cm

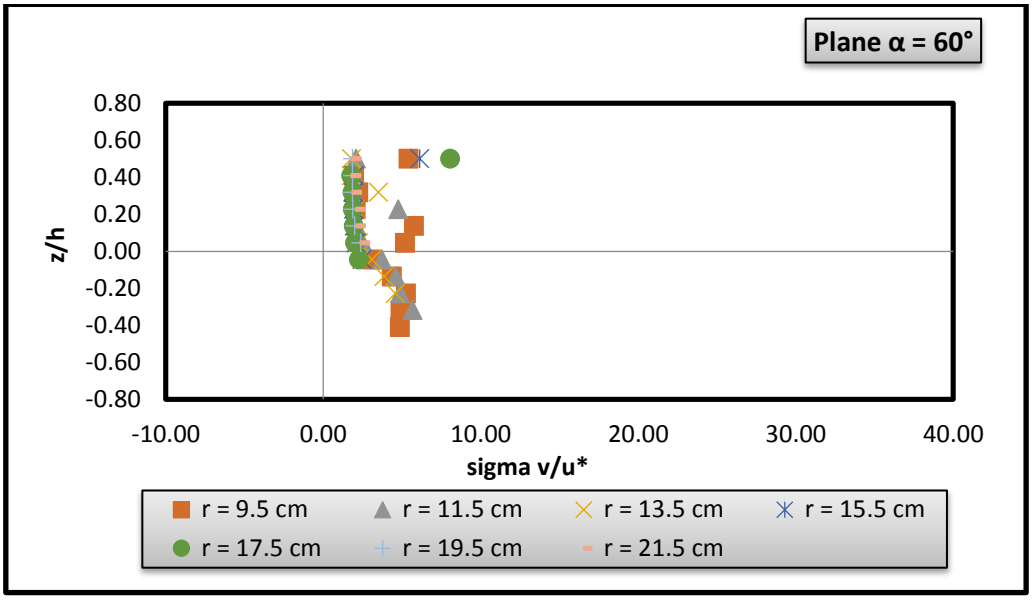
Plane α = 60°
0.80
0.60
0.40
0.20
0.00
-0.20
-0.40
-0.60
-0.80
z/h
-10.00
0.00
10.00
20.00
30.00
40.00
sigma v/u*
r = 9.5 cm
r = 11.5 cm
r = 13.5 cm
r = 15.5 cm
r = 17.5 cm
r = 19.5 cm
r = 21.5 cm

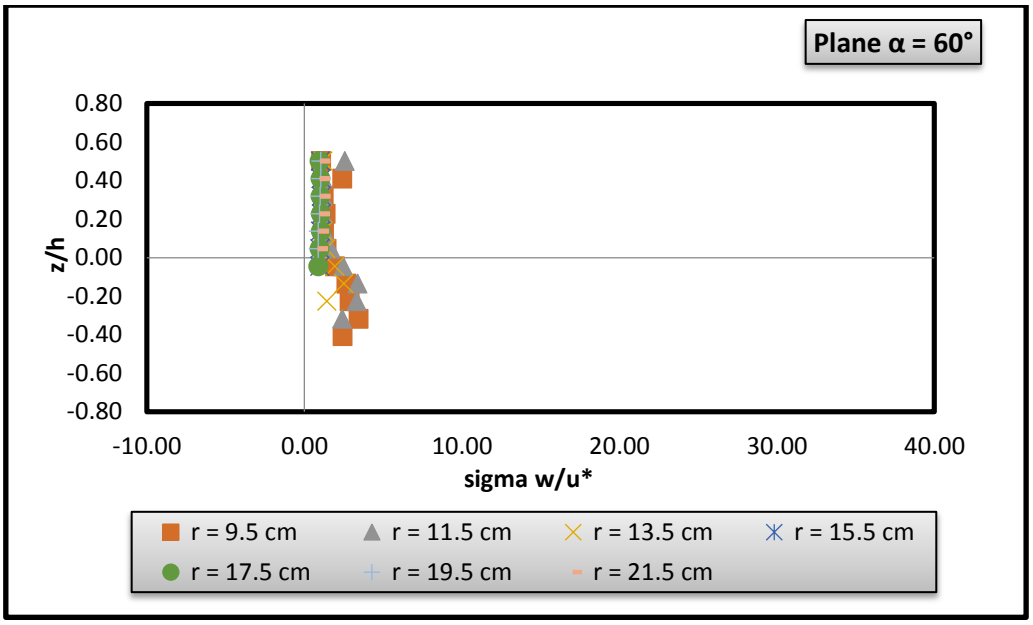
Plane α = 60°
0.80
0.60
0.40
0.20
0.00
-0.20
-0.40
-0.60
-0.80
z/h
-10.00
0.00
10.00
20.00
30.00
40.00
sigma w/u*
r = 9.5 cm
r = 11.5 cm
r = 13.5 cm
r = 15.5 cm
r = 17.5 cm
r = 19.5 cm
r = 21.5 cm

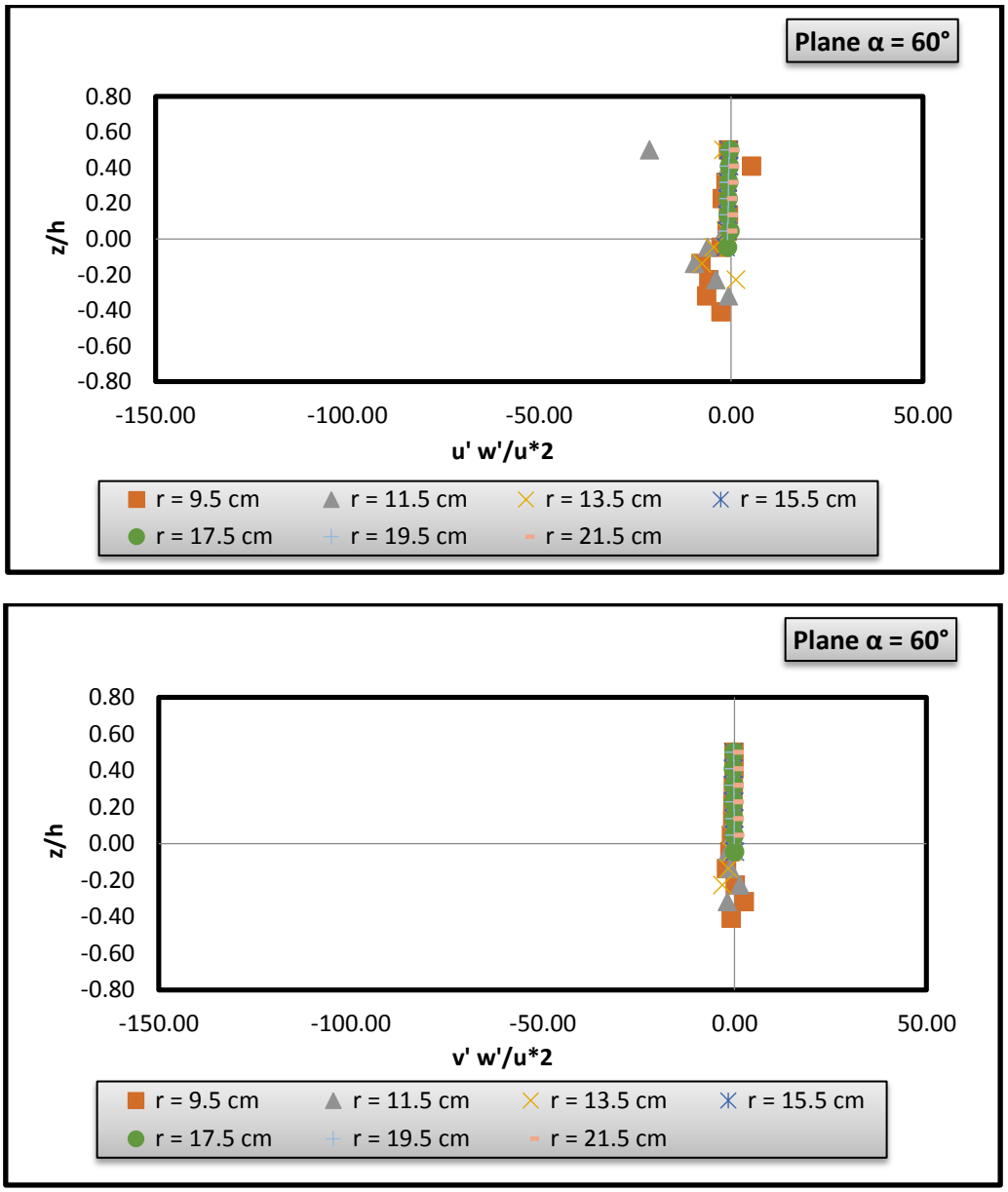

Fig 4.34 Distribution of normalized turbulence intensities and Reynolds stresses in upstream of inclined pier (α =60°).

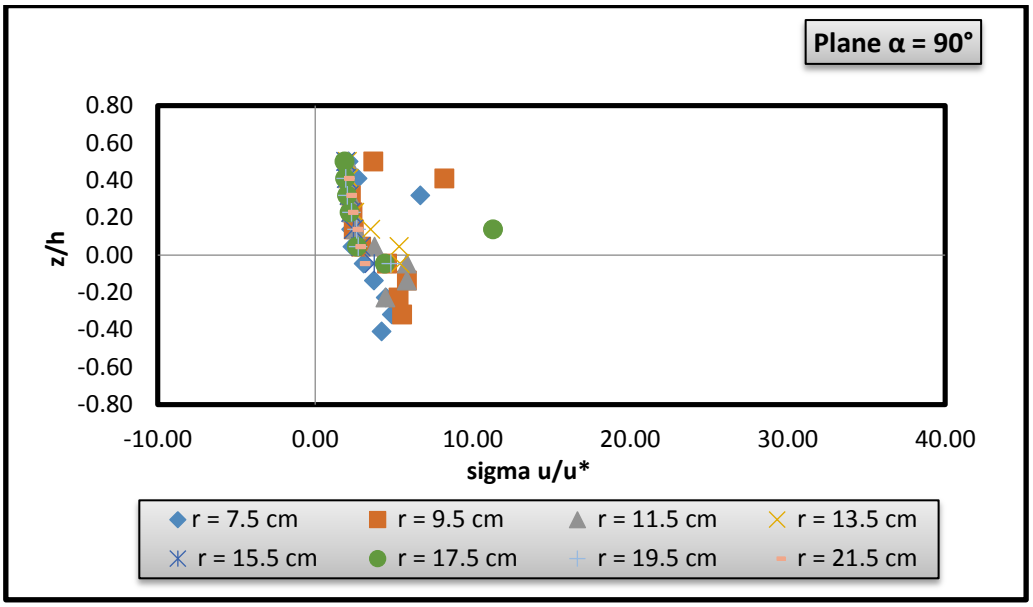
Plane α = 90°
0.80
0.60
0.40
0.20
0.00
-0.20
-0.40
-0.60
-0.80
z/h
-10.00
0.00
10.00
20.00
30.00
40.00
sigma u/u*
r = 7.5 cm
r = 9.5 cm
r = 11.5 cm
r = 13.5 cm
r = 15.5 cm
r = 17.5 cm
r = 19.5 cm
r = 21.5 cm

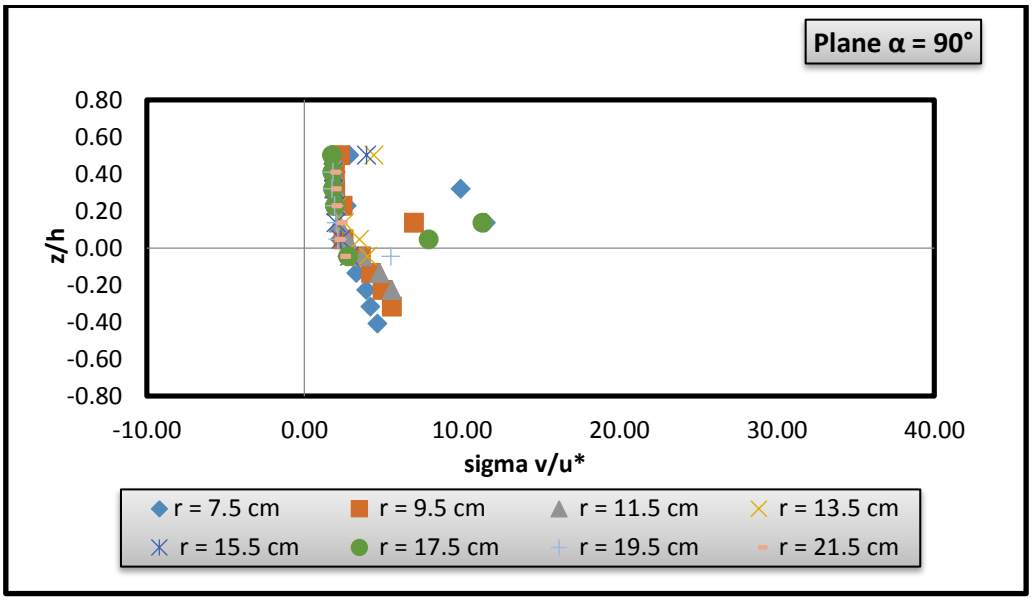
Plane α = 90°
0.80
0.60
0.40
0.20
0.00
-0.20
-0.40
-0.60
-0.80
z/h
-10.00
0.00
10.00
20.00
30.00
40.00
sigma v/u*
r = 7.5 cm
r = 9.5 cm
r = 11.5 cm
r = 13.5 cm
r = 15.5 cm
r = 17.5 cm
r = 19.5 cm
r = 21.5 cm

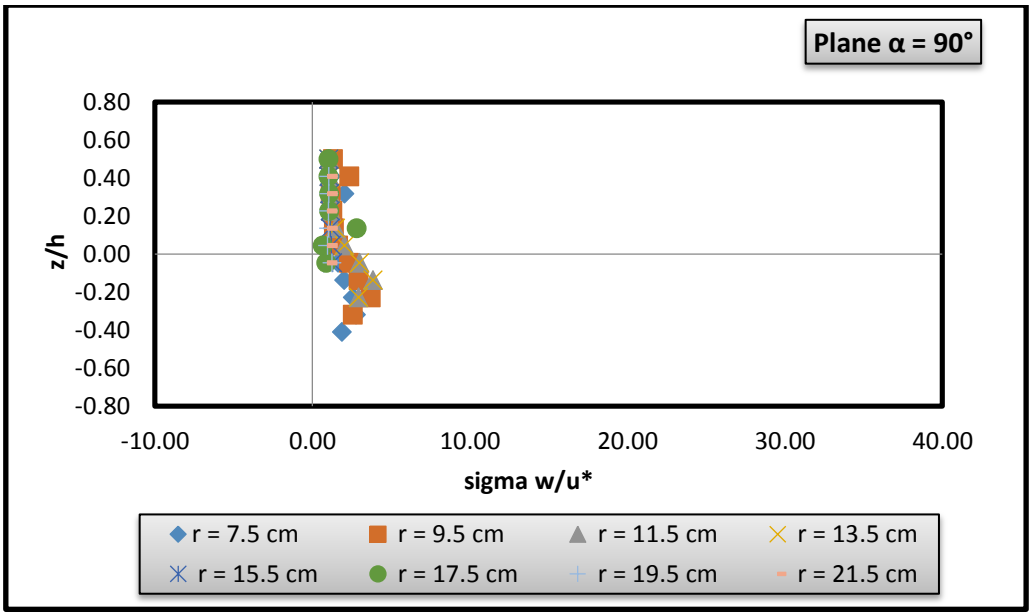
Plane α = 90°
0.80
0.60
0.40
0.20
0.00
-0.20
-0.40
-0.60
-0.80
z/h
-10.00
0.00
10.00
20.00
30.00
40.00
sigma w/u*
r = 7.5 cm
r = 9.5 cm
r = 11.5 cm
r = 13.5 cm
r = 15.5 cm
r = 17.5 cm
r = 19.5 cm
r = 21.5 cm

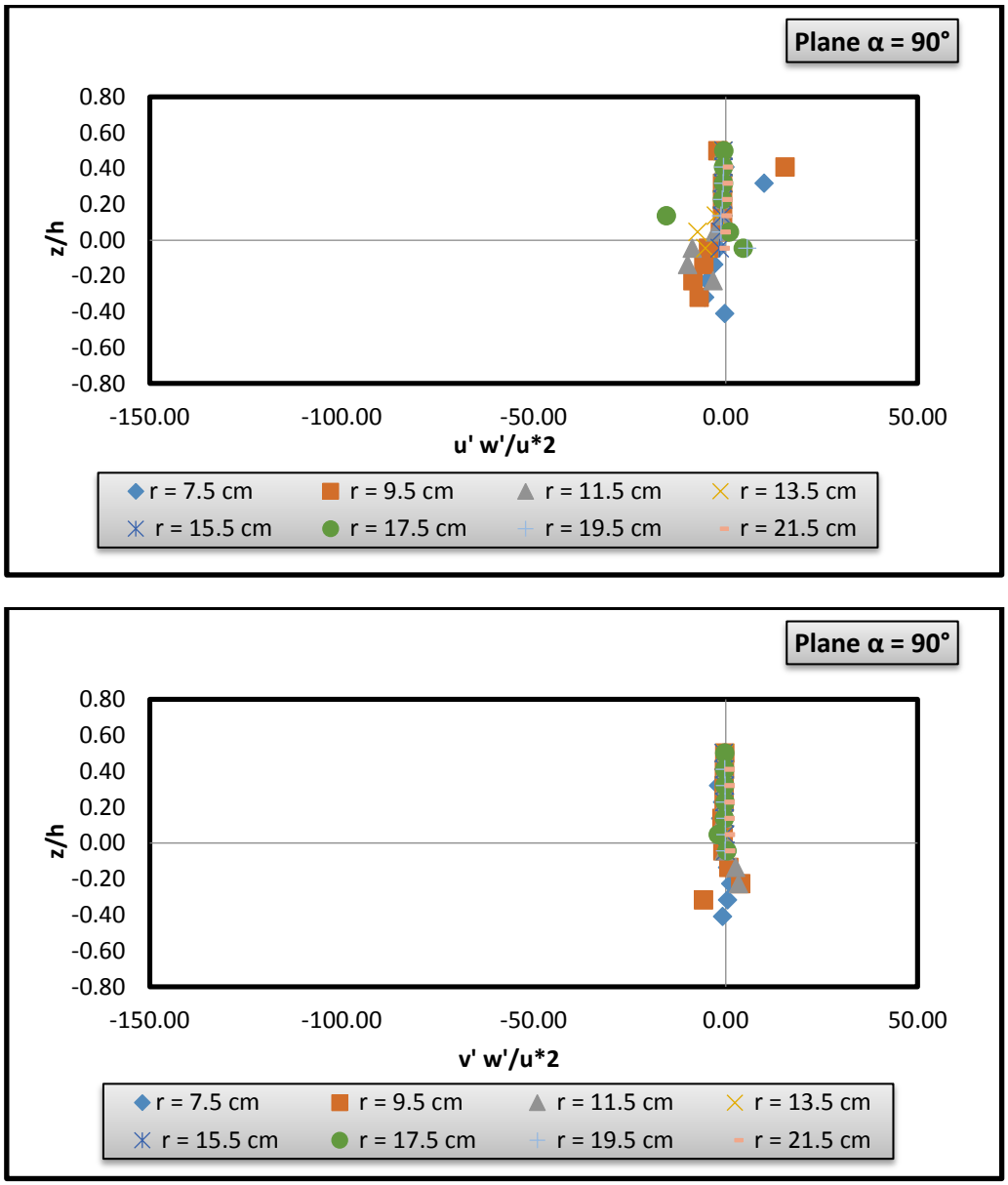

Fig 4.35 Distribution of normalized turbulence intensities and Reynolds stresses in side stream of inclined pier (α =90°).

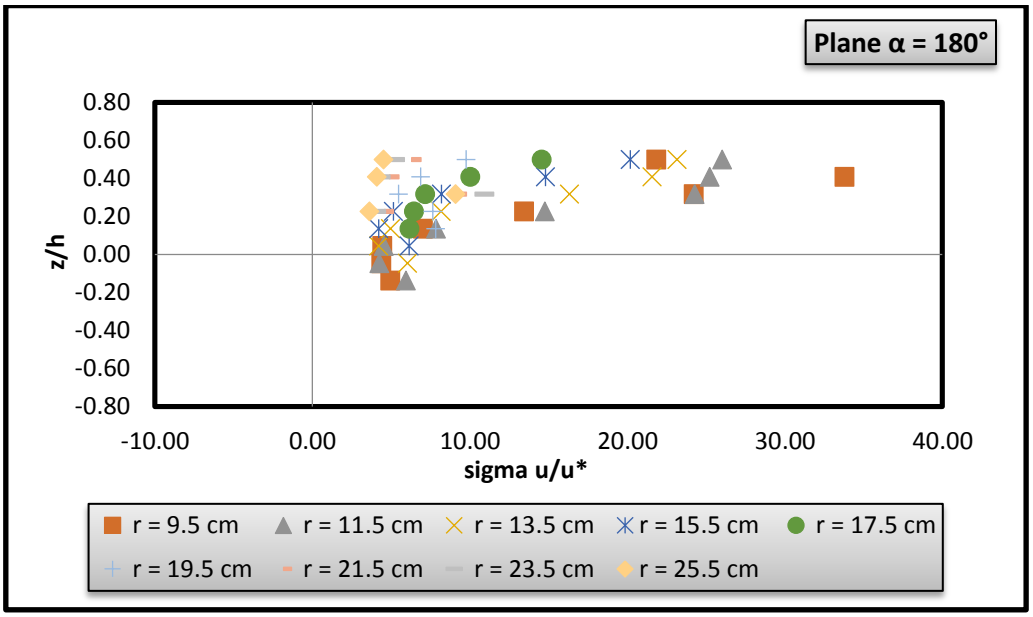
Plane α = 180°
0.80
0.60
0.40
0.20
0.00
-0.20
-0.40
-0.60
-0.80
z/h
-10.00
0.00
10.00
20.00
30.00
40.00
sigma u/u*
r = 9.5 cm
r = 11.5 cm
r = 13.5 cm
r = 15.5 cm
r = 17.5 cm
r = 19.5 cm
r = 21.5 cm
r = 23.5 cm
r = 25.5 cm

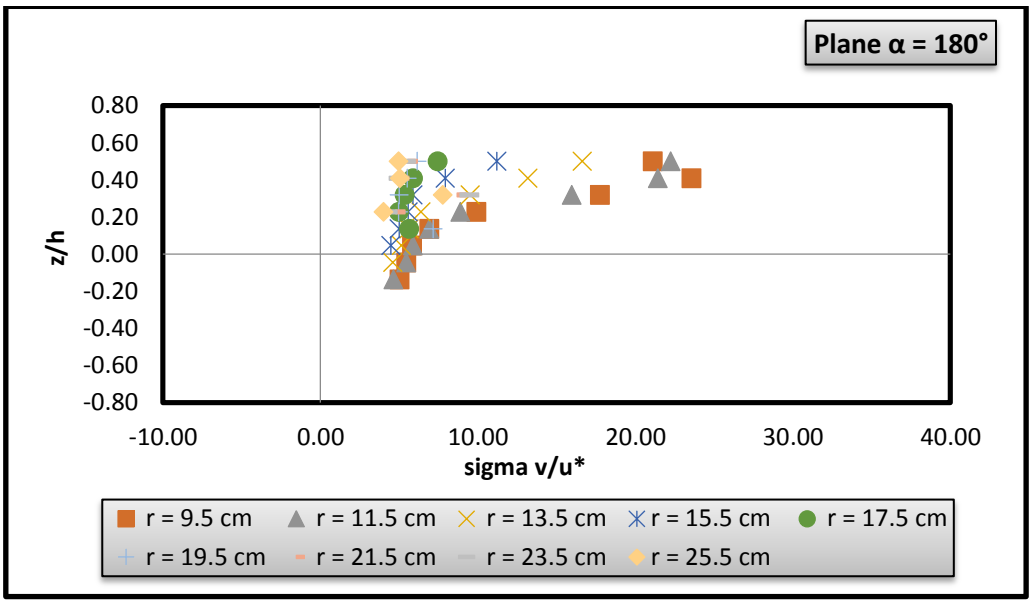
Plane α = 180°
0.80
0.60
0.40
0.20
0.00
-0.20
-0.40
-0.60
-0.80
z/h
-10.00
0.00
10.00
20.00
30.00
40.00
sigma v/u*
r = 9.5 cm
r = 11.5 cm
r = 13.5 cm
r = 15.5 cm
r = 17.5 cm
r = 19.5 cm
r = 21.5 cm
r = 23.5 cm
r = 25.5 cm

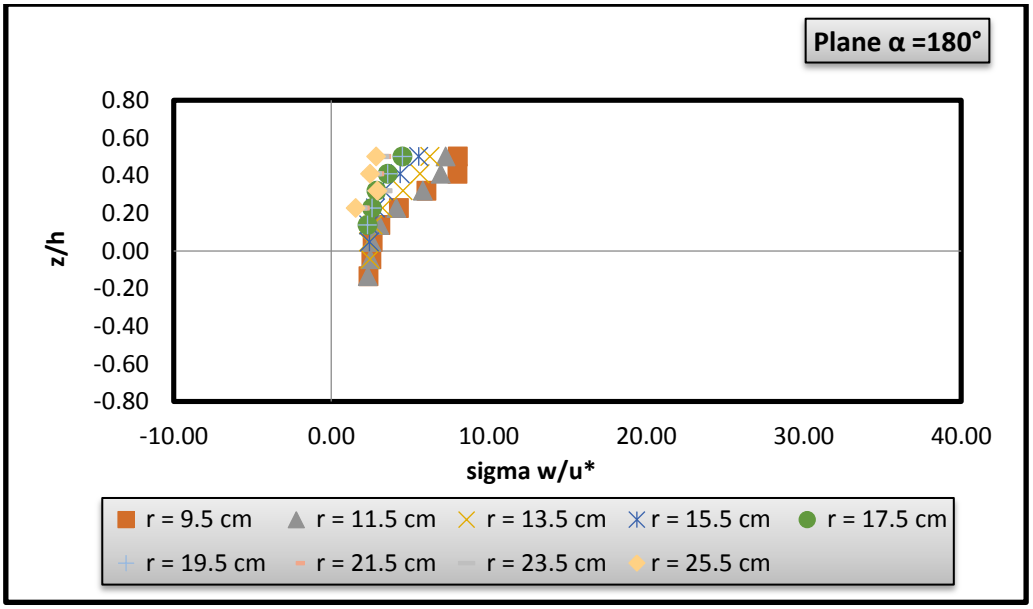
Plane α =180°
0.80
0.60
0.40
0.20
0.00
-0.20
-0.40
-0.60
-0.80
z/h
-10.00
0.00
10.00
20.00
30.00
40.00
sigma w/u*
r = 9.5 cm
r = 11.5 cm
r = 13.5 cm
r = 15.5 cm
r = 17.5 cm
r = 19.5 cm
r = 21.5 cm
r = 23.5 cm
r = 25.5 cm

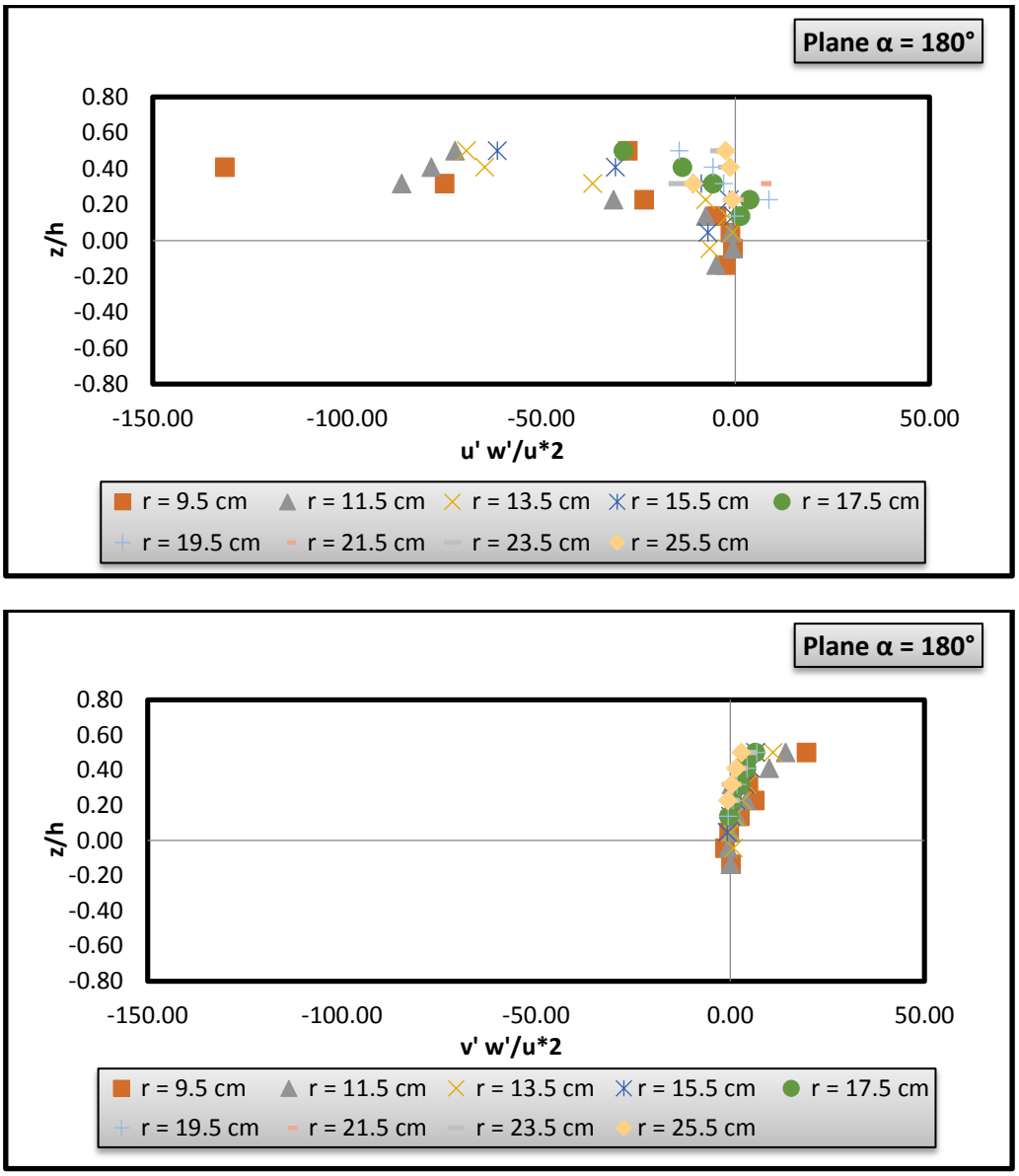

Fig 4.36 Distribution of normalized turbulence intensities and Reynolds stresses in downstream of inclined pier (α =180°).

4.5 Comparative study of the turbulence characteristics

Here we have concerned with the comparative study of the turbulence characteristics of vertical pier (setup 1) with the inclined pier (setup 2), in upstream of the piers(0°),in side stream of the piers (90°) and in downstream of the piers (180°) at various radial locations of 9.5 cm, 11.5 cm, 13.5 cm, and 15.5 cm. After comparison we come up with following points.

- **In upstream region**

1. Turbulent intensities have positive value in this region, with their values decreasing towards the water surface and increasing within the scour hole and having its greater value in setup 2.
2. The longitudinal component of Reynolds stress ($-\overline{u'w'}$) has negative values everywhere and greater value near the bottom of scour hole in setup 1.

- **In side stream of piers**

1. Turbulent intensities have the same trend as in upstream region.
2. Longitudinal component $(-\overline{u'w'})$ of Reynolds stress of negative value is dominant over $(-\overline{v'w'})$ component Reynolds stress with its greater value in setup 2.

- **In wake region**

1. In this plane, close to pier the magnitude of the three components of turbulence intensity are almost many times of the respected values in the upstream region.
2. Reynolds stress in this plane have much higher value but shows no conclusive trend.

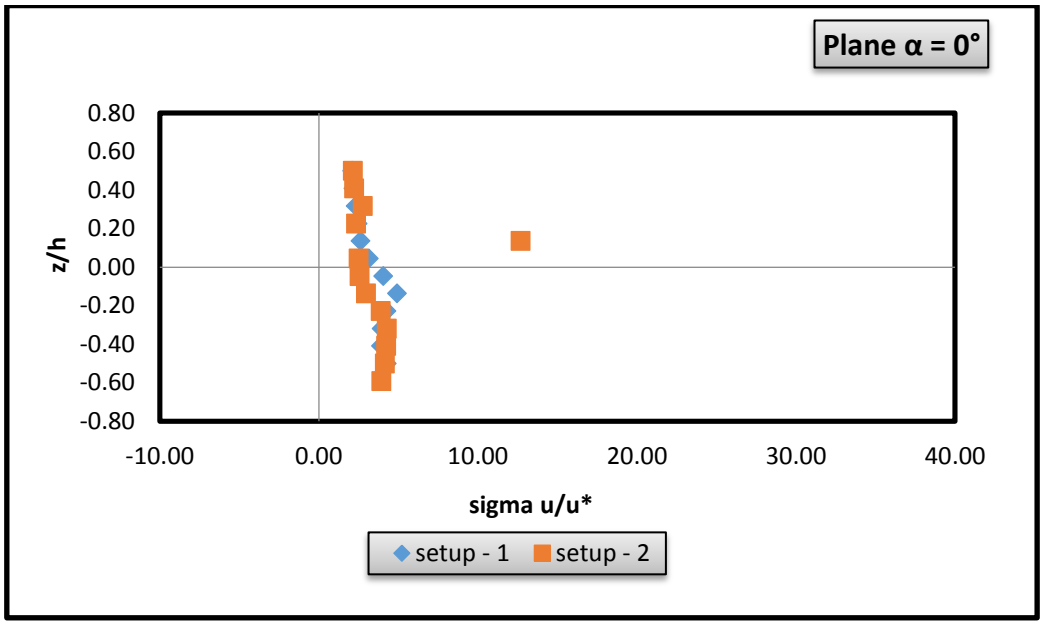
Plane α = 0°
0.80
0.60
0.40
0.20
0.00
-0.20
-0.40
-0.60
-0.80
z/h
-10.00
0.00
10.00
20.00
30.00
40.00
sigma u/u*
setup - 1
setup - 2

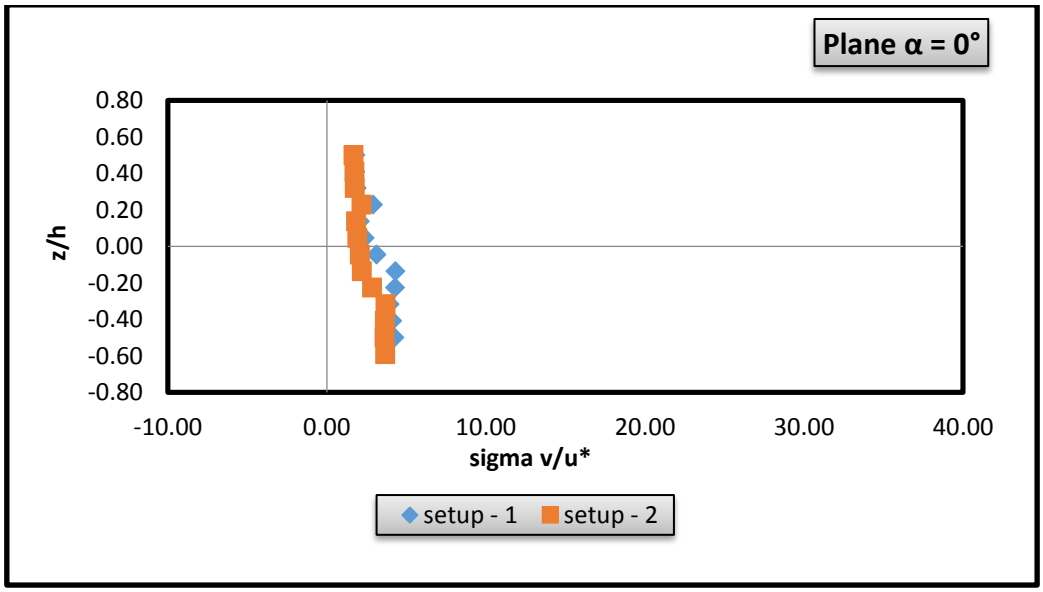
Plane α = 0°
0.80
0.60
0.40
0.20
0.00
-0.20
-0.40
-0.60
-0.80
z/h
-10.00
0.00
10.00
20.00
30.00
40.00
sigma v/u*
setup - 1
setup - 2

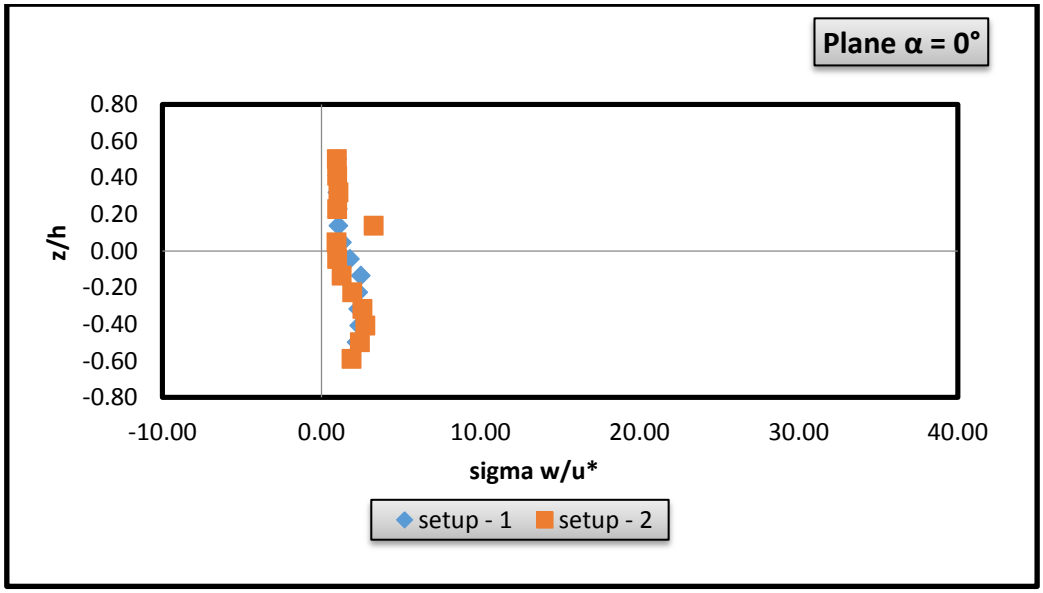
Plane α = 0°
0.80
0.60
0.40
0.20
0.00
-0.20
-0.40
-0.60
-0.80
z/h
-10.00
0.00
10.00
20.00
30.00
40.00
sigma w/u*
setup - 1
setup - 2

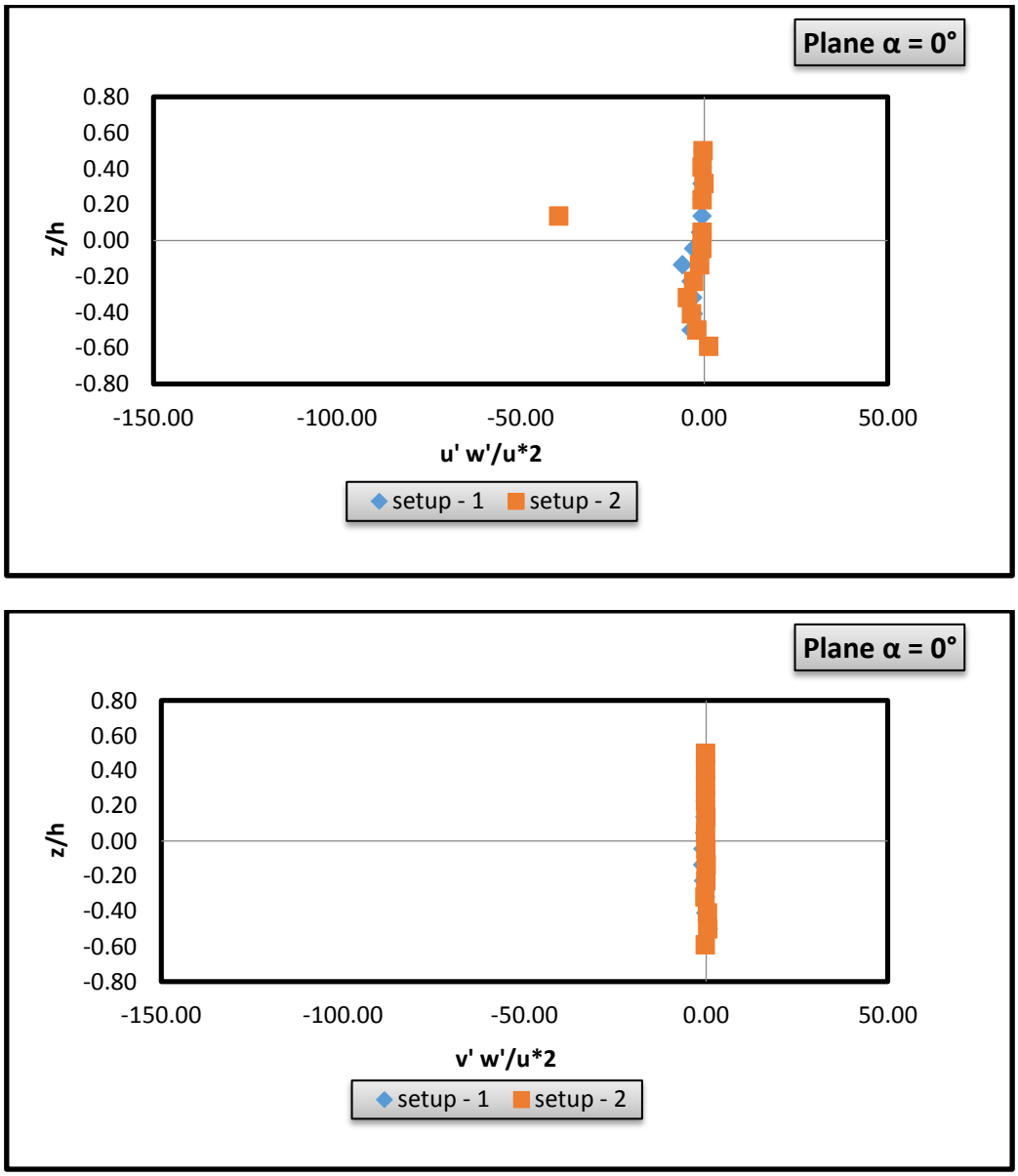

Fig 4.37 Comparison of normalized turbulence intensities and Reynolds stresses in upstream of vertical and inclined pier (α =0°) at r = 9.5 cm.

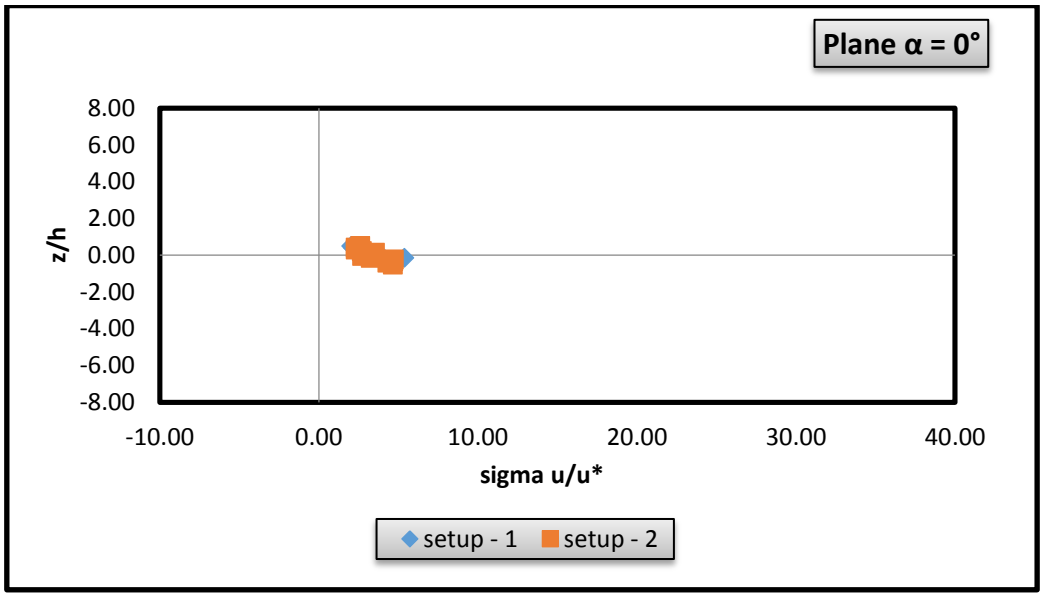
Plane α = 0°
8.00
6.00
4.00
2.00
0.00
-2.00
-4.00
-6.00
-8.00
z/h
-10.00
0.00
10.00
20.00
30.00
40.00
sigma u/u*
setup - 1
setup - 2

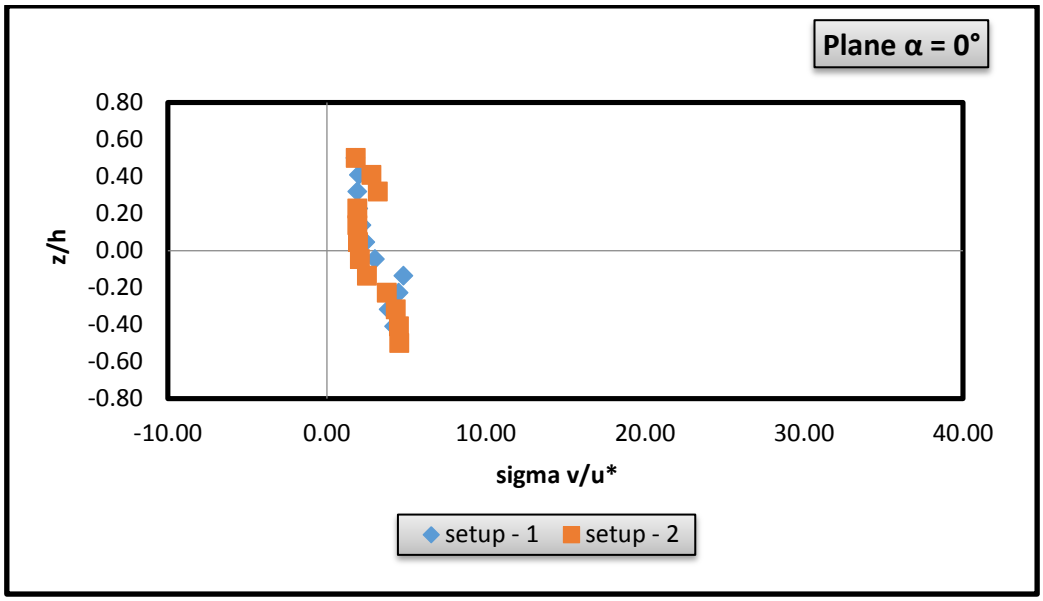
Plane α = 0°
0.80
0.60
0.40
0.20
0.00
-0.20
-0.40
-0.60
-0.80
z/h
-10.00
0.00
10.00
20.00
30.00
40.00
sigma v/u*
setup - 1
setup - 2

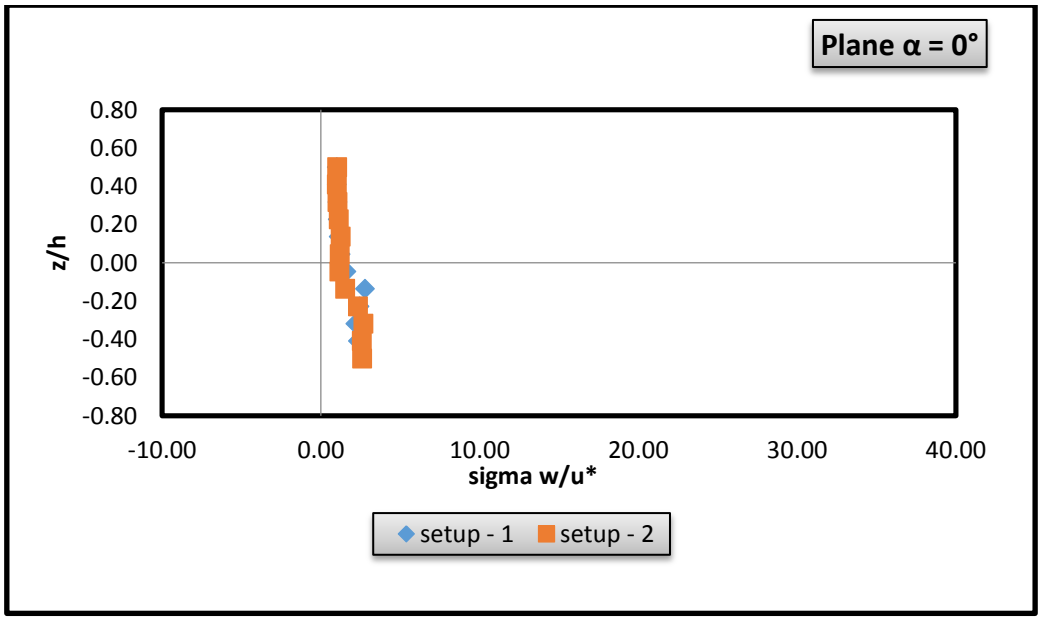
Plane α = 0°
0.80
0.60
0.40
0.20
0.00
-0.20
-0.40
-0.60
-0.80
z/h
-10.00
0.00
10.00
20.00
30.00
40.00
sigma w/u*
setup - 1
setup - 2

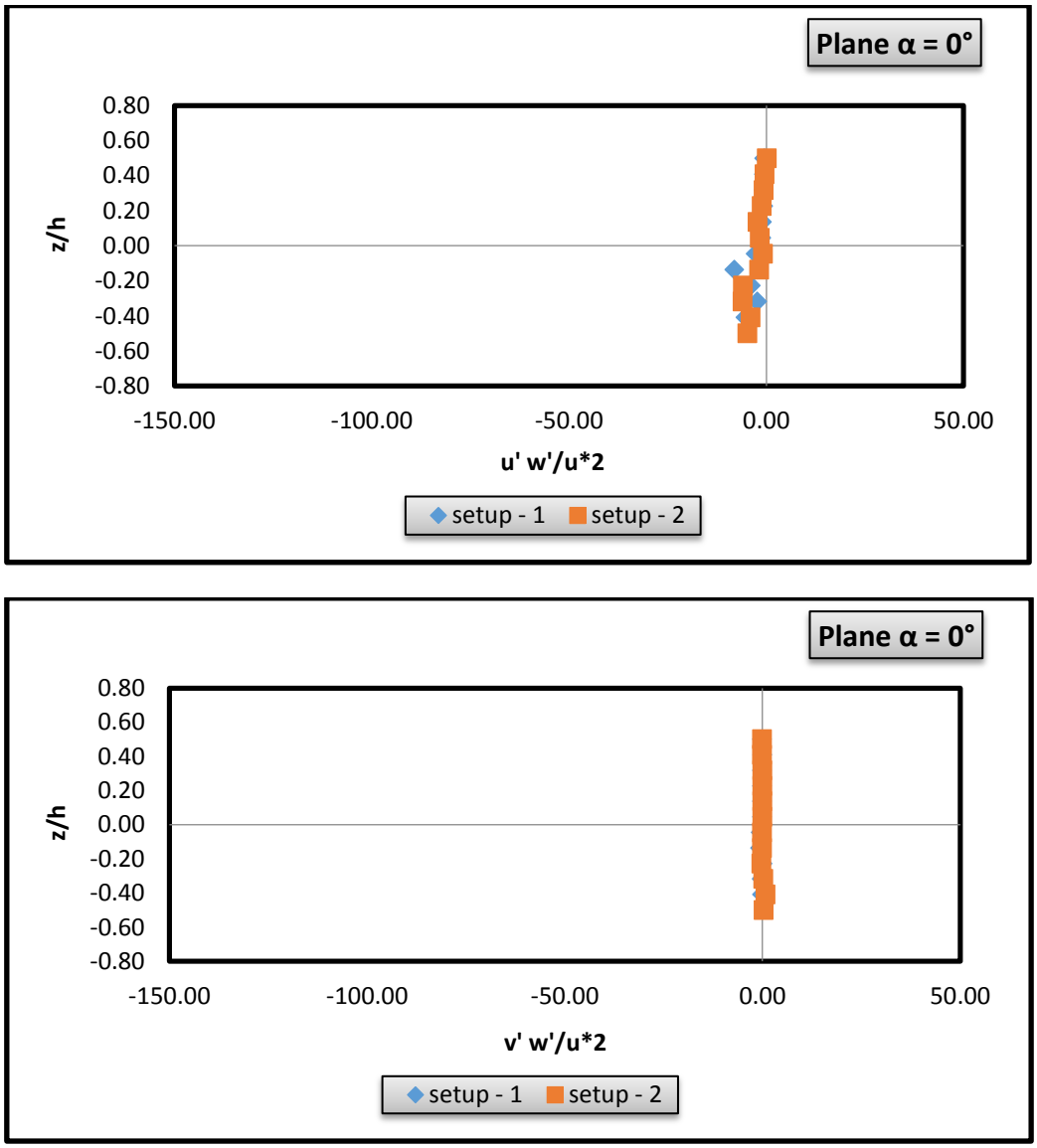

Fig 4.38 Comparison of normalized turbulence intensities and Reynolds stresses in upstream of vertical and inclined pier (α =0°) at r = 11.5 cm.

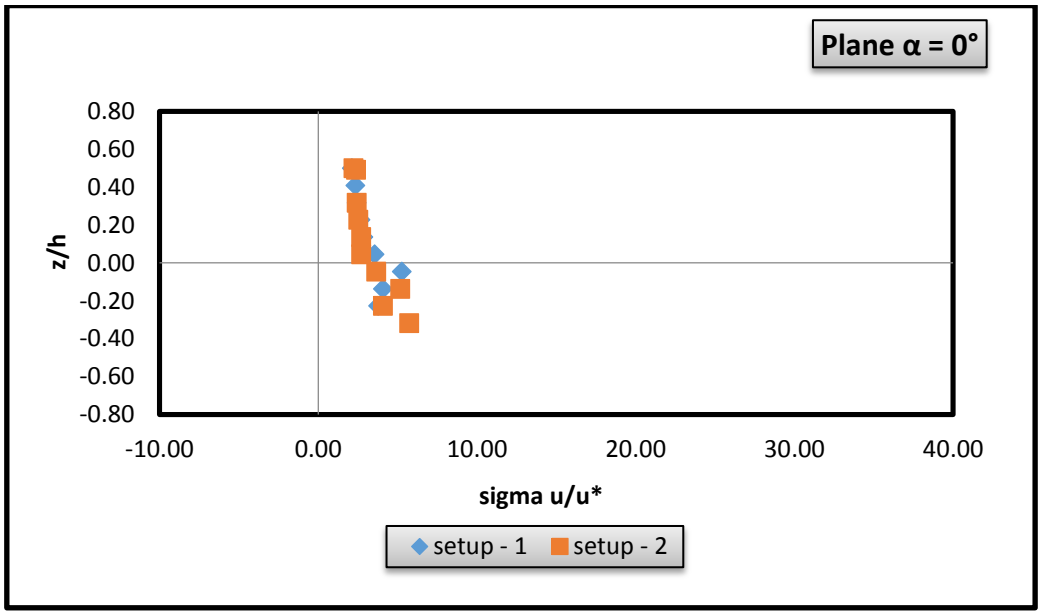
Plane α = 0°
0.80
0.60
0.40
0.20
0.00
-0.20
-0.40
-0.60
-0.80
z/h
-10.00
0.00
10.00
20.00
30.00
40.00
sigma u/u*
setup - 1
setup - 2

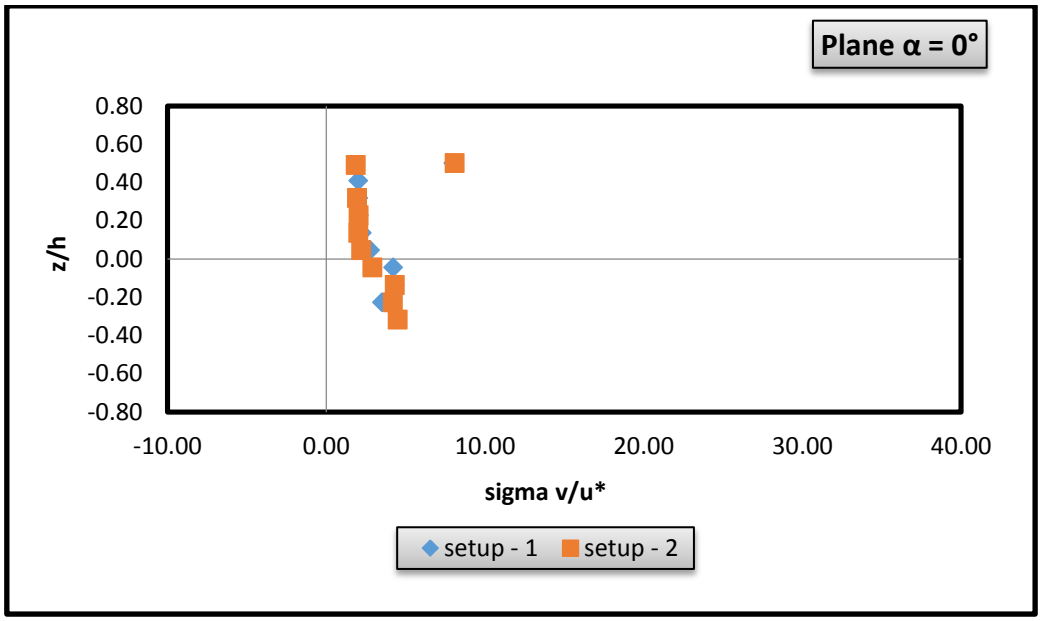
Plane α = 0°
0.80
0.60
0.40
0.20
0.00
-0.20
-0.40
-0.60
-0.80
z/h
-10.00
0.00
10.00
20.00
30.00
40.00
sigma v/u*
setup - 1
setup - 2

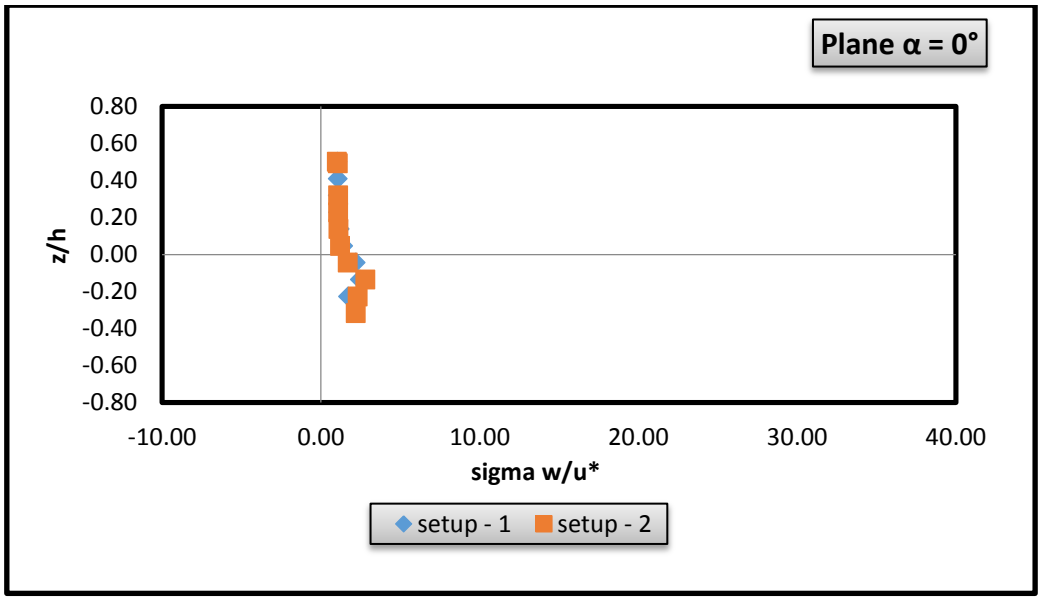
Plane α = 0°
0.80
0.60
0.40
0.20
0.00
-0.20
-0.40
-0.60
-0.80
z/h
-10.00
0.00
10.00
20.00
30.00
40.00
sigma w/u*
setup - 1
setup - 2

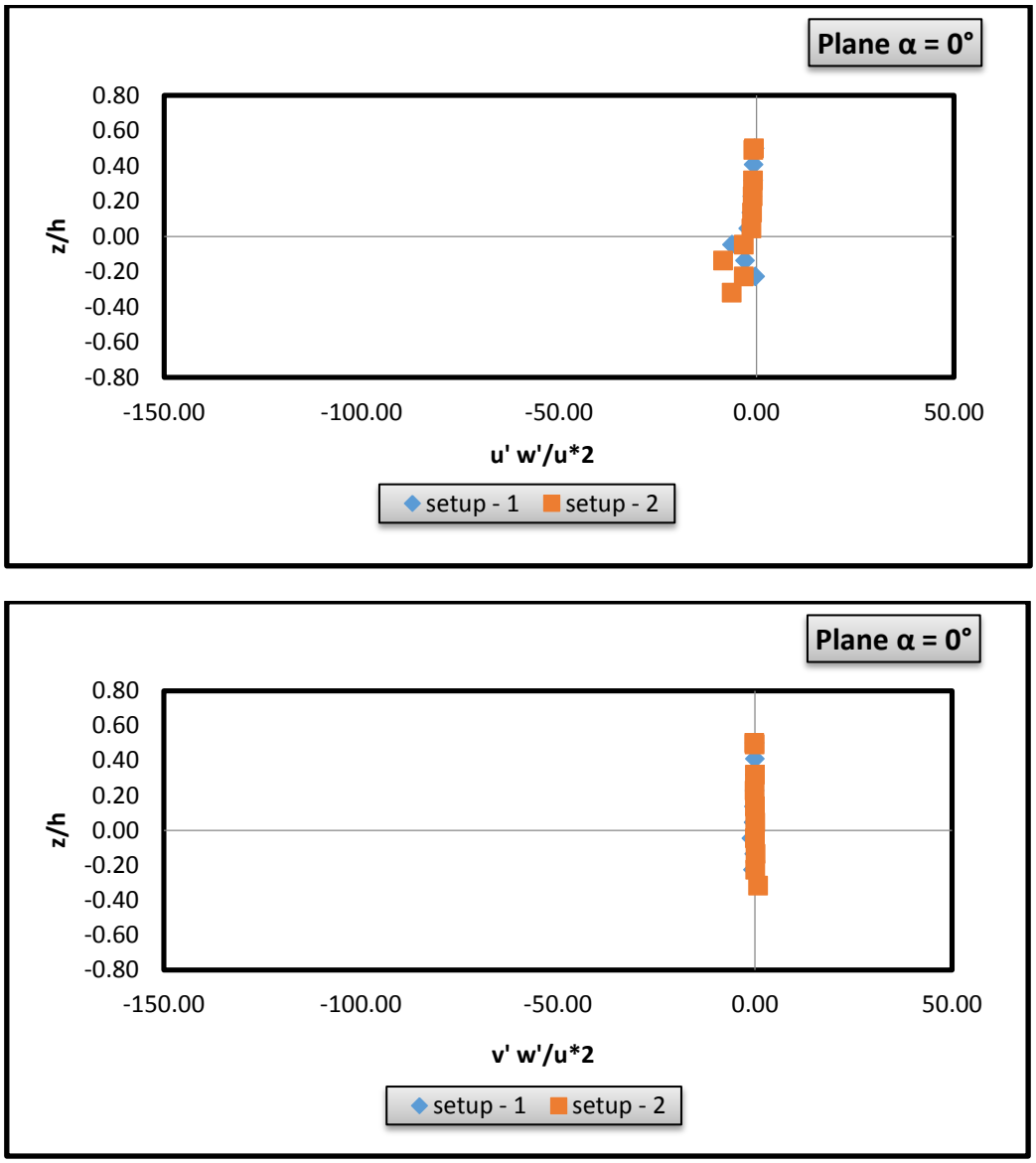

Fig 4.39 Comparison of normalized turbulence intensities and Reynolds stresses in upstream of vertical and inclined pier (α =0°) at r = 13.5 cm.

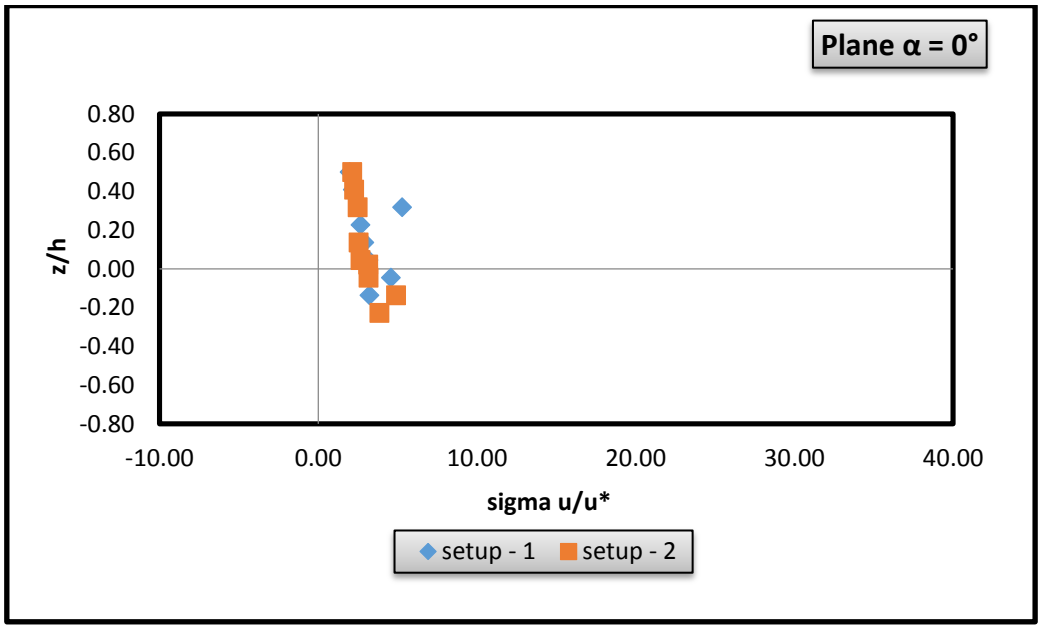
Plane α = 0°
0.80
0.60
0.40
0.20
0.00
-0.20
-0.40
-0.60
-0.80
z/h
-10.00
0.00
10.00
20.00
30.00
40.00
sigma u/u*
setup - 1
setup - 2

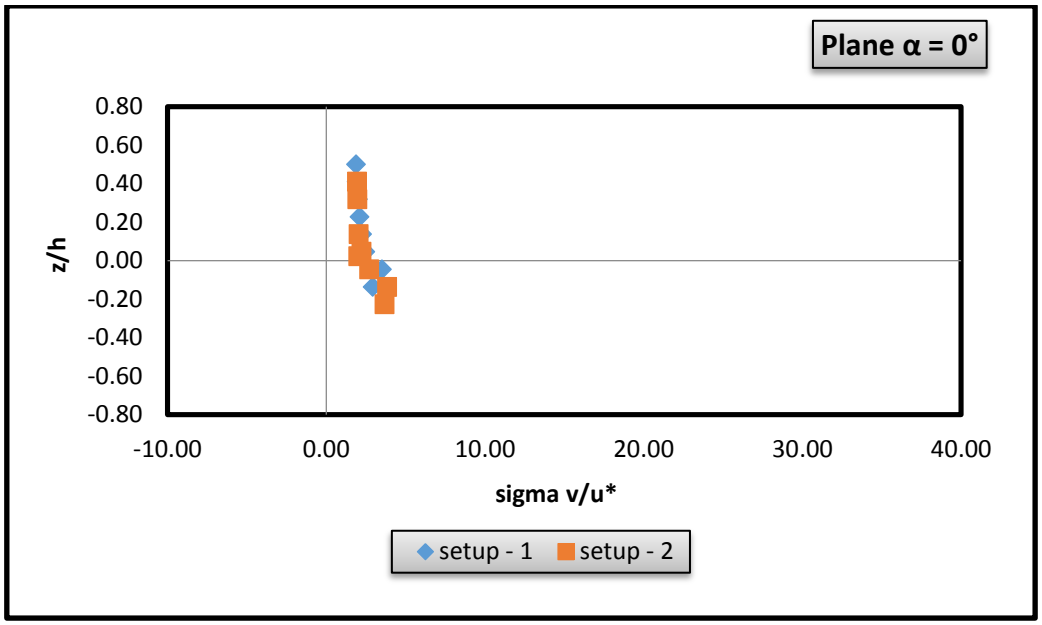
Plane α = 0°
0.80
0.60
0.40
0.20
0.00
-0.20
-0.40
-0.60
-0.80
z/h
-10.00
0.00
10.00
20.00
30.00
40.00
sigma v/u*
setup - 1
setup - 2

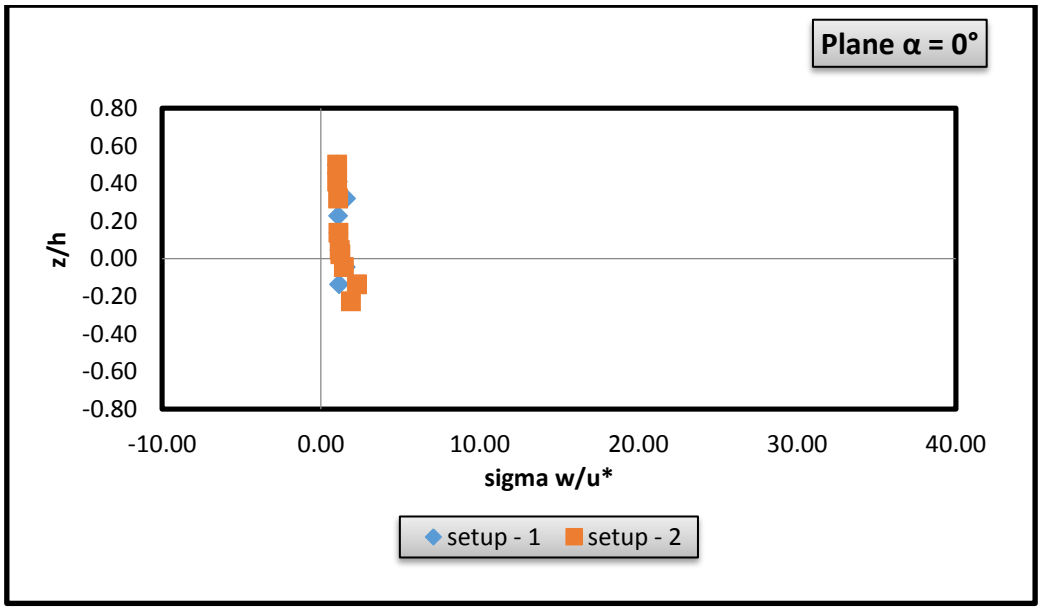
Plane α = 0°
0.80
0.60
0.40
0.20
0.00
-0.20
-0.40
-0.60
-0.80
z/h
-10.00
0.00
10.00
20.00
30.00
40.00
sigma w/u*
setup - 1
setup - 2

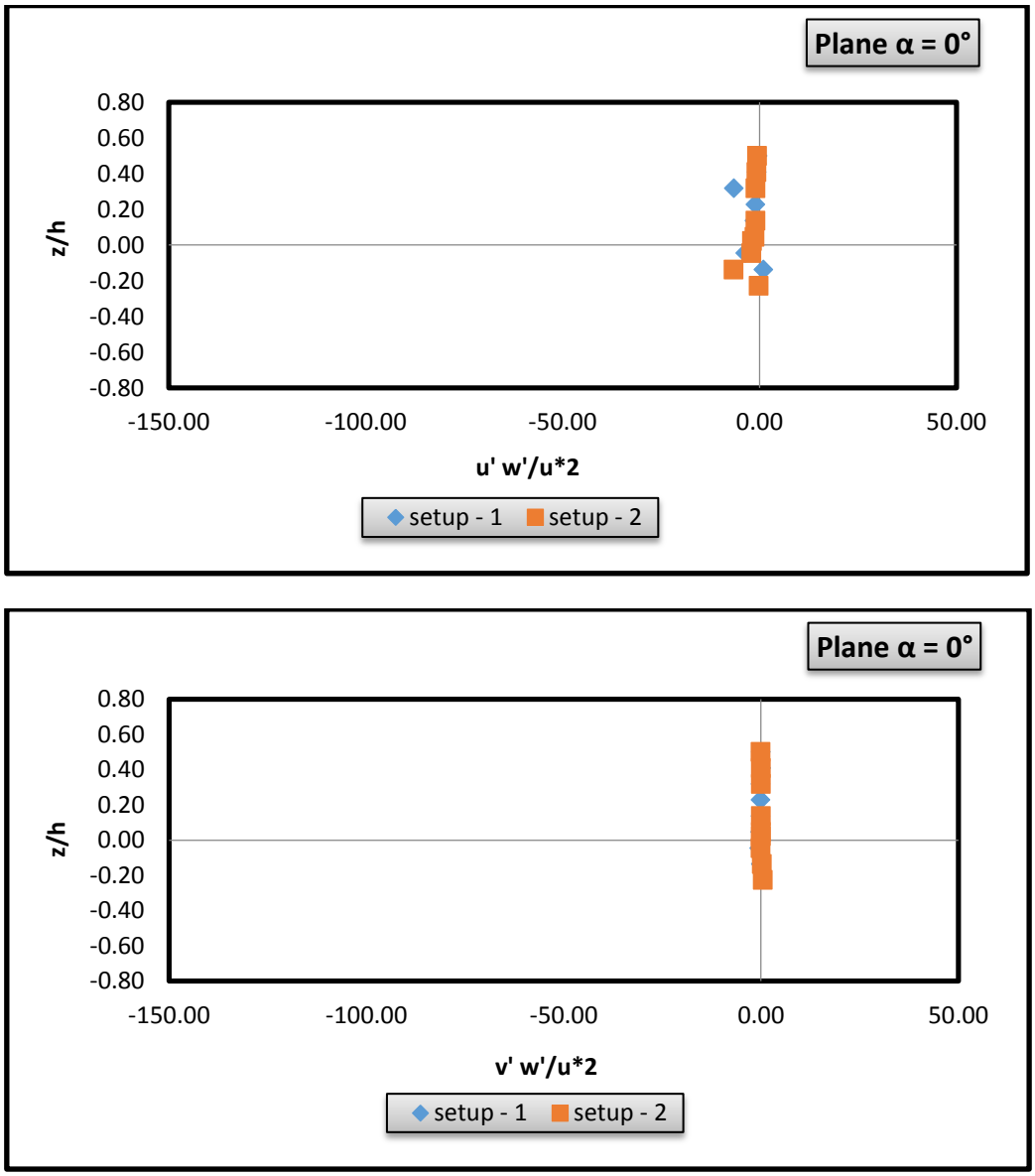

Fig 4.40 Comparison of normalized turbulence intensities and Reynolds stresses in upstream of vertical and inclined pier (α =0°) at r = 15.5 cm.

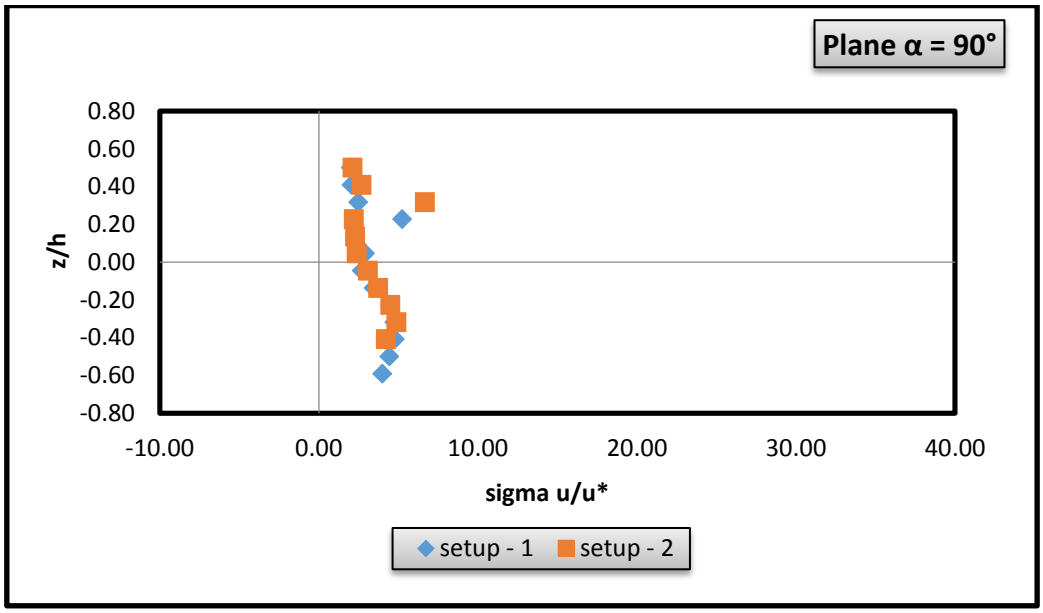
Plane α = 90°
0.80
0.60
0.40
0.20
0.00
-0.20
-0.40
-0.60
-0.80
z/h
-10.00
0.00
10.00
20.00
30.00
40.00
sigma u/u*
setup - 1
setup - 2

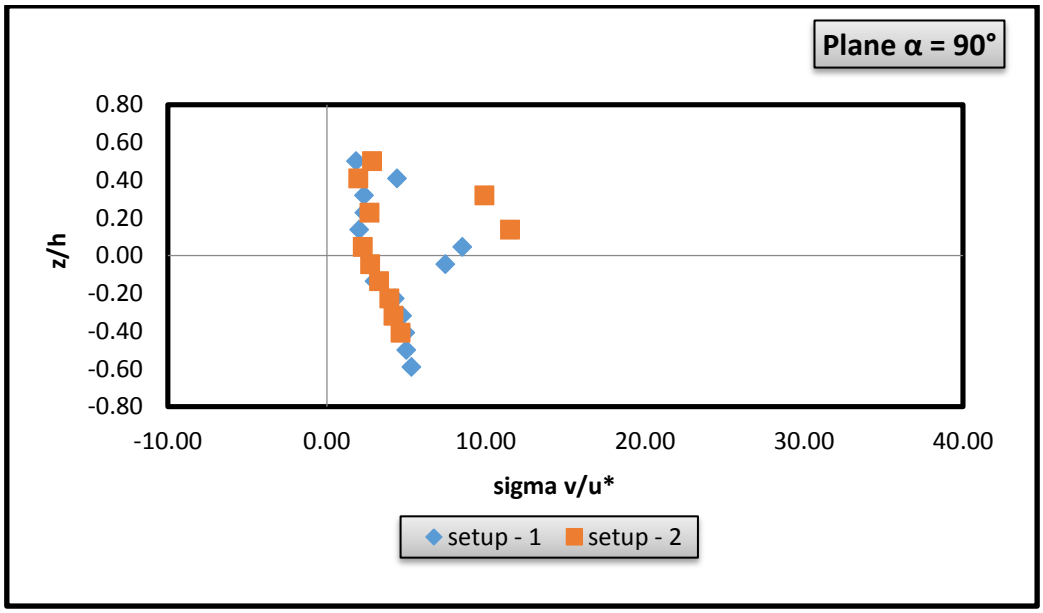
Plane α = 90°
0.80
0.60
0.40
0.20
0.00
-0.20
-0.40
-0.60
-0.80
z/h
-10.00
0.00
10.00
20.00
30.00
40.00
sigma v/u*
setup - 1
setup - 2

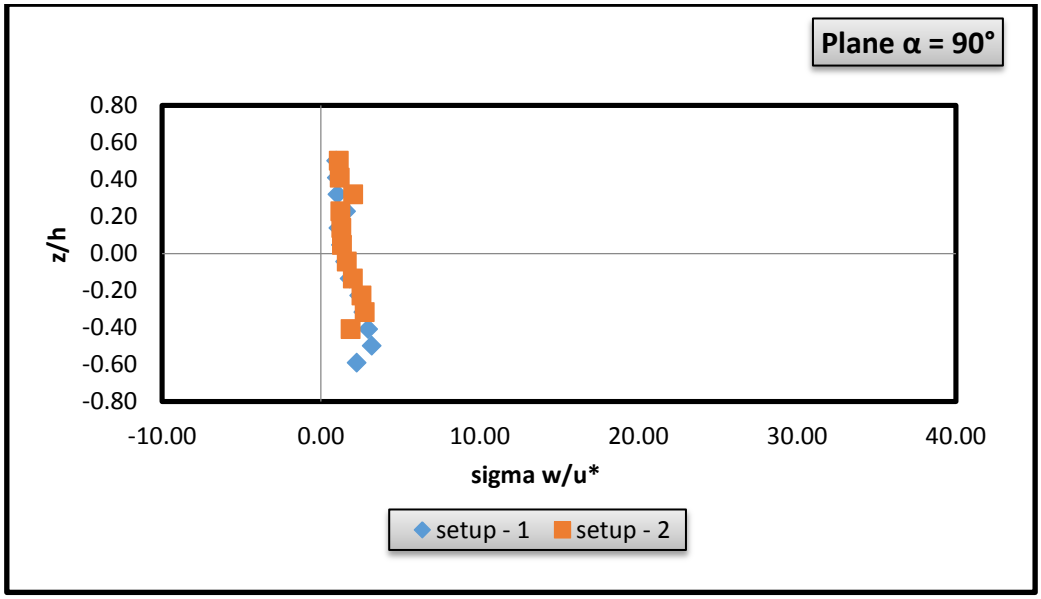
Plane α = 90°
0.80
0.60
0.40
0.20
0.00
-0.20
-0.40
-0.60
-0.80
z/h
-10.00
0.00
10.00
20.00
30.00
40.00
sigma w/u*
setup - 1
setup - 2

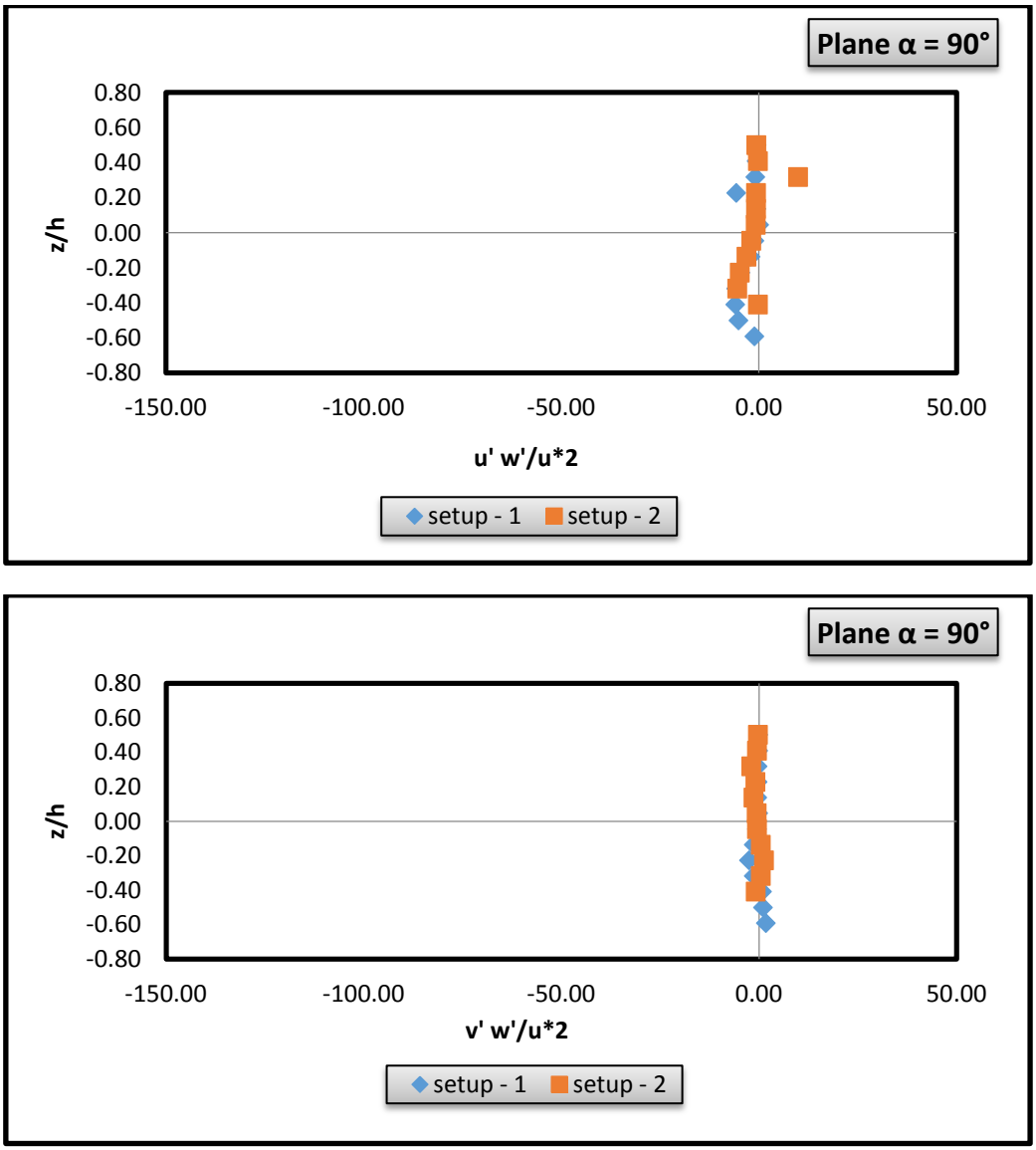

Fig 4.41 Comparison of normalized turbulence intensities and Reynolds stresses in side stream of vertical and inclined pier (α = 90°) at r = 7.5 cm.

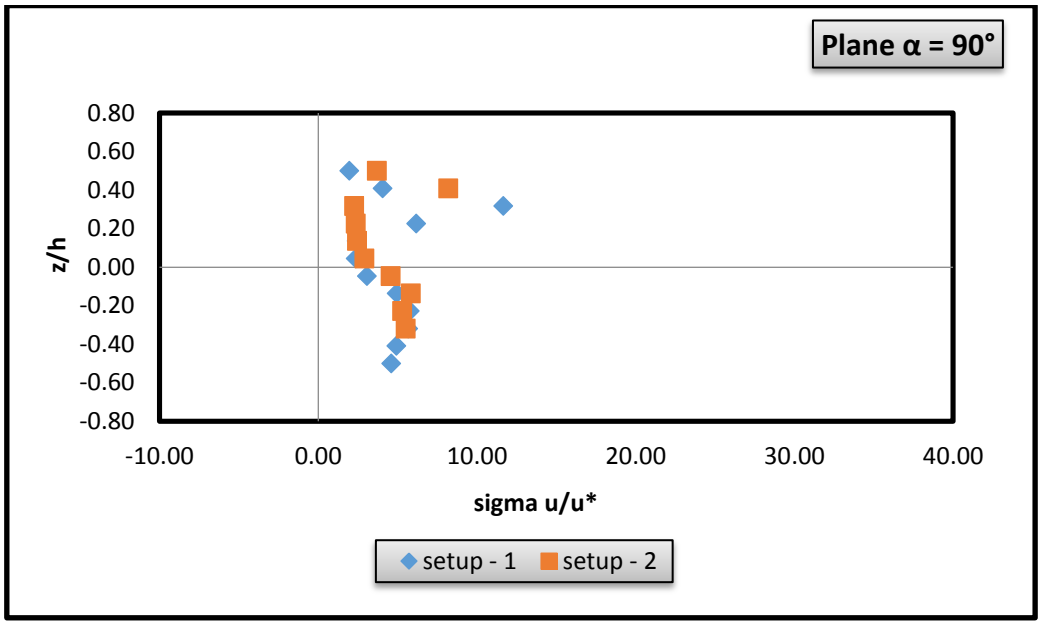
Plane α = 90°
0.80
0.60
0.40
0.20
0.00
-0.20
-0.40
-0.60
-0.80
z/h
-10.00
0.00
10.00
20.00
30.00
40.00
sigma u/u*
setup - 1
setup - 2

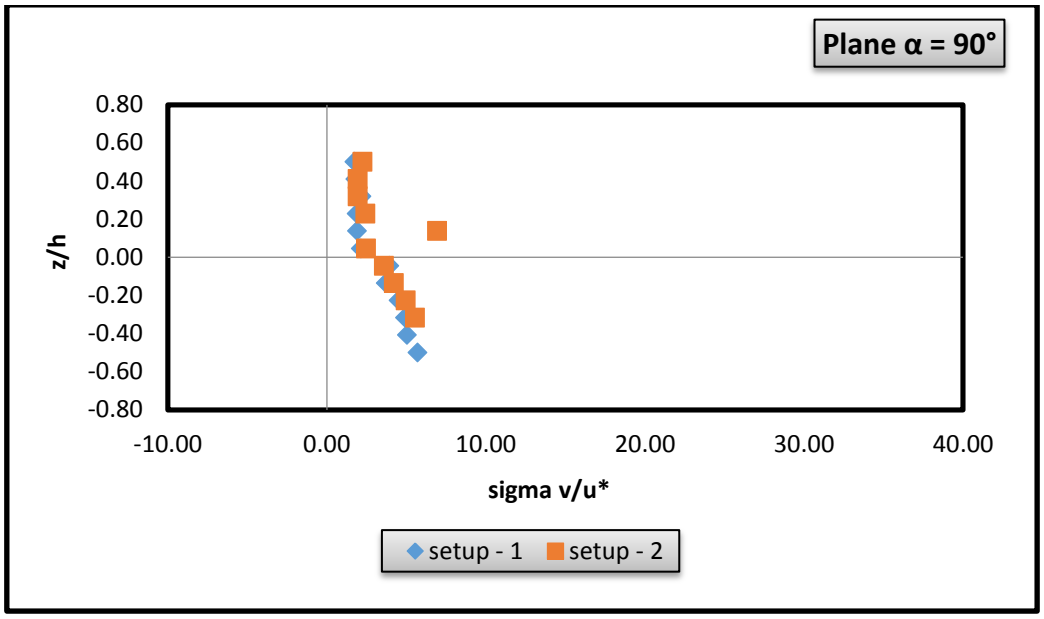
Plane α = 90°
0.80
0.60
0.40
0.20
0.00
-0.20
-0.40
-0.60
-0.80
z/h
-10.00
0.00
10.00
20.00
30.00
40.00
sigma v/u*
setup - 1
setup - 2

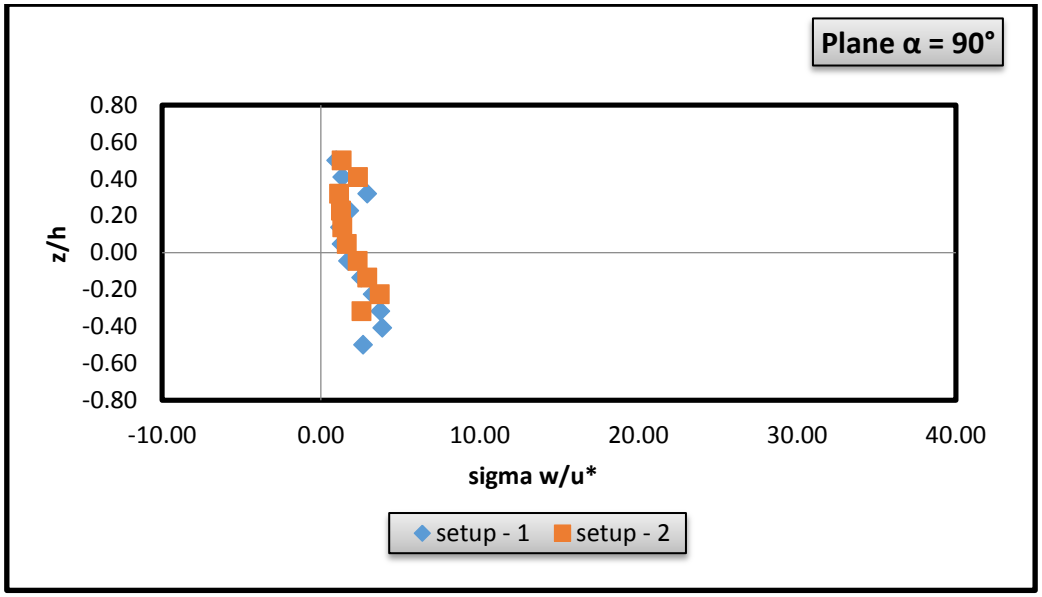
Plane α = 90°
0.80
0.60
0.40
0.20
0.00
-0.20
-0.40
-0.60
-0.80
z/h
-10.00
0.00
10.00
20.00
30.00
40.00
sigma w/u*
setup - 1
setup - 2

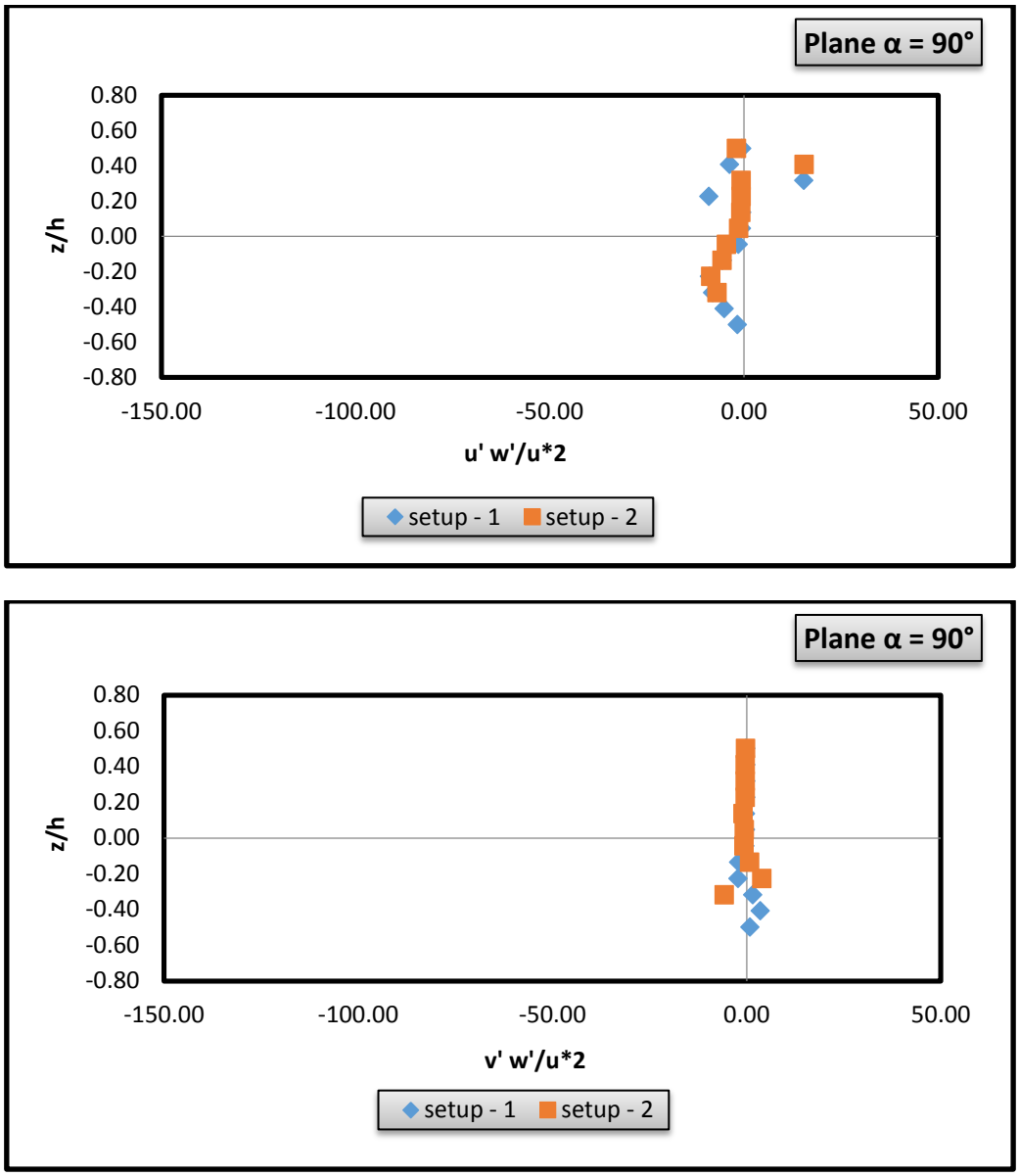

Fig 4.42 Comparison of normalized turbulence intensities and Reynolds stresses in side stream of vertical and inclined pier (α = 90°) at r = 9.5 cm.

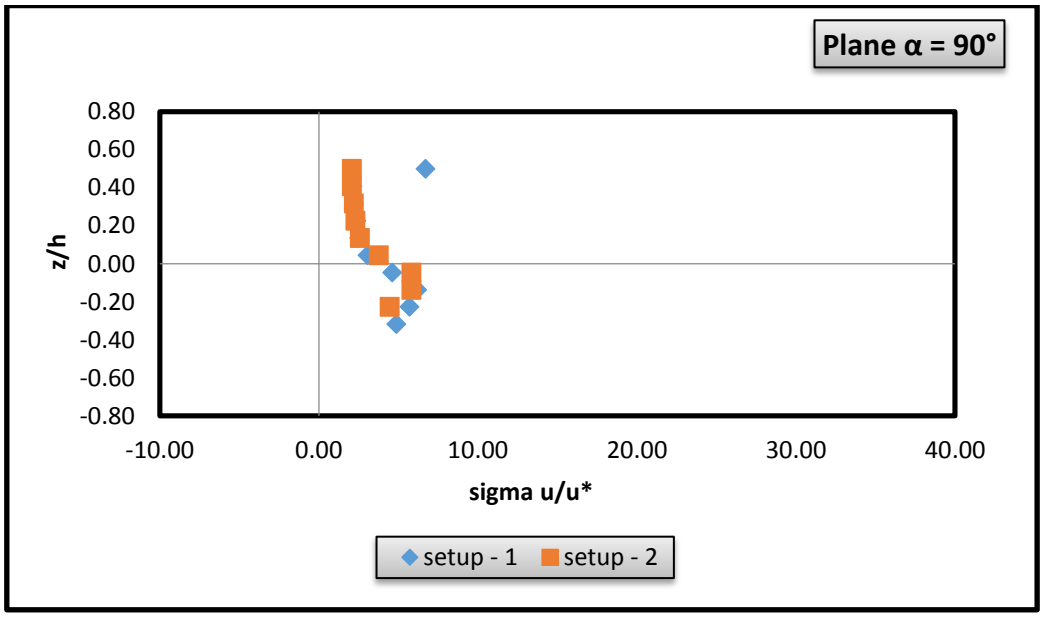
Plane α = 90°
0.80
0.60
0.40
0.20
0.00
-0.20
-0.40
-0.60
-0.80
z/h
-10.00
0.00
10.00
20.00
30.00
40.00
sigma u/u*
setup - 1
setup - 2

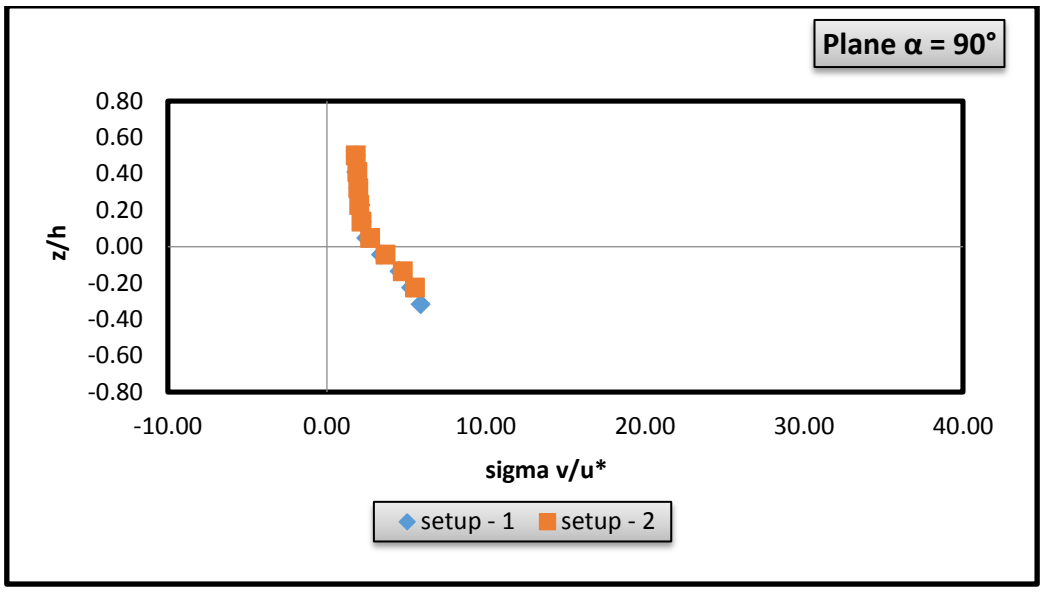
Plane α = 90°
0.80
0.60
0.40
0.20
0.00
-0.20
-0.40
-0.60
-0.80
z/h
-10.00
0.00
10.00
20.00
30.00
40.00
sigma v/u*
setup - 1
setup - 2

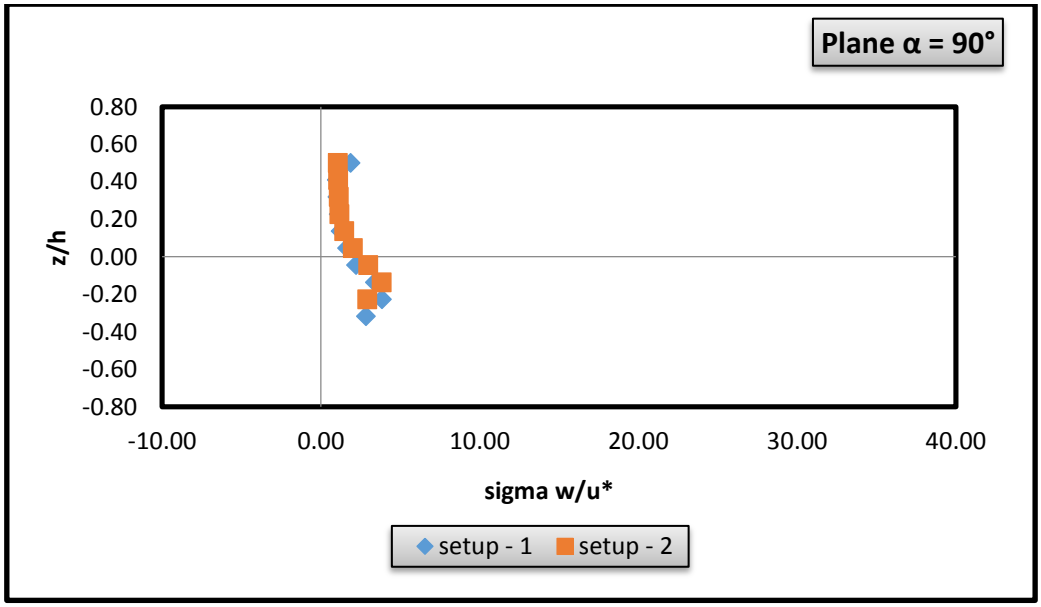
Plane α = 90°
0.80
0.60
0.40
0.20
0.00
-0.20
-0.40
-0.60
-0.80
z/h
-10.00
0.00
10.00
20.00
30.00
40.00
sigma w/u*
setup - 1
setup - 2

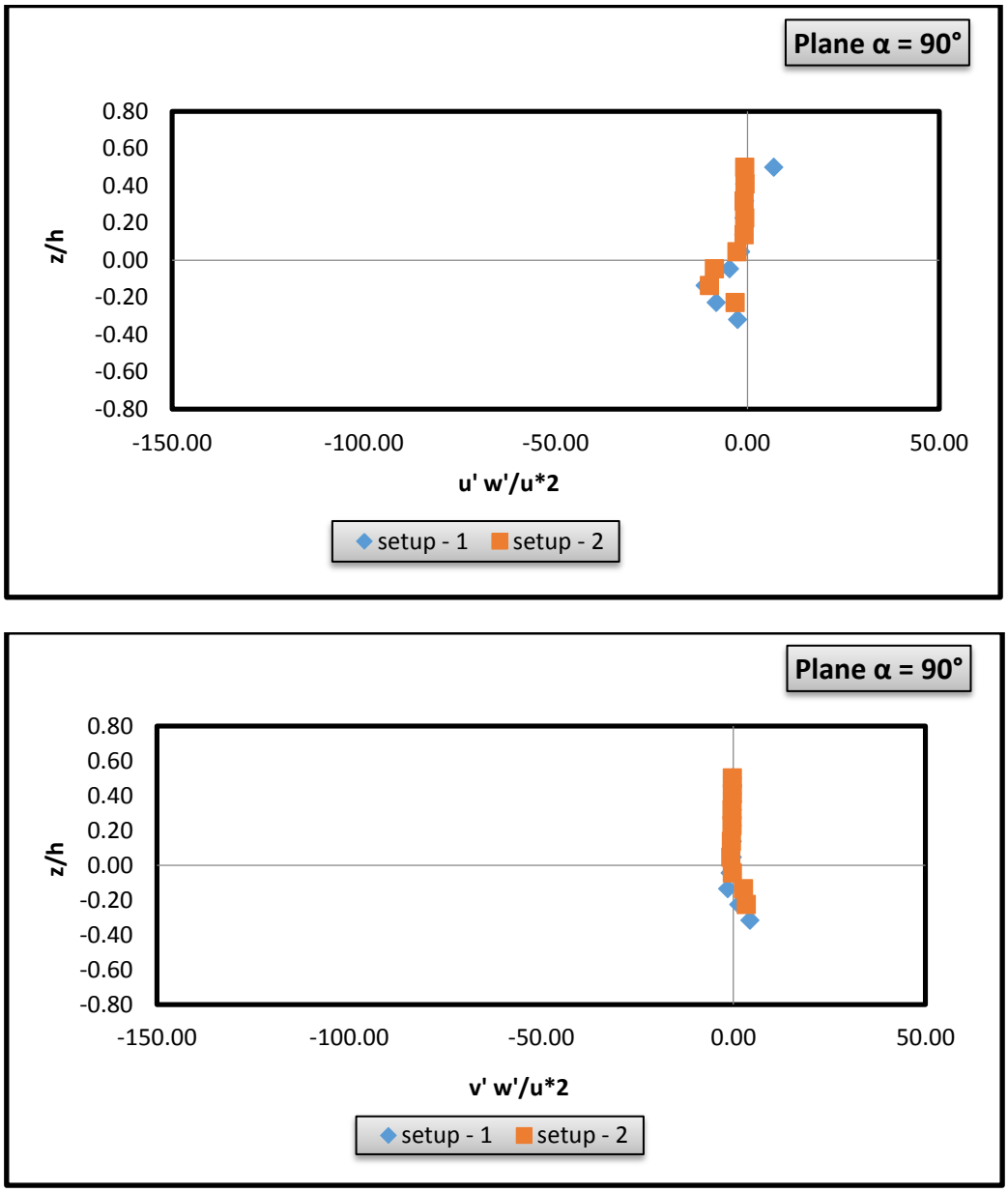

Fig 4.43 Comparison of normalized turbulence intensities and Reynolds stresses in side stream of vertical and inclined pier (α = 90°) at r = 11.5 cm.

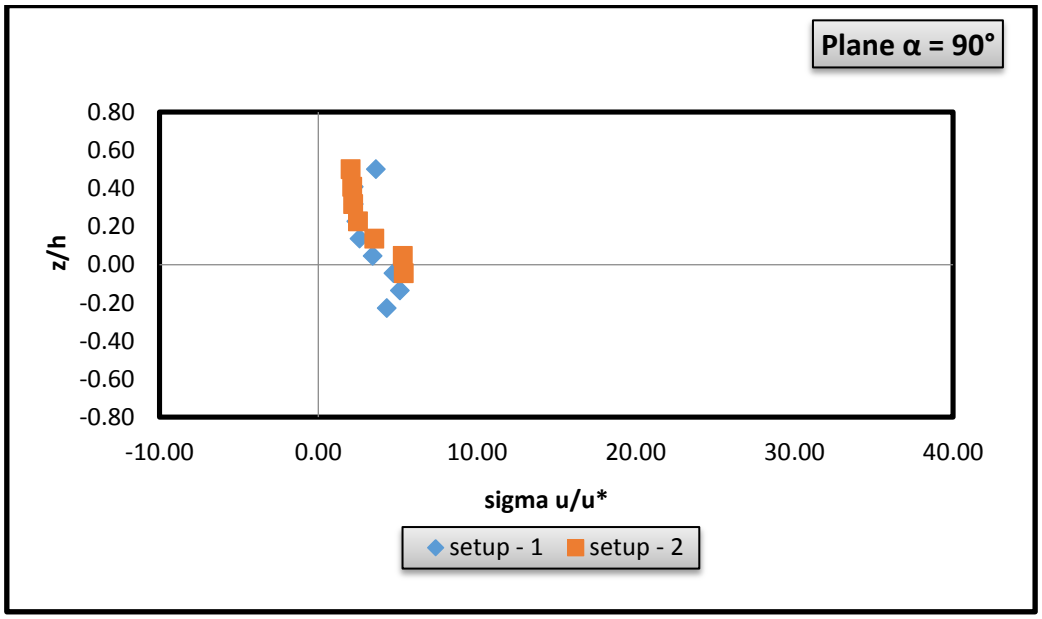
Plane α = 90°
0.80
0.60
0.40
0.20
0.00
-0.20
-0.40
-0.60
-0.80
z/h
-10.00
0.00
10.00
20.00
30.00
40.00
sigma u/u*
setup - 1
setup - 2

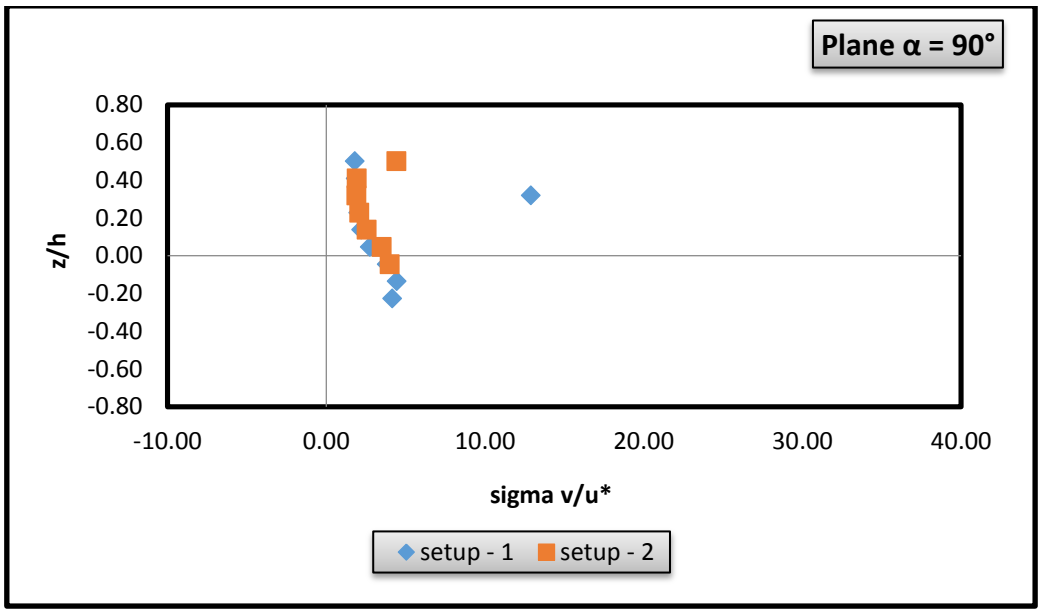
Plane α = 90°
0.80
0.60
0.40
0.20
0.00
-0.20
-0.40
-0.60
-0.80
z/h
-10.00
0.00
10.00
20.00
30.00
40.00
sigma v/u*
setup - 1
setup - 2

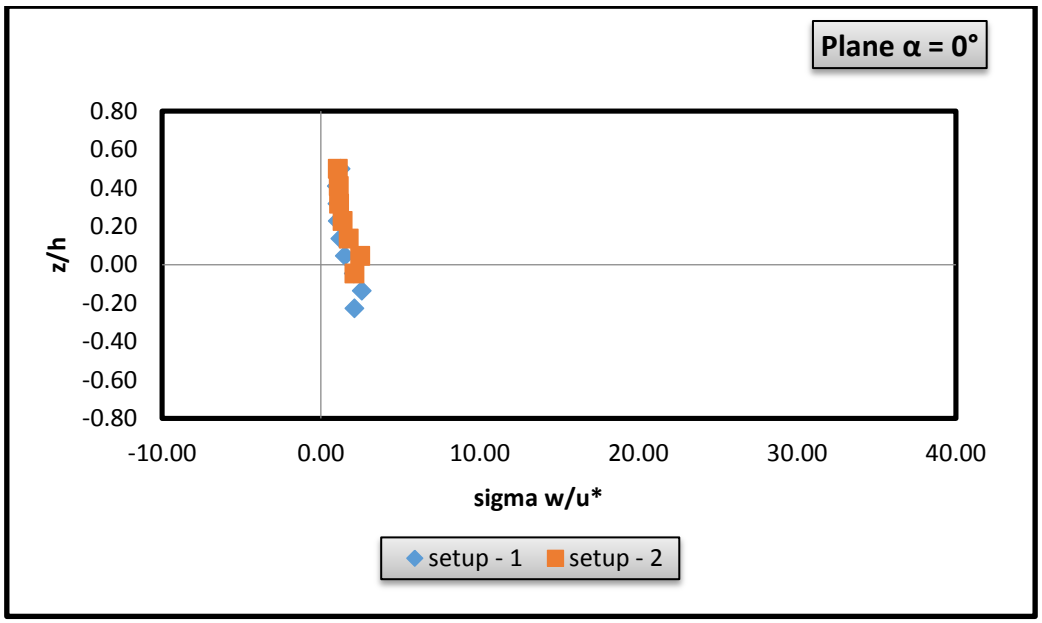
Plane α = 0°
0.80
0.60
0.40
0.20
0.00
-0.20
-0.40
-0.60
-0.80
z/h
-10.00
0.00
10.00
20.00
30.00
40.00
sigma w/u*
setup - 1
setup - 2

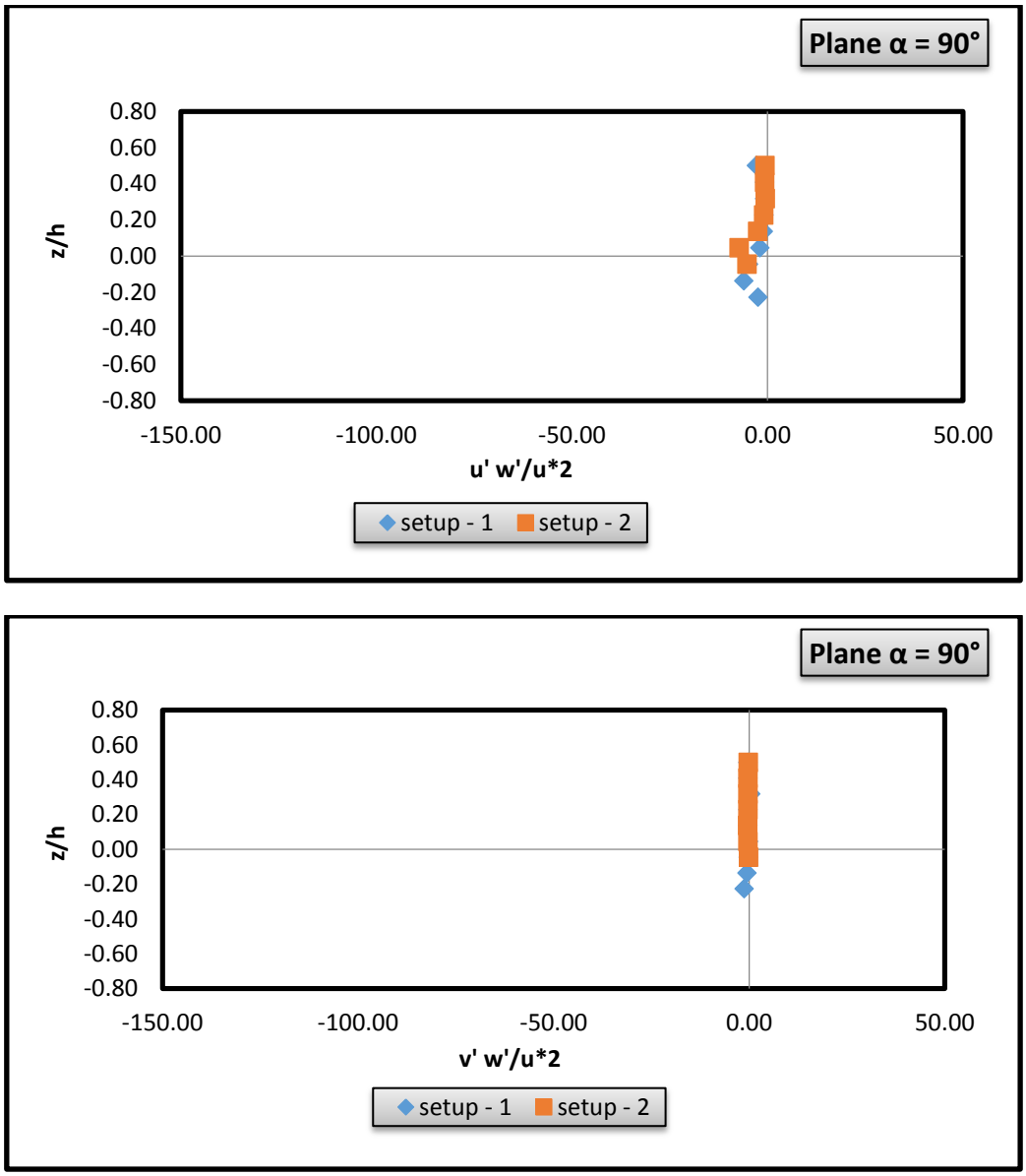

Fig 4.44 Comparison of normalized turbulence intensities and Reynolds stresses in side stream of vertical and inclined pier (α = 90°) at r = 13.5 cm.

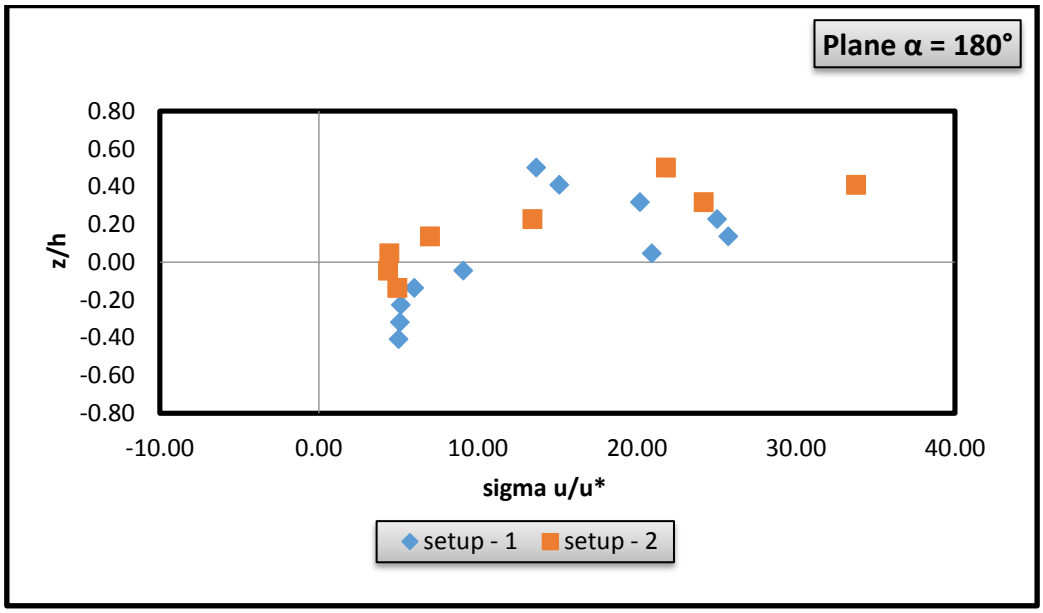
Plane α = 180°
0.80
0.60
0.40
0.20
0.00
-0.20
-0.40
-0.60
-0.80
z/h
-10.00
0.00
10.00
20.00
30.00
40.00
sigma u/u*
setup - 1
setup - 2

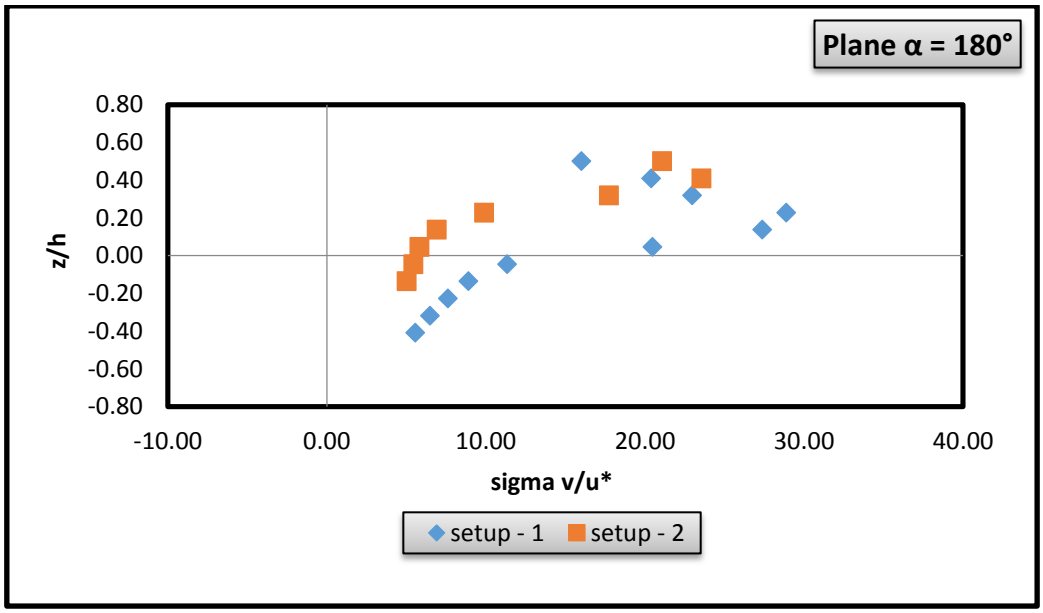
Plane α = 180°
0.80
0.60
0.40
0.20
0.00
-0.20
-0.40
-0.60
-0.80
z/h
-10.00
0.00
10.00
20.00
30.00
40.00
sigma v/u*
setup - 1
setup - 2

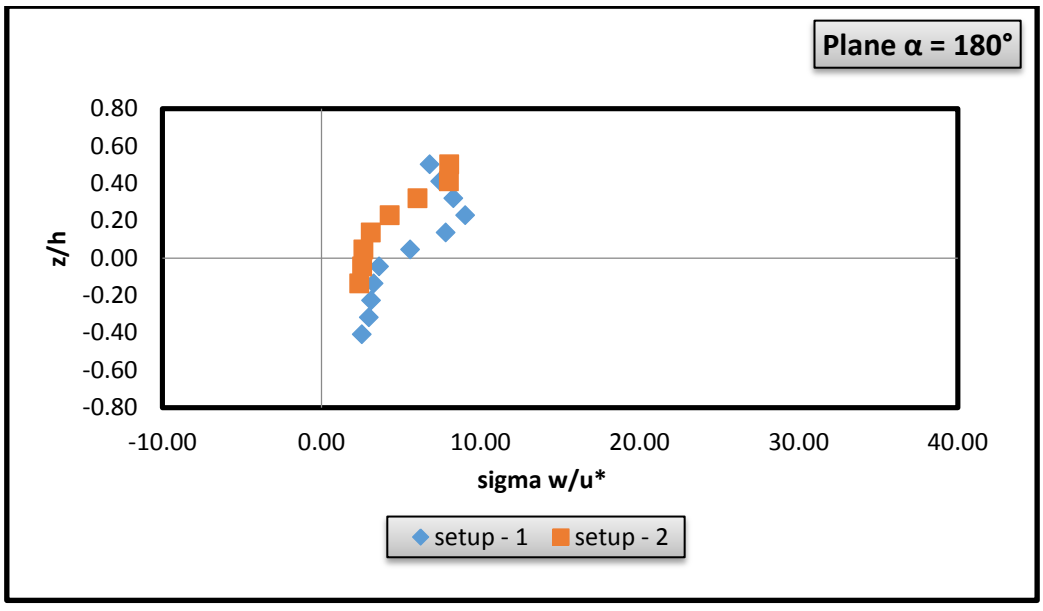
Plane α = 180°
0.80
0.60
0.40
0.20
0.00
-0.20
-0.40
-0.60
-0.80
z/h
-10.00
0.00
10.00
20.00
30.00
40.00
sigma w/u*
setup - 1
setup - 2

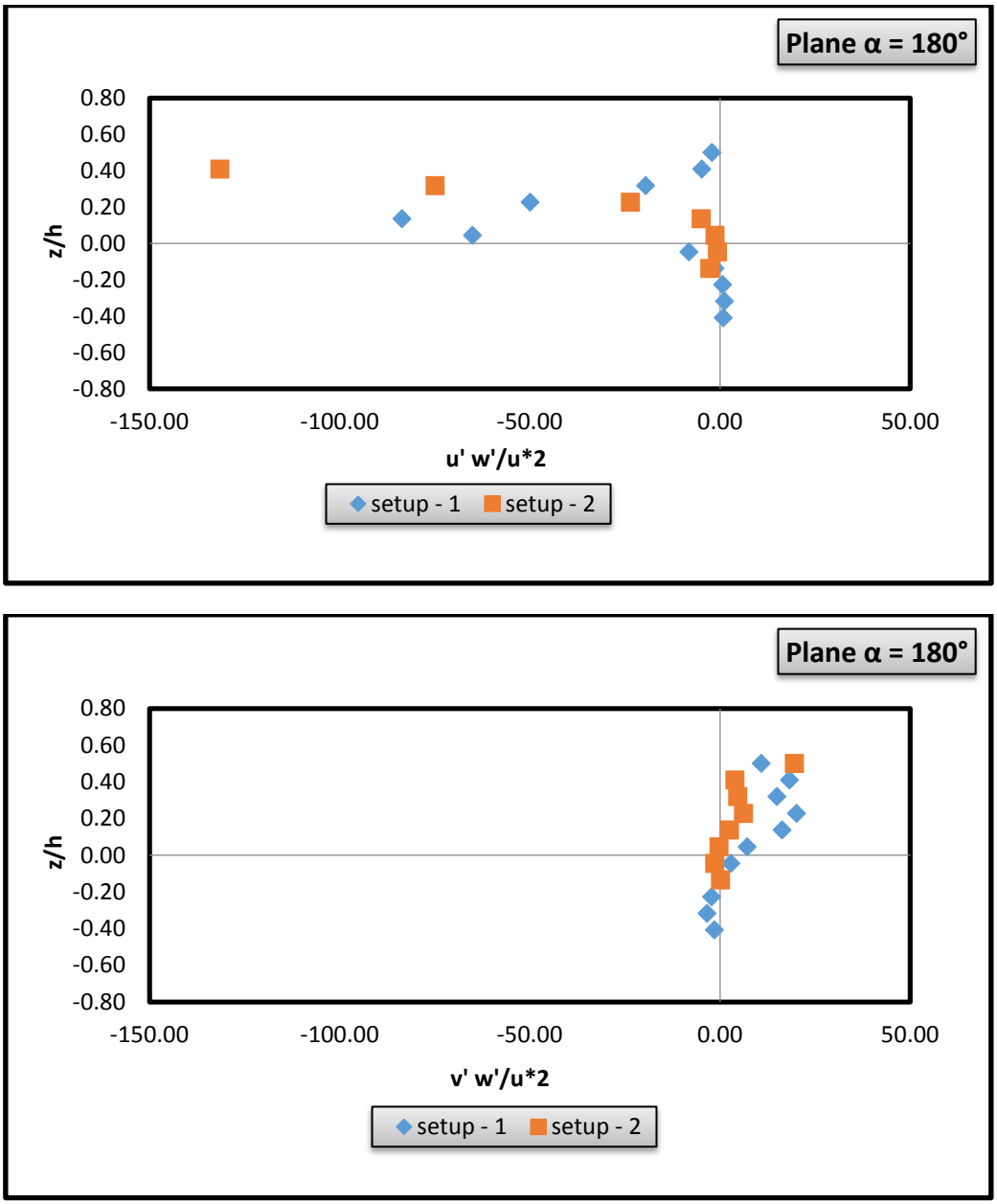

Fig 4.45 Comparison of normalized turbulence intensities and Reynolds stresses in downstream of vertical and inclined pier (α = 180°) at r = 9.5 cm.

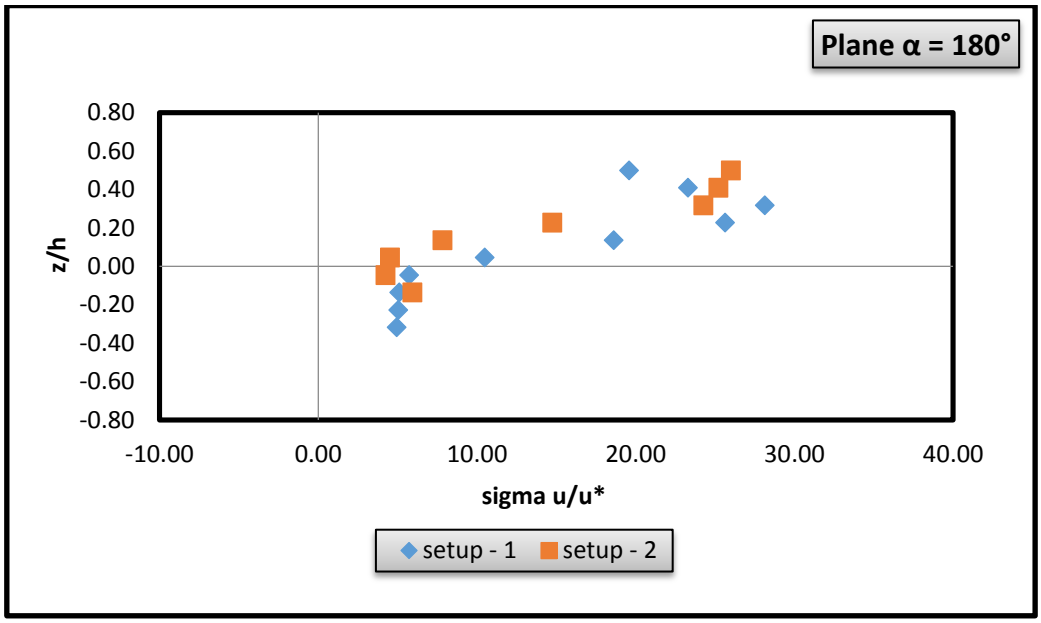
Plane α = 180°
0.80
0.60
0.40
0.20
0.00
-0.20
-0.40
-0.60
-0.80
z/h
-10.00
0.00
10.00
20.00
30.00
40.00
sigma u/u*
setup - 1
setup - 2

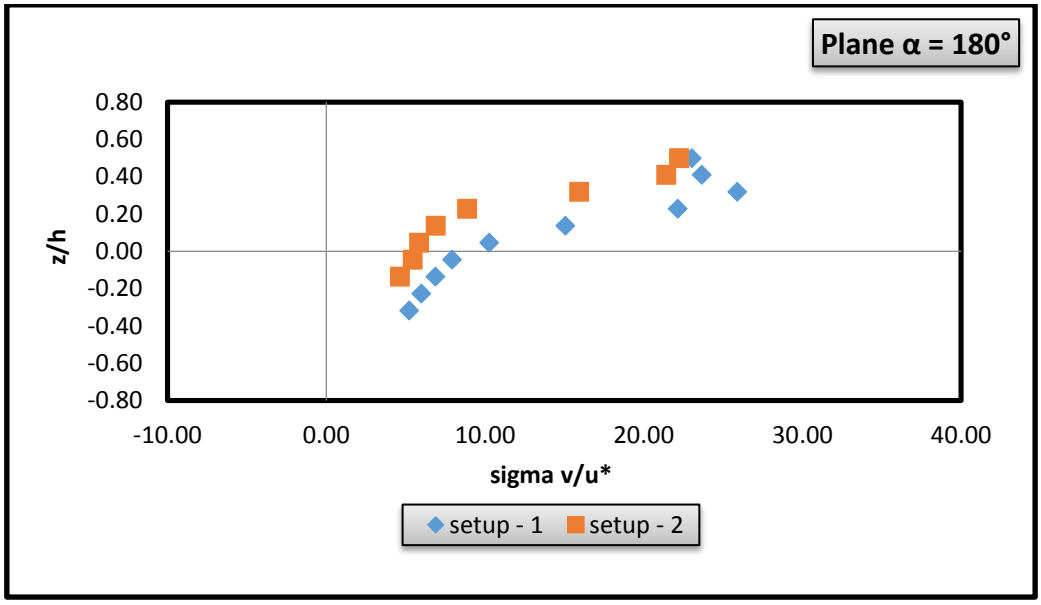
Plane α = 180°
0.80
0.60
0.40
0.20
0.00
-0.20
-0.40
-0.60
-0.80
z/h
-10.00
0.00
10.00
20.00
30.00
40.00
sigma v/u*
setup - 1
setup - 2

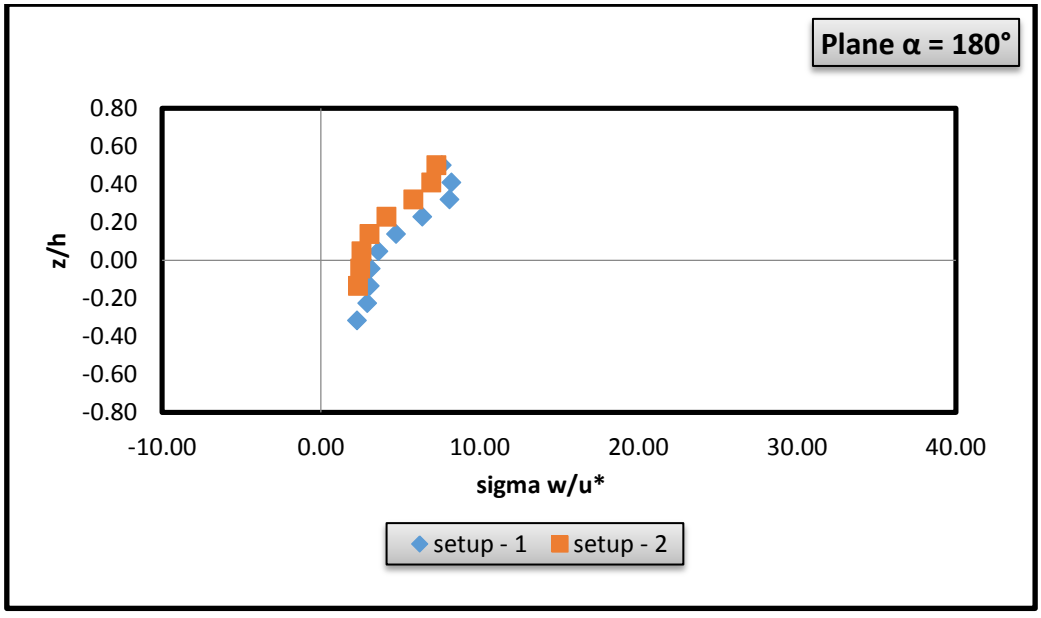
Plane α = 180°
0.80
0.60
0.40
0.20
0.00
-0.20
-0.40
-0.60
-0.80
z/h
-10.00
0.00
10.00
20.00
30.00
40.00
sigma w/u*
setup - 1
setup - 2

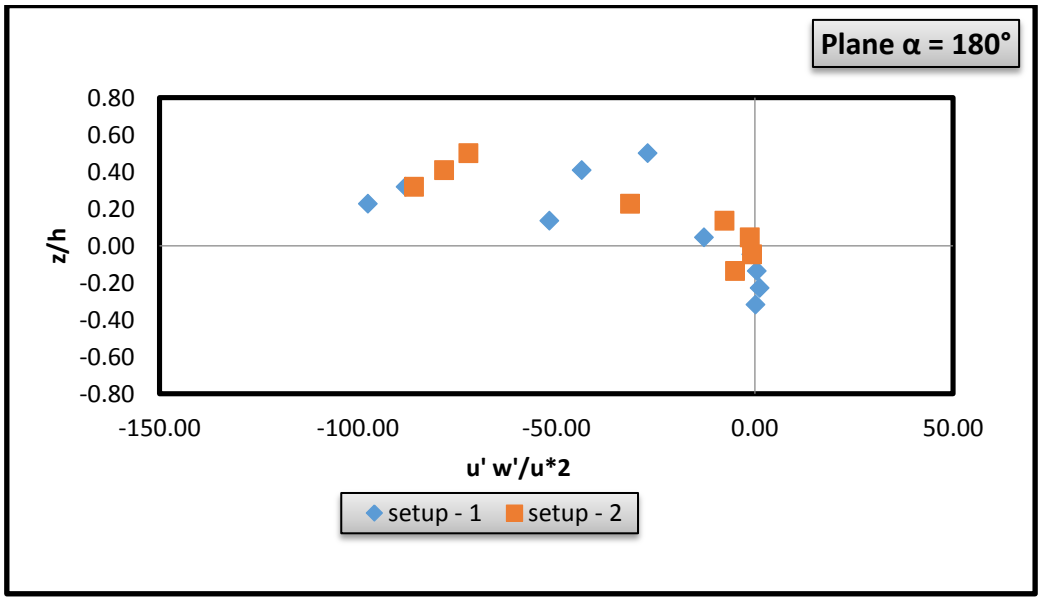

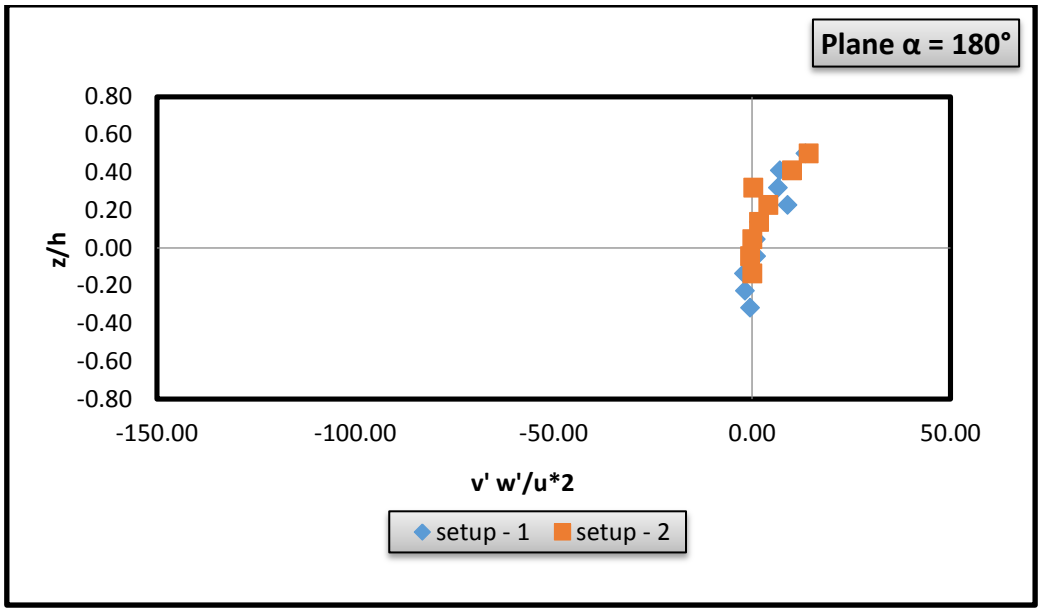

Fig 4.46 Comparison of normalized turbulence intensities and Reynolds stresses in downstream of vertical and inclined pier (α = 180°) at r = 11.5 cm.

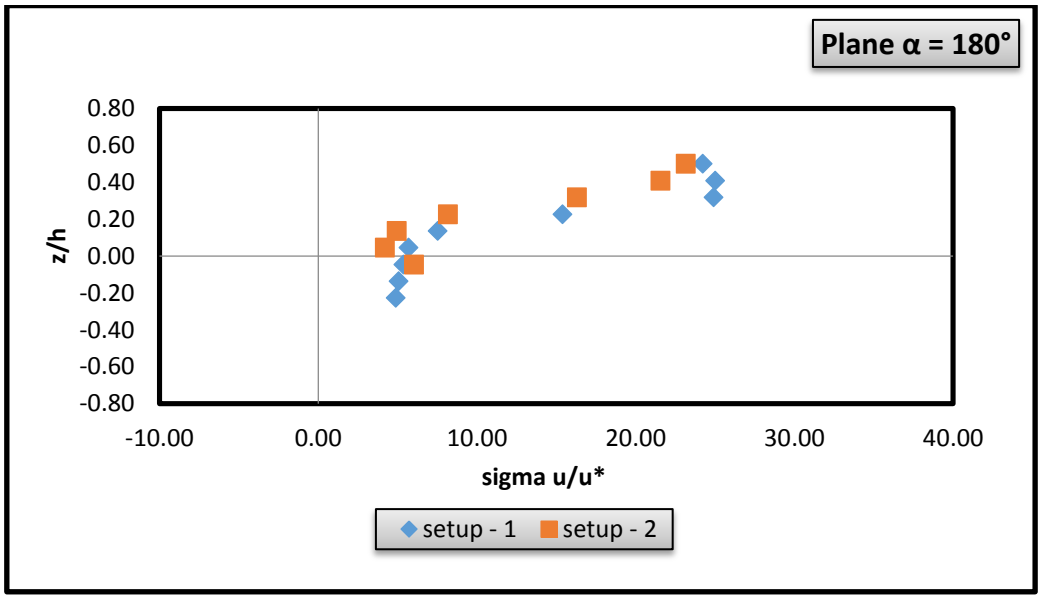
Plane α = 180°
0.80
0.60
0.40
0.20
0.00
-0.20
-0.40
-0.60
-0.80
z/h
-10.00
0.00
10.00
20.00
30.00
40.00
sigma u/u*
setup - 1
setup - 2

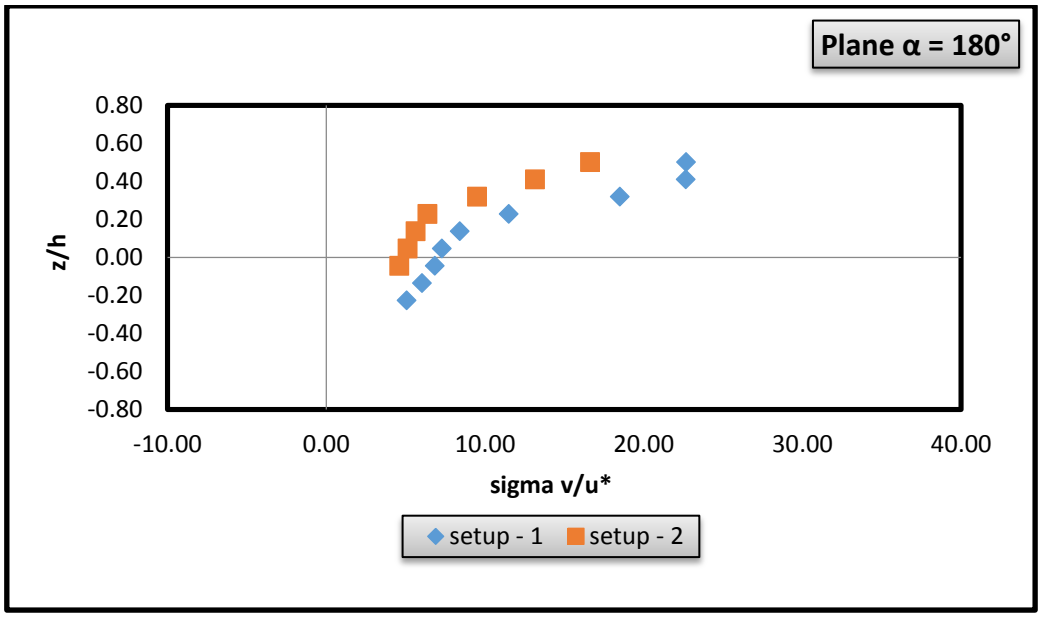
Plane α = 180°
0.80
0.60
0.40
0.20
0.00
-0.20
-0.40
-0.60
-0.80
z/h
-10.00
0.00
10.00
20.00
30.00
40.00
sigma v/u*
setup - 1
setup - 2

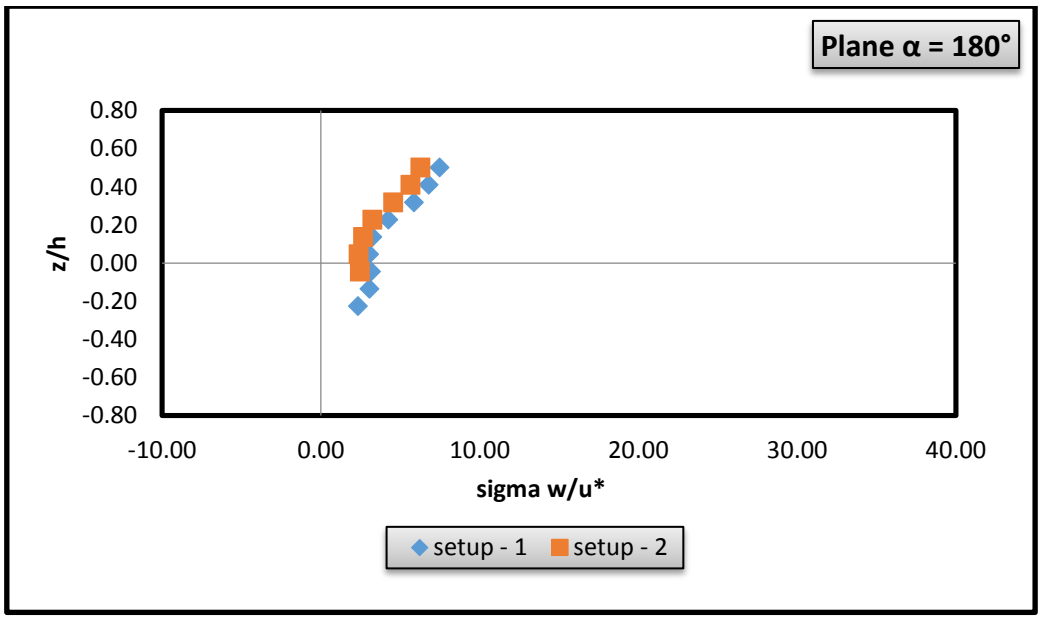
Plane α = 180°
0.80
0.60
0.40
0.20
0.00
-0.20
-0.40
-0.60
-0.80
z/h
-10.00
0.00
10.00
20.00
30.00
40.00
sigma w/u*
setup - 1
setup - 2

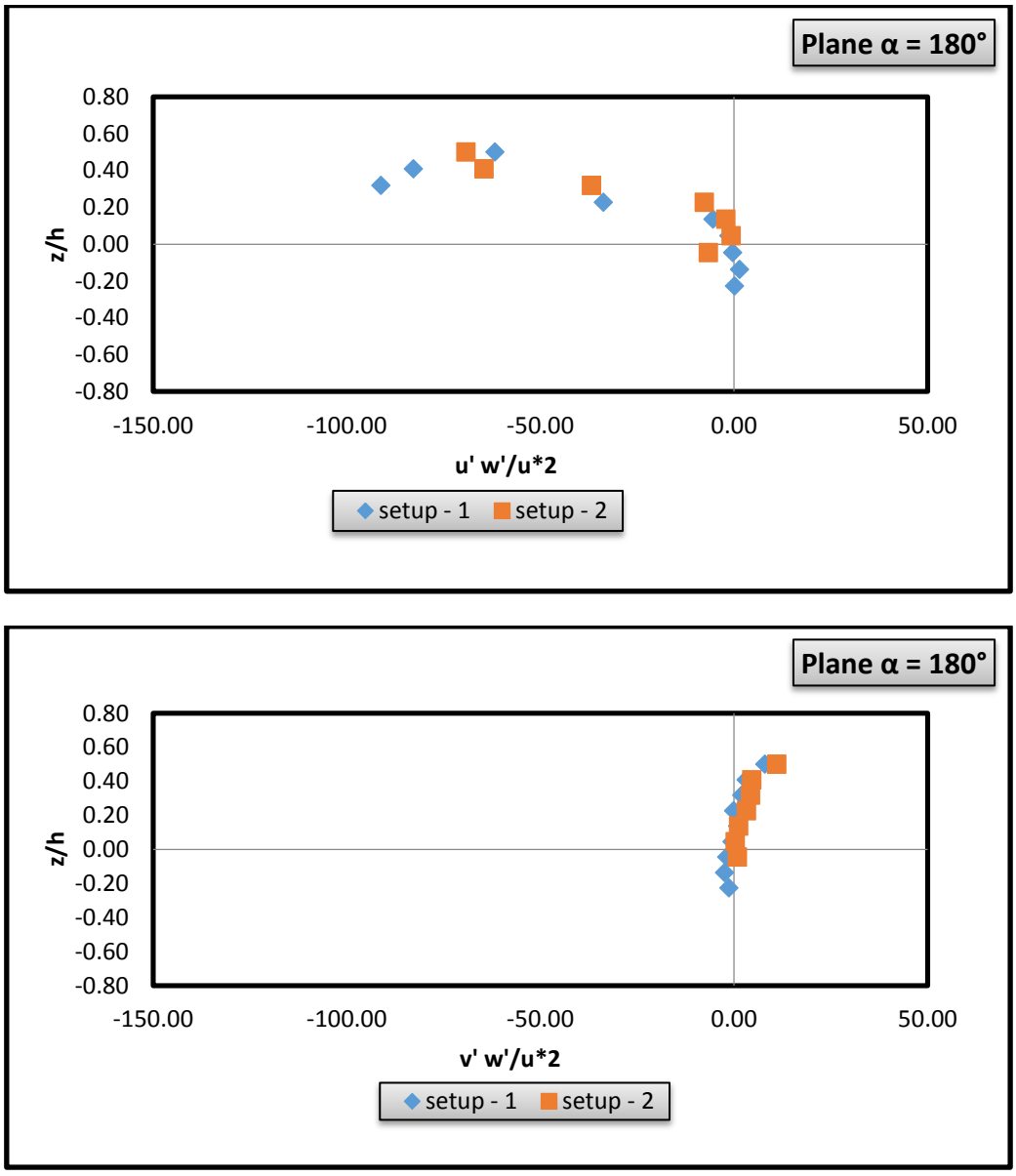

Fig 4.47 Comparison of normalized turbulence intensities and Reynolds stresses in downstream of vertical and inclined pier (α = 180°) at r = 13.5 cm.

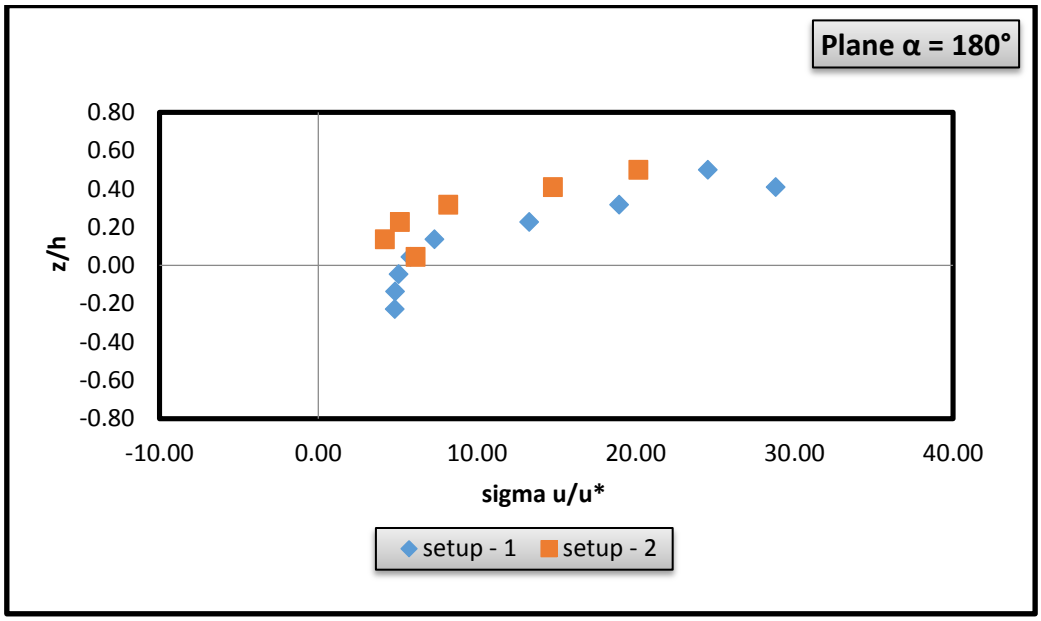
Plane α = 180°
0.80
0.60
0.40
0.20
0.00
-0.20
-0.40
-0.60
-0.80
z/h
-10.00
0.00
10.00
20.00
30.00
40.00
sigma u/u*
setup - 1
setup - 2

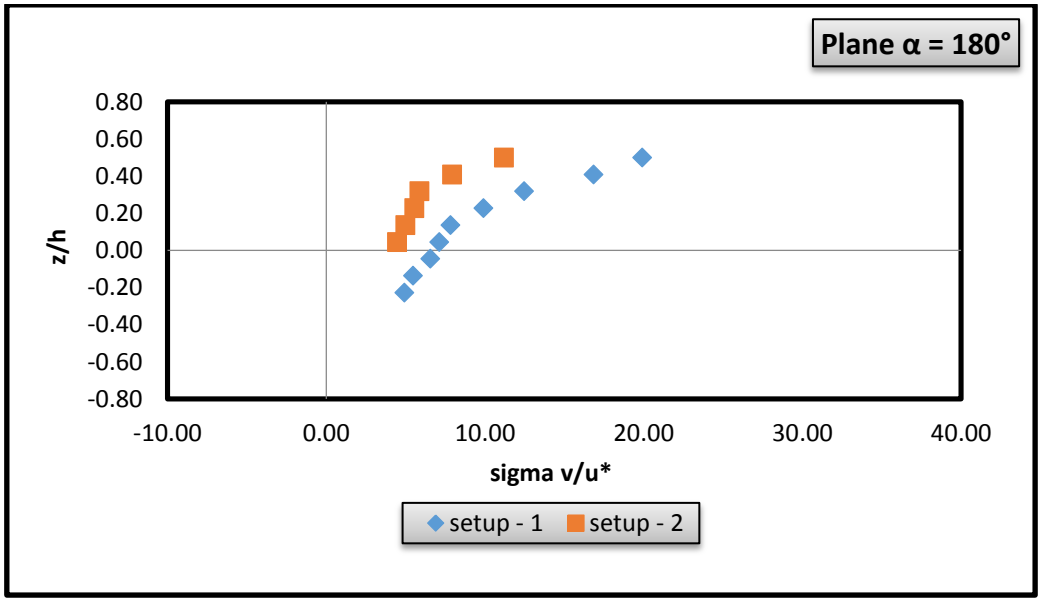
Plane α = 180°
0.80
0.60
0.40
0.20
0.00
-0.20
-0.40
-0.60
-0.80
z/h
-10.00
0.00
10.00
20.00
30.00
40.00
sigma v/u*
setup - 1
setup - 2

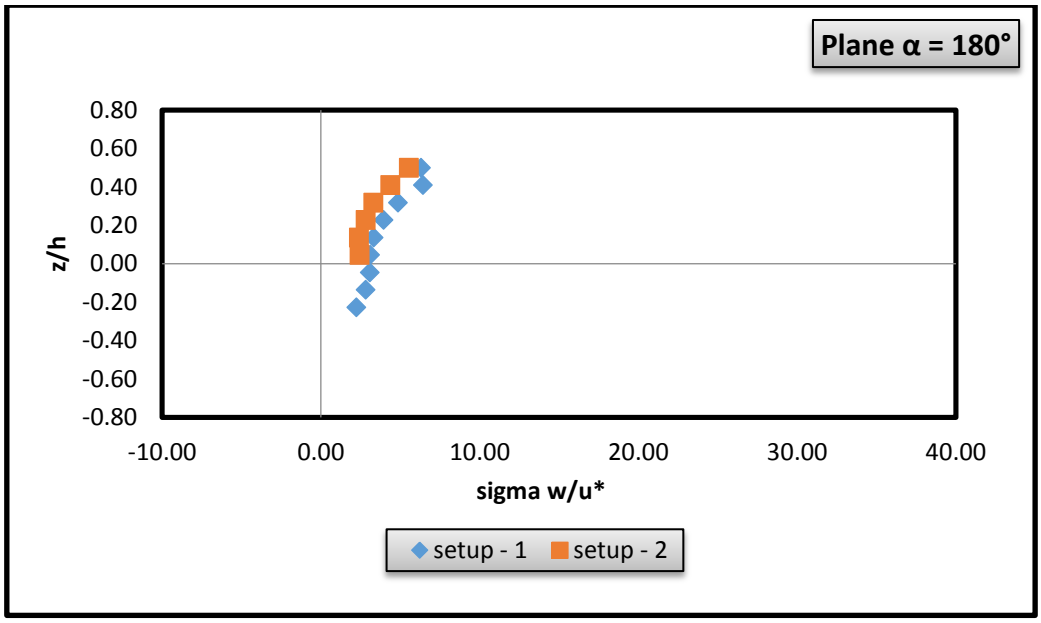
Plane α = 180°
0.80
0.60
0.40
0.20
0.00
-0.20
-0.40
-0.60
-0.80
z/h
-10.00
0.00
10.00
20.00
30.00
40.00
sigma w/u*
setup - 1
setup - 2

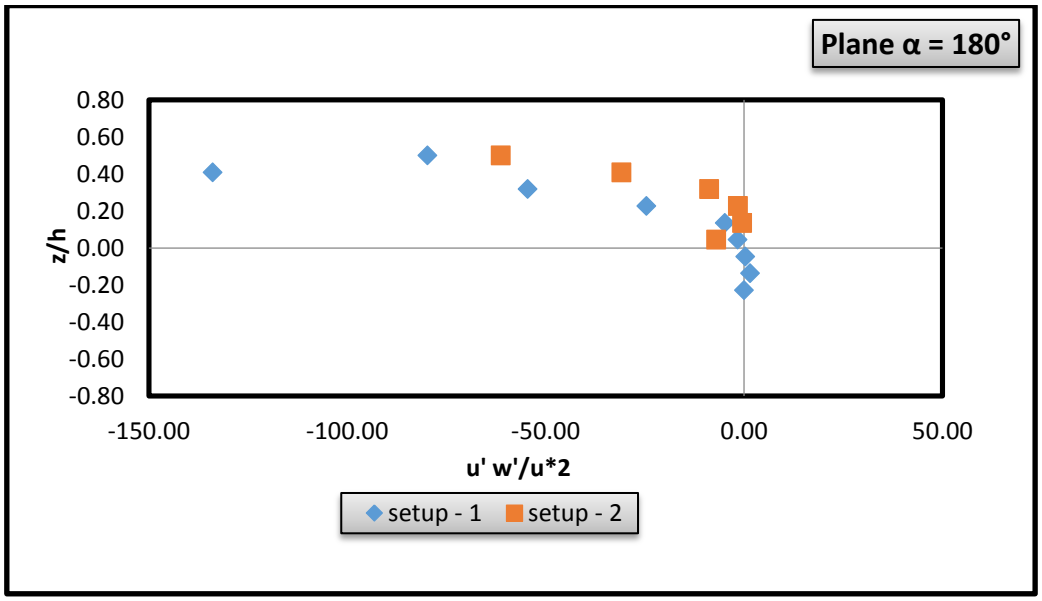

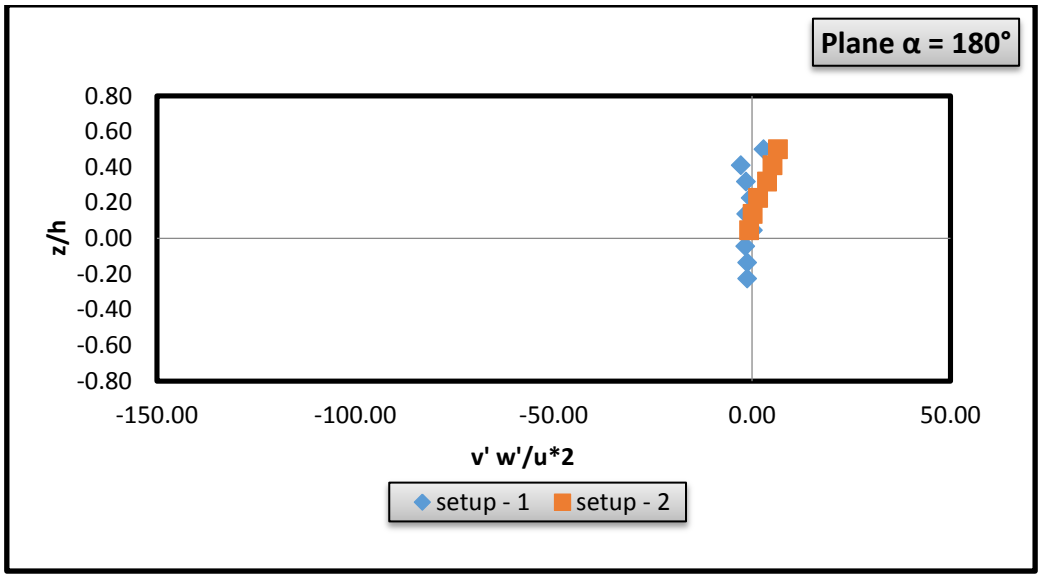

Fig 4.48 Comparison of normalized turbulence intensities and Reynolds stresses in downstream of vertical and inclined pier (α = 180°) at r = 15.5 cm.

CONCLUSION

Experimental results are presented in this study concerning velocity and turbulence characteristics in vertical and inclined pier within the scour hole. In upstream plane near to the pier existence of a strong down flow is detected. The *v* component is almost negligible in the upper zone while $z > 0$. In the downstream plane, just near the pier the *u* component reveals reversal of flow near the water surface. The *w* component is always in the upward direction in the wake region and this is contrary to the flow pattern in the upstream plane. The magnitudes of intensity of turbulence are high and flow is less organized in the wake region while it is relatively more organized in the upstream plane. It is showed that the vertical component of velocity occurring in upstream of the pier losses its strength as the pier inclined towards downstream. It shows that the important variable that effect scour depth and flow characteristics is the slope of the leading edge of abutment to the vertical. Scour depth reduction of approximate 7 % is obtained when pier is inclined 5° towards downstream as compare to vertical pier. Such reduction of scour hole will lead to considerable saving in the construction of the bridge pier. Degree of inclination must be decided after acknowledging structural aspect as well. Results of the present study shall become useful input to the future use of inclined piers.

REFRENCES

1. Ahmed, F., and Rajaratnam N. (1998). “Flow around bridge piers” J. Hydr Engr., 12(3), 288-300.
2. Ashtiani and A. A. Kordkandi (2012). “Flow field around single and tandem piers” Flow Turbulence Combust (2013) 90:471–490.
3. Breusers, H. N. C., Nicollet, G., and Shen, H. W. (1977). “Local scour around cylindrical pier.” J. Hydr. Res., Delft, The Netherlands, 15, 211-252.
4. Breusers, N.N.C., and Raudkivi A.J. (1991). Scouring, design manual, No. 2, International Association for Hydraulic Reaseach, Balkema.
5. Ettema, R. (1980). “Scour at bridge piers.” Rep. no. 216, School of Engrg., Univ. of Auckland, New Zealand.
6. Kumar and U. C. Kothyari (2005). “Flow characteristics within the scour hole around a circular bridge pier”. Hydro., 599-608.
7. Kumar,A.(2007). “Scour around circular compound bridge piers.”Ph.D.thesis, Dept. of Civil Engineering Indian Institute of Tech., Roorkee, India.
8. Kumar and U. C. Kothyari (2012). “Three-Dimensional Flow Characteristics within the Scour Hole around Circular Uniform and Compound Piers”. Journal of Hydraulic Engineering,Vol.138,No.5,May1,2012.©ASCE,ISSN0733-9429/2012/5-420–429/$25.
9. Melville, B.W., And Chiew, Y.M. (1999). “Time scale for local scour at bridge pier.” J. Hydraul. Eng., 125(1), 59-65.
10. Melville, B.W. (1997). “Pier and abutment scour: integrated approach.” J. Hydraul. Eng., 123(2), 125-136.
11. W. H. Graf and B. Yulistiyanto (1998). “Experiments on flow upstream of a cylinder”. Ecole Polytechnique Federale, Lausanne, Switzerland.
12. Zafer Bozkus and Murat Cesme (2010) “Reduction of scouring depth by using inclined pier” NRC research press web site at cjce.nrc,ca on 30 oct. 2010.
13. Zafer Bozkus and Osman Yildiz (2004) “Effect of inclination of bridge pier on scouring depth” ASCE 0733-9429(2004)130:8(827).